高速公路動態交通時間狀態特性之分析、預測與應用

學生：黃益三　　指導教授：藍武王 博士
許鉅秉 博士

國立交通大學交通運輸研究所

摘　要

研究動態交通（Traffic dynamics）的時間狀態特性（Temporal features）與預測短期交通的變化，對尋求解決各項交通問題以及改善先進交通管理系統（Advanced traffic management systems, ATMS）等相關領域效能，均扮演相當重要的關鍵角色。然而傳統一維空間時間序列分析方法，對交通動態隨時間狀態演進的特徵，無法充分掌握其訊息；復以過去許多研究著手進行預測之前，未能審慎考量交通特性暨影響預測準確性的因素，均顯示出過去研究不足之處急待解決。

綜觀過去對交通時間序列的分析，不外乎著重於線性型態的研究，當然，也有為數不少相當有貢獻的研究係著重於探討車輛軌跡在時間-空間上的交互作用；然而這些研究的資料仍僅限於使用模擬模型所產生，其實驗結果缺乏實證交通資料的驗證。因此，本研究利用 Takens 法則，以多維空間方法進行分析，佐以最大里亞帕諾夫指數（the largest Lyapunov exponent）以及吸引子維度（Correlation dimension），在多維空間中仔細觀察交通流量、速率及佔有率，隨時間演進之軌跡，並藉此發展出一套檢驗動態交通在時間狀態特性的準則。

此外，在本研究中，採用輻狀基底函數類神經網路（Radial Basis Function Neural Network, RBFNN）以及即時回饋學習演算法（Real-time recurrent learning algorithm, RTRL），探討在不同量測尺度、時間稽延、空間維度以及不同時段的情況下，對短期動態交通預測的影響程度；同時在不同預測方法中，利用一階自我迴歸隨機時間序列（First-order autoregressive stochastic time series）與確定性一階微分方程式（Deterministic first-order differential-delay equation），成對比較了[線性-即時回饋學習演算法]與[簡單非線性法-即時回饋學習演算法]在預測能力方面的差異特性。

最後，經由中山高速公路實測資料，進行時間狀態特性的實證研究與短期交通預測的敏感度分析，其結果顯示：隨著量測尺度、歷史資料、觀察時段不同，交通流量、速率及佔有率在多維空間中呈現不同非線性時間形態；而藉由流量-速率-佔有率，三者成對觀察中發現透過時間順序的遞進，多維空間不啻提供更多有效訊息。另外，使用輻狀基底函數類神經網路以及即時回饋學習演算法在短期交通

預測方面，具有令人滿意的結果；但是預測準確度也同時會受到量測尺度、時間稽延以及不同時段的影響。本研究的實證成果可做為未來發展交通管理的架構參考，特別是在動態的交通控制方面。

關鍵詞：時間狀態特性、重構狀態空間、時間順序、輻狀基底函數類神經網路、即時回饋學習演算法。

TEMPORAL FEATURES OF FREEWAY TRAFFIC DYNAMICS: ANALYSIS, PREDICTION AND APPLICATION

Student: Yi-San Huang

Advisor: Lawrence W. Lan
Jiuh-Biing Sheu

Institute of Traffic and Transportation
National Chiao Tung University

Abstract

The characterization of the dynamics of traffic states remains fundamental to seeking for the solutions of diverse traffic problems while short-term prediction of dynamic traffic states remains critical in the field of advanced traffic management systems (ATMS) and related areas. However, the scarcity of information provided by conventional one-dimensional traffic time-series data and the hasty prediction without deliberately taking into account the characteristics of traffic dynamics as well as affected factors may have shed light on the lack which need to be solved urgently.

Conventional analysis of traffic time series may play a part in the investigation of traffic patterns characterized by linear statistics. A certain number of studies working at the vehicle trajectories or their interactions within a time-space domain have significant contributions. Nevertheless, most of the results simulated by formulated models are not easy to be calibrated by real data. To gain more insights in traffic dynamics in the temporal domain, this paper explored traffic patterns in higher-dimensional state spaces, where we attempted to map the one-dimensional traffic series into appropriate multidimensional space by Takens' algorithm. After such a state space reconstruction, we then made use of the largest Lyapunov exponent to depict the rate of expansion or contraction of traffic state trajectories in the reconstructed spaces. The correlation dimension was further estimated to examine if the traffic state trajectories exhibited chaotic-like or stochastic-like motions. In accordance with the above procedures, a novel filtering approach was proposed to inspect the characteristics of real-world temporal traffic flow dynamics.

In addition, a radial basis function neural network (RBFNN) and a real-time recurrent learning algorithm (RTRL) were proposed to learn about whether or not the dynamics of short-term traffic states characterized in different time intervals, collected in diverse time lags, dimensions and times of day have significant influence on the performance

of the proposed model relative to the published forecasting methods. Furthermore, we also dabble in comparing pair predictability of linear method-RTRL algorithms and simple nonlinear method-RTRL algorithms individually using a first-order autoregressive stochastic time series AR(1) and a deterministic first-order differential-delay equation.

Finally, an empirical study and a sensitivity analysis were conducted. Wherein, flow, speed, and occupancy time-series data as well as the speed-flow, speed-occupancy, and flow-occupancy paired data collected from dual-loop detectors on a freeway of Taiwan was processed in the empirical study and the same traffic data was fulfilled in the sensitivity analysis with various time intervals, time lags and times of day. The numerical results revealed that different nonlinear traffic patterns could emerge depending on the observed time-scale, history data and time-of-day. In addition, with consideration of sequential order and spatiotemporal features, more information about traffic dynamical evolution was extracted. On the other hand, the performances of RBFNN and RTRL algorithms in predicting short-term traffic dynamics are satisfactorily accepted. Furthermore, it is found that the dynamics of short-term traffic states characterized in different time intervals, collected in diverse time lags and times of day may have significant effects on the prediction accuracy of the proposed algorithms. The above findings may support that the proposed methods in this study can be used to develop traffic management schemes which are practically applicable in dynamic control.

Keywords: temporal traffic pattern, reconstructed state spaces, sequential order, radial basis function neural network, real-time recurrent learning algorithm

TEMPORAL FEATURES OF FREEWAY TRAFFIC DYNAMICS: ANALYSIS, PREDICTION AND APPLICATION

TABLE OF CONTENTS

LIST OF FIGURES

PAGE

LIST OF TABLES


E S A
1896

CHAPTER 1 INTRODUCTION

1.1 Background and Motivations

Traffic patterns are those characteristics of vehicle groups passing a point or short segment during a specified span or traveling over longer sections of highway. Various applications of cooperative driving or any kind of driver information and assistance systems are strongly dependent on actual and predicted traffic features. In terms of temporal features, traffic time-series data measured in different time scales or intervals serve different purposes. In planning, for instance, one might wish to estimate the annual traffic volume over the planned horizon for proposed infrastructure alternatives. The annual volume is then used for estimating the expected saving in travel time for economic feasibility studies. For design purposes, however, hourly traffic volume is often required to determine the facilities' capacity. Thus, accurately predicting the hourly flow variations would become essential to avoid an over- or under-design of new facilities. For operational purposes, much shorter-term traffic information, such as minute-flow, is essential for real-time traffic management and control. In addition to flow, other traffic data in temporal perspectives such as occupancy and speed are also crucial for various practical purposes. Further, traffic occurs in space and time, i.e., spatiotemporal features. If we explore the spatiotemporal traffic patterns, more insightful information may provide us an understanding of freeway traffic that can be used for effective traffic management, traffic control, organization and other engineering applications, which should increase freeway capacity, improve traffic safety and result in high-quality mobility. In particular, surveying the congested traffic patterns could give us necessary information for efficient collective management strategies, including such well-know methods as ramp metering and traffic assignment. Varaiya (2005) pointed out that effective management on highway congestion through investigation of traffic patterns can significantly reduce congestion. As such,

disclosure of the traffic dynamical patterns deserves in-depth exploration.

Traffic time series represent the evolution or temporal variation of any traffic variables measured in a sequential (chronological) order. The diverse characteristics of traffic time series, from random series, short-term correlation, non-stationary series to seasonal fluctuations, can be depicted according to various observing time intervals. Conventional analysis of time series may shed light on investigating into the features of time-series data such as trend, seasonality, outliers and discontinuities against time. Such a measure may merely apply to describing general linear phenomena such as mathematical moments mean, variance, auto-covariance and autocorrelation rather than the whole spectra of nonlinear dynamic phenomena, which exhibit not only trend but also the resulting anomalous fluctuation. The intrinsic information behind traffic fluctuation, which is an essence for many advanced traffic control and management practices in intelligent transportation systems (ITS), may need an advanced method to exploit. Therefore, researching the features of traffic time series via an innovative technique deserves in-depth exploration, too.

On the other hand, accurately characterizing and predicting the traffic dynamics, especially measured in short time intervals, has become a prerequisite in the development of advanced traffic management systems (ATMS). Here, traffic dynamics (or termed as traffic time series) refer to are regarded as temporal evolution of such traffic states as flow, speed and occupancy, measured in a sequential (chronological) order with identical time intervals. Numerous adaptive intelligent signal control mechanisms, for instance, are established on the basis of instantaneous or predicted 5-minute or shorter flow data. Smart incident detection may require 1-minute or shorter traffic states as inputs. Lam *et al*. (2002) further pointed out that the short-term traffic forecasting results can be used for validation of the regional and territory-wide transport models required in various transport studies, such as the freight transport study and parking demand study, and the development of traffic flow simulator to provide the off-line short-term travel time and traffic flow forecasting database. Due to the complex nature of traffic time series with considerable fluctuations and noises, accurately capturing and predicting short-term traffic dynamics is more challenging than the long-term (e.g., hourly or daily traffic) dynamics wherein conspicuous fluctuations have essentially been smoothed out. In view of traffic dynamics measured in different ways would provide more informative insights into its complex nature, developing the prediction models to better elucidate its evolution, measured in different time intervals, periods, lags, and times of day, deserves in-depth exploration. And this also motivates our study.

With regard to the fact that how to apply the results of characterizing and predicting the traffic dynamics to help developing methods for real time traffic control is an extensive issue which furthers more research in the development of advanced traffic management systems (ATMS). For instance, recurrent traffic congestion has been recognized as a critical issue to solve in the development of advanced freeway traffic dynamics systems. Generally speaking, recurrent traffic congestion often happens during peak hours and affects most of commuters day after day. If we can reduce the top fluctuation of flows, we may postpone the peak hour, which mainly bring about traffic block to eliminate most of delay by some control rules. However, it had been inefficient to stop on-ramp vehicles entering freeway whenever one fond the flows increase drastically in the twinkling of an eye. So, it is necessary to develop a forward strategy to control fluctuation of flows. Otherwise the suddenly high flow will influence obviously the next step flow. Therefore, we would like to learn whether or not the critical problems of recurrent congestion and non-recurrent congestion daily occur could be alleviated or avoided via the characterizing and predicting of traffic dynamics. The significance is the fourth reason to trigger our study.

1.2 Objectives and Values

In view of the scarcity of information provided by one-dimensional traffic time series, and the lack of considering sequential order in fundamental diagrams proposed by traffic stream models, the main objective of this study was to characterize evolutional state trajectories in appropriately reconstructed state spaces and chronological relationship for paired- and three- traffic variables in multiple dimensions at an isolated station as well as between two nearby stations. From successive days with coarse scales to within a day using subtle observation (20-second, 1-minute, etc.), then to several days with different time intervals, we have attempted to gain in-depth insights into the evolution of traffic time series. By investigating the temporal patterns of traffic dynamics in reconstructed state spaces, we can understand the characteristics of traffic series and further develop effective managements, such as incident detection, extended delay prevention and ramp metering other than those known in one-dimensional space. Furthermore, a close look at traffic time series not only provides useful information for application in ITS, but improves upon the shortage of linear models for conventional stochastic processes. Aside from the above temporal patterns, we believe that this analysis may have a sense as the first step for understanding of complex behavior of spatiotemporal features of congested traffic patterns.

With considering the above features of traffic dynamics exhibited in multidimensional state spaces and predictabilities between various techniques suiting different types of traffic series, the second purpose of this study is to propose a radial basis function neural network-based (RBFNN) and a real-time recurrent learning-based (RTRL) algorithm to know whether or not the dynamics of short-term traffic states characterized in different time intervals, collected in diverse time lags and times of day have significant influence on the performance of the proposed model relative to the published forecasting methods. In addition to assessing the relative performance of the proposed RBFNN and RTRL algorithms, we further compare the pair predictability of linear method versus RTRL algorithms and simple nonlinear method versus RTRL algorithms individually using a first order autoregressive time series AR(1) and a deterministic function to elucidate the significance that the characteristics of traffic dynamics affect the accuracy of prediction. After a well-trained network is built and various techniques are compared, the accurate understanding for traffic dynamics and reliable prediction would be anticipated.

1.3 Benefits and Significance

In this study, we adopt three traffic variables, flow, speed and percent occupancy, to explore the temporal features of traffic dynamics. To see the benefits of inspecting features of a time series, we set an example to elucidate the conceptual difference between numeric data and features. For instance, one normally does not have a distinct awareness that traffic is light or heavy when one is told that the traffic volume equals 20 vehicles per lane with a 1-minute time interval. At most, one perhaps can ask when the traffic volume occurs during the day to help discriminate between light and heavy traffic. Nevertheless, as depicted in Figure 1-1, one easily gets confused, since the specific volume, 20 vehicles per minute, happens at several time points during the day. Therefore, the information provided by traffic data is extremely limited, in particular when figures are derived from one variable.

From Figure 1-2 (a), it can be seen that heavy traffic seemingly occurs, because traffic speed drops off and occupancy increases, at two time points in the day, around 10:00 am and 14:00 pm, when the other two curves of variables, speed and occupancy, are added in Figure 1-1. Meanwhile, the corresponding traffic dynamics with volumes equal to 52 vehicles per 3 minutes and 154 vehicles per 9 minutes are displayed in Figures 1-2 (b) and (c) respectively. For the larger intervals, it seems that the associated information is getting less. However, no matter what time scale we employ,

the useful information provided by traffic data is incomplete and even misunderstood compared with that provided by features shown in Figure 1-3. From Figure 1-3, it can be clearly seen that traffic series measured with different time scales reveal similar trends or structures. As the time scale used as a measurement becomes smaller, fluctuations surging along with the general patterns become more conspicuous. Specifically, the traffic time series patterns in one dimension from day to day look very similar but never exactly repeat. The patterns are essentially non-reproducible (with oscillations) each day.

In spite of the benefits of features, the display of traffic dynamics in multidimensional spaces may reveal more valuable information. To see the benefits of a time series presented in reconstructed state spaces in this study and illustrate two well-known nonlinear time series: the first one is Lorenz series generated by Eq. (1.1), which is known as a deterministic (chaotic) time series. The second one is a random time series generated by Eq. (1.2), which is proven as a stochastic (random) time series (Sprott and Rowlands, 1995).

$$dX/dt=10(Y-X);\ dY/dt=28X-Y-XZ;\ dZ/dt=XY-8Z/3 \quad (1.1)$$

$$X_{n+1}=AX_n+B(modC) \quad (1.2)$$

For the one-dimensional plots, $x(t)$ versus t, shown in Figure 1-4, we notice that a chaotic time series (Figure 1-4(a)) is less distinguishable from a random time series (Figure 1-4(b)). Namely, it is faint to distinguish, by visualization method, between a chaotic system and a stochastic system because both have very similar irregularity in one-dimensional space; however, it seems existent a few rules in the Lorenz time series. If we reconstruct these two time series in a three-dimensional state spaces, $x(t)$ versus $x(t+\tau)$ versus $x(t+2\tau)$, where τ is a proper time lag, we would see the difference as shown in Figure 1-5. Notice that the chaotic system has revealed discernible structure (Figure 1-5(a)), in which the trajectories are governed by certain deterministic rules. In contrast, the random system does not reveal any structure at all, which plots just scatter uniformly in the three-dimensional state spaces (Figure 1-5(b)). This illustration provides good advice that a very simple tool, which is one of methods of nonlinear time series, can reveal certain deterministic rules in multidimensional state spaces.

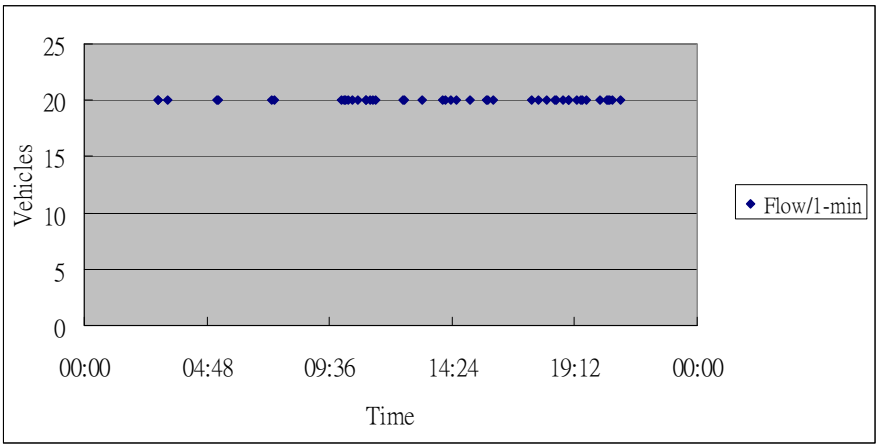

Figure 1-1 Time points with volume equaling 20 vehicles/1-minute in a workday

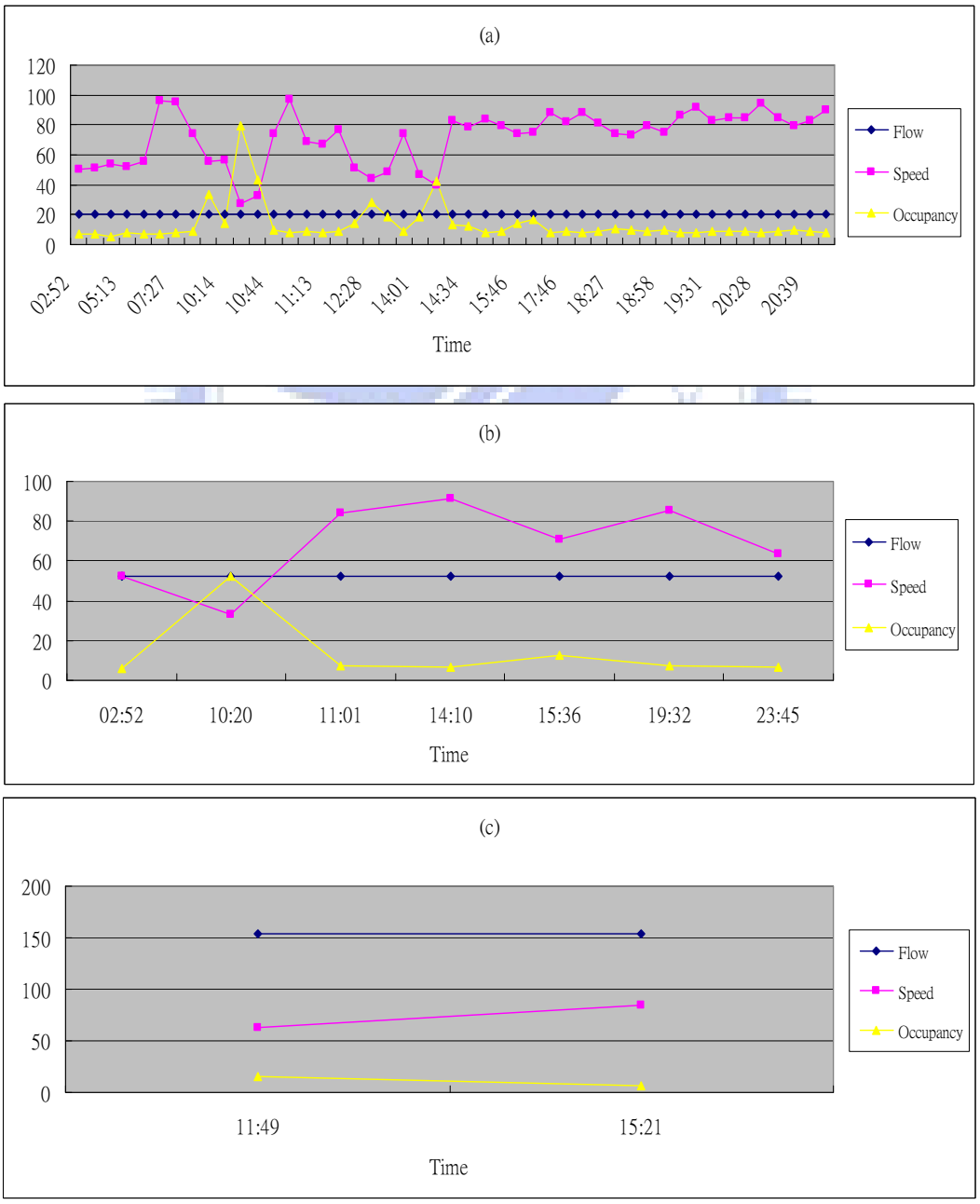

Figure 1-2 Numerical variation of traffic variables with 3 time scales in a workday

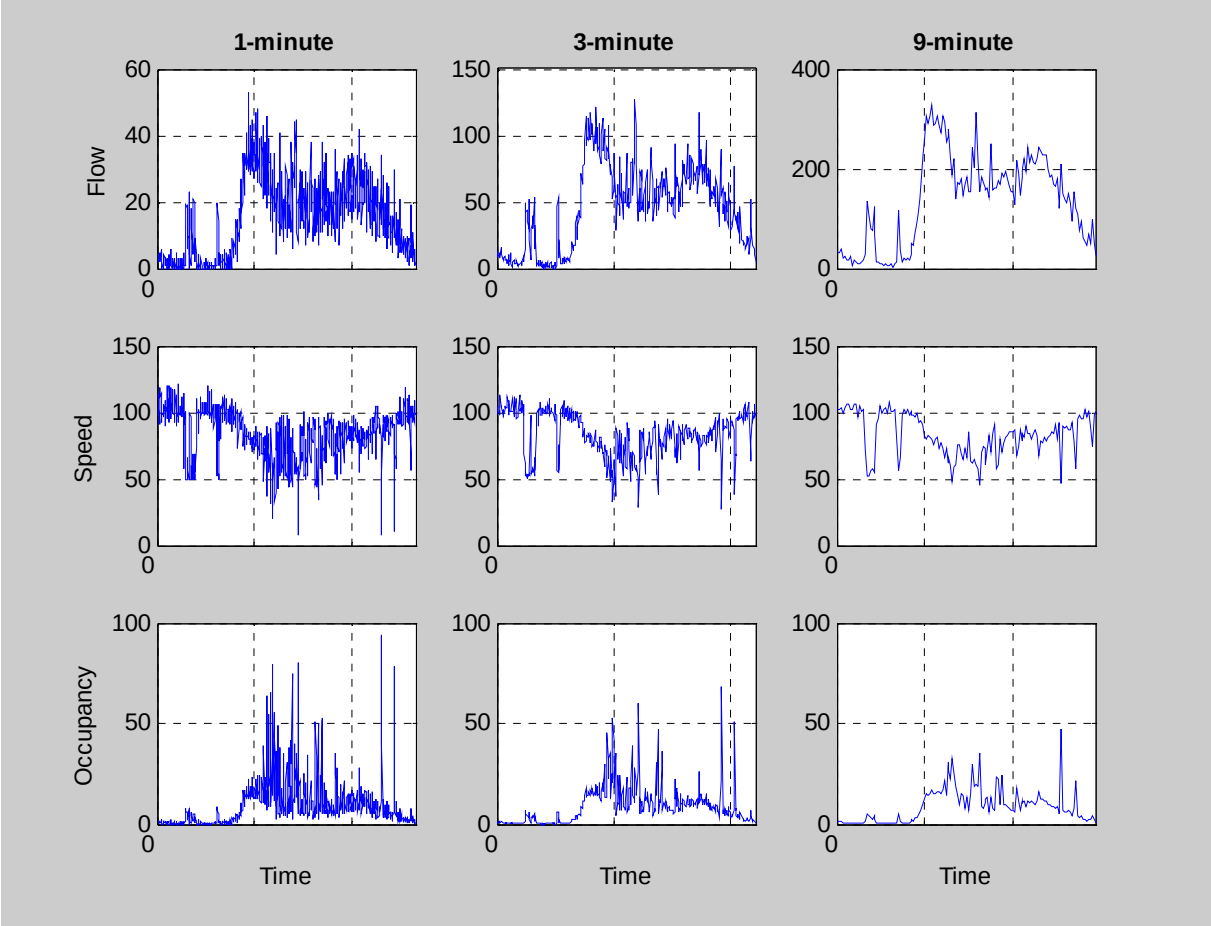

Figure 1-3 Features of 24-hour traffic time series with 4 time intervals

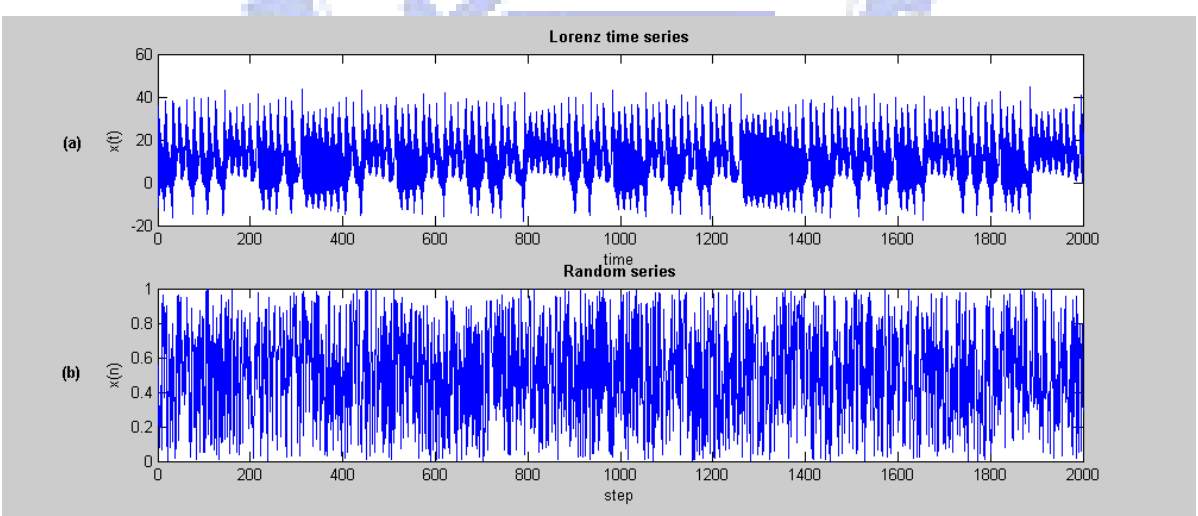

Figure 1-4 One-dimensional plots for Lorenz and a random time series

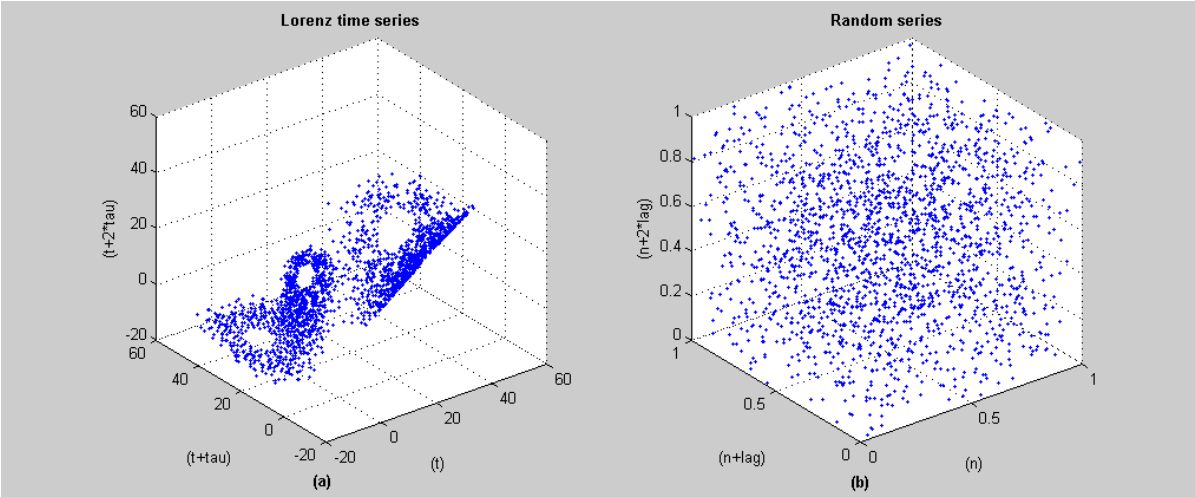

Figure 1-5 Three-dimensional state spaces plots for Lorenz and a random time series

Through the state space reconstruction, one may find out the noticeable patterns for a chaotic system. However, one still cannot figure out how the series trajectories would evolve over time because mapping the one-dimensional series into higher dimension does not explain its sequential order. To see the importance of the sequential order, this study further demonstrates another nonlinear time series, known as Logistic map, generated by Eq. (1.3).

$$x(n+1)=3.75x(n)(1- x(n)) \tag{1.3}$$

Let the initial condition of the series be $x(0)=0.1$. Figure 1-6 presents the difference of the series in two-dimensional state spaces with revealing and without revealing its sequential dynamics. One can clearly observe the back-forth dynamical behaviors by only taking the sequential order of the series into consideration (Figure 1-6(a) marked with numbers). In contrast, without considering its sequential order the series can only reveal its patterns, not the dynamical behaviors (Figure 1-6(b)).

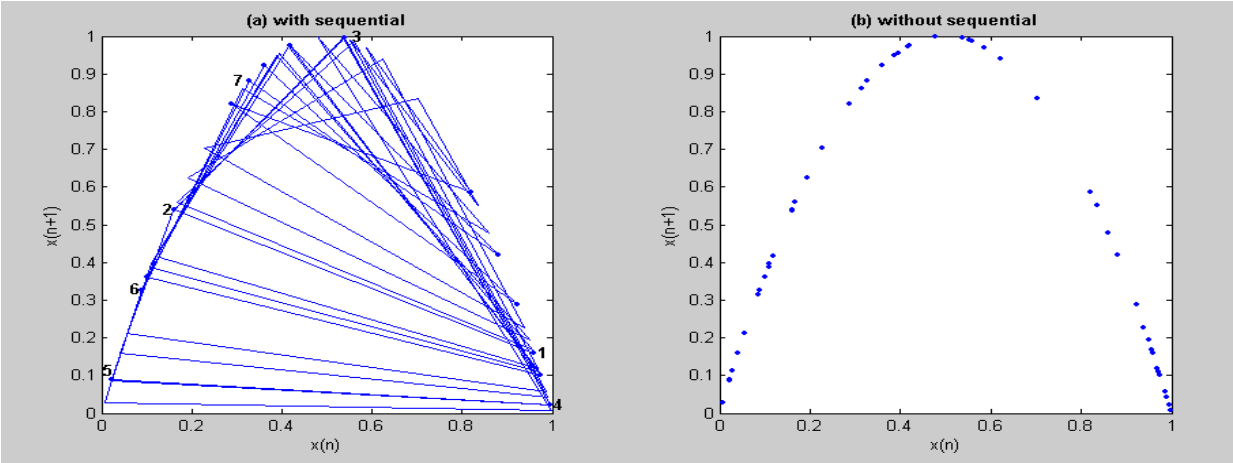

Figure 1-6 Logistic map $x(n+1)=3.75x(n)(1- x(n))$, where $x(0)=0.1$

Next, another well-known example is further demonstrated in Figure 1-7 to elucidate the significance of tracing when we face the intangible variance of traffic dynamics. In this figure, the relationship between speed and flow without sequential order is displayed in the top left plot (entitled original data (a)), while the identical relationship between speed and flow, when completely shuffled, without sequential order is displayed next to the original data (a), and which we name surrogate data (b). From the above two plots, it seems that the distribution representation only tells us the numerical relationship between the two traffic variables rather than the rationale of the dynamics. However, when their sequential order is taken into consideration, the slight difference between the original data and the surrogate data can be seen, depicted as original data (c) and surrogate data (d) respectively in Figure 1-7. Moreover, if a small area from the original data (c) is selected and the sequential order tracked, then we find the trace scattering depicted in the original data (a) and original data(c) of the right hand side plots, which represent the plots of ten points in the early hours and morning peak hours. Obviously, there are distinct differences between the original data (plot (a) and (c)) and the surrogate data (plot (b) and (d)) after tracing along the ten points. Accordingly, such tracings play an important role in investigating traffic dynamics.

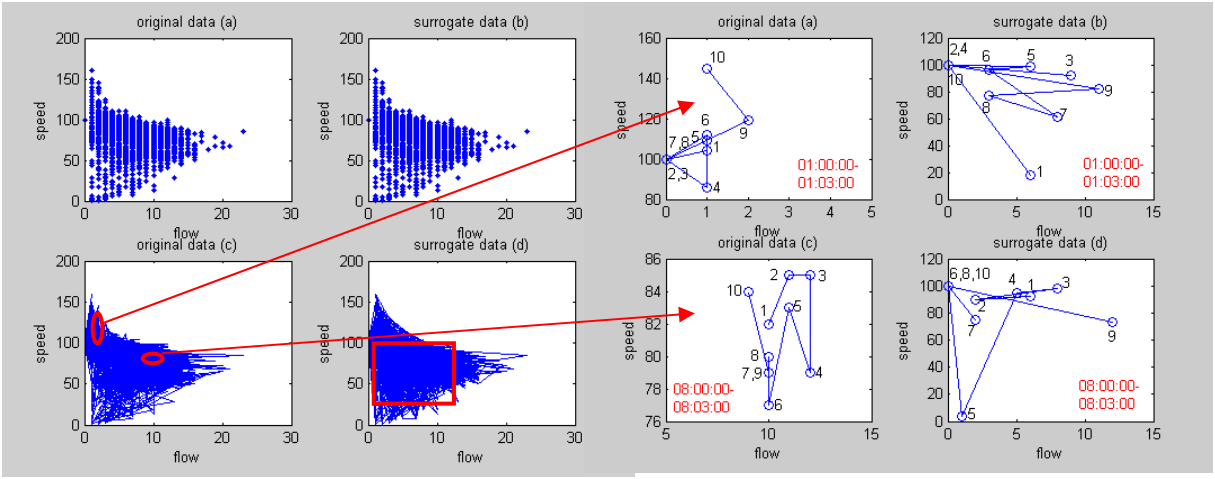

Figure 1-7 The relationship between speed and flow with/without tracing

The above illustrations imply that one can gain insights into a time series by looking at its patterns in multidimensional state spaces, rather in a conventional one-dimensional space, and by considering its sequential order to realize its actual dynamical behaviors. Some challenging issues may arise from these implications. For instance, what is the most appropriate time lag? How high the dimension should be embedded to reveal the best features? Do nonlinear phenomena really exhibit in the nature of traffic dynamics? What types of nonlinear phenomena may exist? What are the core logics for modeling the traffic sequential orders? Why do we need to predict? What is the best prediction? What is the cause and effect relationship between features and prediction? What is the difference of predictability between various techniques? The following chapters will address these issues in detail.

1.4 Limitation and Scope

In this study, traffic time series were directly extracted from dual-loop detectors installed at a given 3~4-lane mainline segment of the northbound Sun Yat-Sen Freeway of Taiwan, located in the northern area of Taipei County. The traffic series extracted from “isolated” stations can only provide us to explore the temporal patterns of traffic dynamics, not spatiotemporal features over several adjacent segments. This is the restriction of our empirical investigation. In addition, traffic state trajectories in this dissertation refer to traffic variables (flow, time-mean-speed, percent occupancy), which were tracked and recorded in reconstructed state spaces over time rather than vehicles changing their position with time evolution.

1.5 Organization and Framework

The following chapters of the dissertation begin with the literature review and description of our rationales for methodology development, followed by a brief of preliminary testing and discussion of analytical results. We conclude with an elaboration of the research and follow-up for future work. Figure 1-8 is the framework of dissertation and Figure 1-9 is the research framework.

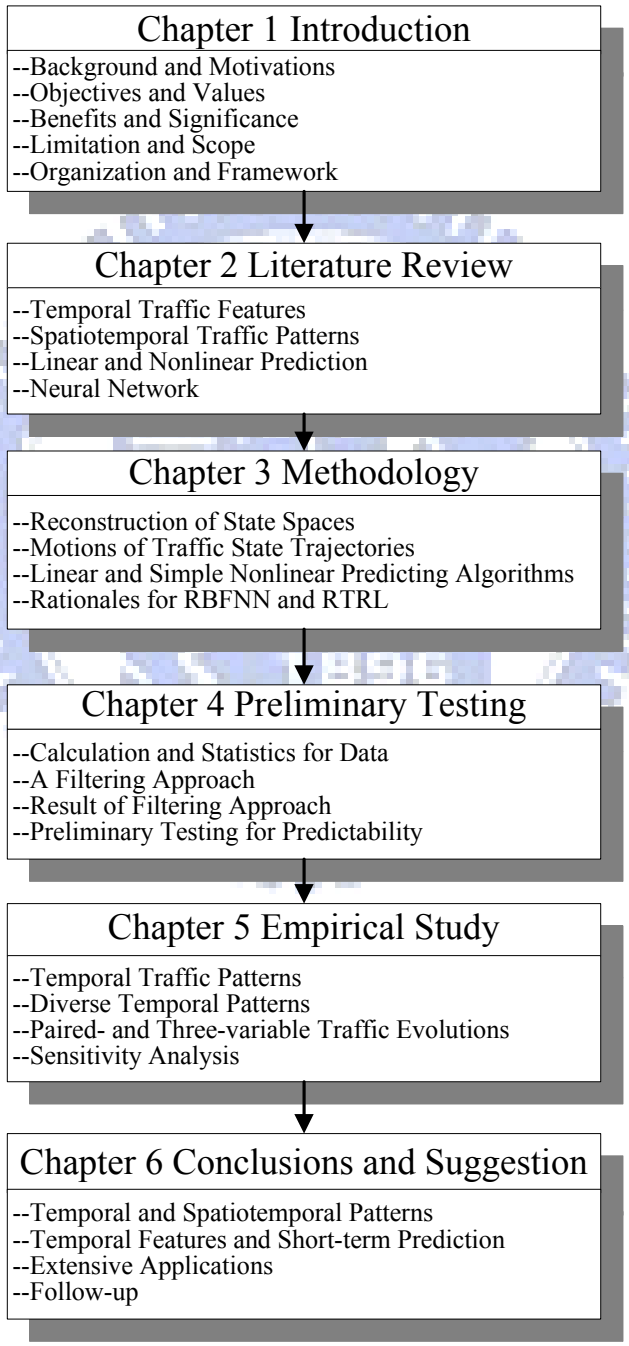

Figure 1-8 Framework of dissertation

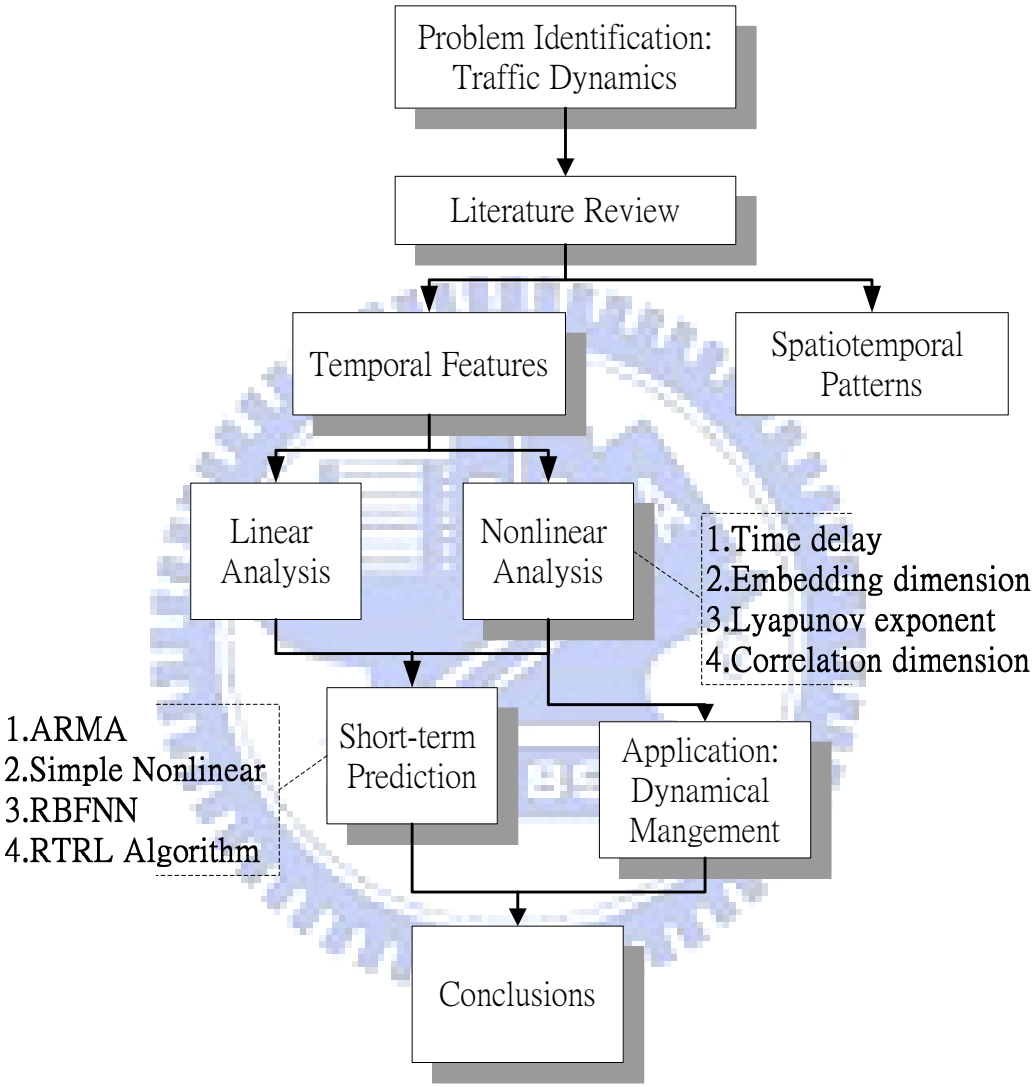

Figure 1-9 Research framework

CHAPTER 2 LITERATURE REVIEW

Numerous researchers have devoted their efforts to the study of traffic dynamics, and we can categorize their achievements into four types: temporal features, spatiotemporal patterns, linear and nonlinear prediction and artificial neural networks, which are presented in this chapter.

2.1 Characteristics of Temporal Traffic Time Series

Most of the early paradigms have employed stochastic processes to depict the traffic time series by using some presumed mathematical (probabilistic) distributions. Taking headways as an example, May (1990) categorized their features into random, constant, and intermediate states. Wherein, headways categorized as the intermediate case is the most difficult to model, although it is the most frequently encountered case in a real-world situation. Likewise, traffic flows are often modeled by different stochastic processes. For instance, Poisson distributions are widely acknowledged in low-volume conditions where the mean and the variance of counting traffic are about the same. Such traffic conditions can be associated with random headway states. In contrast, binomial distributions are often utilized for near-capacity conditions where the mean of flow rates is typically larger than its variance. These traffic conditions correspond to nearly constant headway states. The intermediate flow count between these two boundary states can be very complex, and has been modeled by different probabilistic distributions. In the late 1970s, autoregressive integrated moving average (ARIMA) processes had become very popular in the study of linear stochastic time series (Box *et al*., 1976; Jenkins and Alavi, 1981). Moreover, a large amount of literature has extended analytical tasks from pure time-series models to dynamically generalized linear models (Ansley *et al*., 1977; Clarke, 1983; Maravall, 1983; Liu, 1991; Chang and Miaou, 1999; Lee and Fambro, 1999; Lingras *et al*., 2000; Williams, 2001;

Williams and Hoel, 2003), and to multivariate time series state space models (Stathopoulos and Karlaftis, 2003) assuming that the dynamics of traffic flow may follow a linear system or can be modeled with a time invariant linear filter by Wold's decomposition.

Other paradigms treat traffic series as a nonlinear system. For instance, Disbro and Frame (1989) utilized chaos theory, a nonlinear system with aperiodic determinism, to describe traffic flow phenomena, and Dendrinos (1994), Zhang and Jarrett (1998), Lan *et al.* (2003a) and Shang *et al.* (2005) in their analysis of traffic data also found that chaotic characteristics exist in traffic systems. In addition, Smith *et al.* (2002) stated that the presence of "chaotic like" behavior cannot be completely dismissed, especially during congestion when traffic flow is unstable and a stronger causative link may be operating in the time dimension. In reality, at times it is very difficult to make such a spatiotemporal analysis of empirical data extracted from "isolated" stationary detectors. Under such restriction - only temporal traffic patterns were investigated, nonlinear phenomena such as equilibrium (stable) fixed points, periodic, quasi-periodic motions or chaotic characteristics, and stochastic or random behaviors could be analyzed in a traffic dynamical system. Therefore, it may not be appropriate to view any traffic series as a pure deterministic or a complete random time series. Instead, traffic flow dynamics may be characterized in a comprehensive spectrum featured in the range between random and deterministic (Lan *et al.*, 2007b). Only through sufficient evidence from field observations can we be sure of the dynamical behaviors of traffic series, thereby in turn, enabling modeling (elucidating or predicting) the traffic series in a more accurate manner for practical applications.

2.2 Spatiotemporal Traffic Patterns

A certain number of previous studies also have aimed at the trajectories of traffic patterns varying in the spatial domain for specific purposes such as geometric design of traffic systems and advanced traffic control. Such spatial traffic patterns, which vary transversely across the highway between lanes and direction of travel and longitudinally along the highway or street, may also provide useful information for control and design purposes, such as incident detection, accident investigation, roadway design, etc. For example, Sheu *et al.* (2004) presented a discrete-time nonlinear stochastic model to characterize the traffic states under the condition of lane-blocking incidents on surface street. In the late 1990s, a "three-phase traffic theory" was developed to depict the spatiotemporal traffic patterns (Kener, 1998, 1999, 2002a, b). Subsequently, several models, including Kerner-Klenov model, CA model,

FOTO and ASDA models, were presented to recognize and track traffic breakdown and spatiotemporal congested patterns (Kener and Klenov, 2002; Kerner *et al*., 2002, 2004). In addition, Kerner (2004) and Kerner *et al*. (2006) further pointed out a few drawbacks of fundamental diagram approaches in describing of spatiotemporal congested freeway patterns. By Kerenr's three-phase traffic theory, the spatiotemporal relationship among traffic variables has been elaborately illustrated. In addition, cellular automaton (CA) simulation has been widely used to explicate the behaviors of traffic flows. Nagel and Schreckenberg (1992) first proposed a CA model to reproduce the basic features of real traffic. In the late 1990s, a considerable number of modified CA models have been developed or extended in the past decade (Nagel, 1996, 1998; Rickert *et al*., 1996; Chowdhury *et al*., 1997; Barlović *et al*., 1998; Nagel *et al*., 1998; Knospe *et al*., 2000; Bham and Benekohal, 2004; Larraga *et al*., 2005). Most of these modified works dealt only with pure traffic flows (only one type of vehicles). Hsu, *et al*. (2007) proposed refined cellular automata (CA) rules to explore the fundamental traffic features and stated that the proposed refined CA models are capable of capturing the essential features of traffic flows.

2.3 Techniques for Linear and Nonlinear Prediction

Techniques for predicting time series can be generally divided into two categories: linear and nonlinear. Linear techniques, such as autoregressive integrated moving average (ARIMA) methods, aim to characterize homogeneous time-series data, either stationary, or non-stationary that can be further transformed into a stationary series (Kalman, 1960; Box and Jenkins, 1970; Granger and Newbold, 1976; Oller, 1985). Additional comparisons between linear technique (ARIMA) and other predicting methods, for instance neural network (NN), non-parametric regression (NPR) and Gaussian maximum likelihood (GML) are also conducted for extensive applications (Smith *et al*., 2002; Tam *et al*., 2004; Lam *et al*., 2006). In contrast, linear models may not be applicable in characterizing inhomogeneous data due to their weakness in transforming the non-stationarity of traffic states into stationarity.

The nonlinear techniques for predicting the inhomogeneous time series are in effect strongly based on the underlying postulation that different time series with equal states may have equal futures and similar states will also evolve similarly, at least in the short run. According to such postulation, Iokibe *et al*. (1995) proposed a fuzzy local reconstruction method which was adequate in prediction of some experimental nonlinear time-series cases. Sakawa *et al*. (1998) proposed a fuzzy neighborhood method which proved effective in some deterministic nonlinear predictions. Lan and

Lin (2001) proposed a phase-space local approximation method for satisfactorily predicting short-interval flow dynamics. In the prediction literature, most successfully modeling for nonlinear time-series data have been generated in laboratory experiments and rarely have they been found outside the laboratory due to the complex fluctuations with noises of most real time-series data. This has stimulated some attempts to combine nonlinearity and stochasticity in modeling and making predictions (Gardiner, 1997; Ragwitz and Kantz, 2000, 2002).

2.4 Neural Network

Undoubtedly, considerable literature has elaborated the predicting approaches from neural network (Clark *et al*., 1993; Dochy *et al*., 1996; Dougherty and Cobbett, 1997; Smith and Demetsky, 1997; Kirby *et al*., 1997) to wavelet analysis (He and Ma, 2002) and to hybrid method (Li, 2002; Soltani, 2002). One of neural network based approaches, called radial basis function neural network (RBFNN), is worth to further illustrate because of its successful application on predicting the traffic dynamics (Wedding and Cios, 1996; Chen and Grant-Muller, 2001) with reasonable training time from practical perspectives. Ham and Kostanic (2001) and Kecman (2001) proposed an effective technique, called OLS (Orthogonal Least Squares), to improve the disadvantages pertaining to the original RBFNN, which had made RBFNN more useful and practical in prediction (Chen *et al*., 1991). Another neural network based approach, real-time recurrent learning (RTRL), is also noteworthy because it is not only able to manipulate the mapping of single input-output, i.e., static process, but also capable of incorporating time sequential order into operating the non-stationary process, in which the chronological order is a very important factor to accurately predict traffic dynamics (Haykin, 1999; Chang *et al*. 2002). Because of the recurrent feedback loops, a recurrent neural network (RNN) is able to process temporal patterns and time-vary systems (Chang and Mak, 1999). Wherein, the real-time recurrent learning algorithm applied to train RNN developed by Williams and Zipser (1989) is one of the successful learning algorithms. In particular, it is suitable for on-line training of RNN (Mak *et al*. 1999). Afterward, Mak *et al*. (1999), Chang and Mak (1999) and Goh (2003) proposed modified learning algorithms as well as an adaptive gradient computation to improve the convergence capability of the RTRL algorithms, which have made RTRL algorithms more useful and practical in prediction.

Despite the improvement in computation of above approaches, most previous literature may either lack empirical analysis of the characteristics of traffic dynamics before prediction, or hastily train a network without considering the effects that influence the

prediction accuracy from diverse perspectives, for example, observing the different training results of traffic series measured in different time intervals, time lags, times of day and in multidimensional state spaces. Accordingly, it is necessary to further understand the pros and cons between various predicting techniques and the affected factors under different scenarios when one would like to thoroughly acquire more information from the procession of prediction.

CHAPTER 3 METHODOLOGY

This chapter mainly describes the methods of this study, including reconstruction of state spaces, motions of traffic state trajectories, linear and simple nonlinear predicting algorithms, RBFNN and RTRL algorithms. In addition, we also use a few well-known examples to elucidate the algorithms and make them readable.

3.1 Reconstruction of State Spaces

Reconstruction of state spaces involves two main steps: (1) determination of appropriate time delay and (2) embedding dimension. In the study, the fundamentals of Takens' method were utilized to determine appropriate time delay. Note that Takens' method has been extensively applied to many disciplines of science and engineering (Abarbanel, 1996; Kantz and Schreiber, 2004). In Takens (1981), it was proved that, under fairly general conditions, the underlying dynamical system could be faithfully reconstructed from time series, in the sense that a one-to-one correspondence can be established between the reconstructed and the true but unknown dynamical systems. Details about the developmental procedures and rationales for state space reconstruction were depicted in the following, including determination of time delay, embedding dimension and how to measure the motion of trajectories in reconstructed space via largest Lyapunov exponent and attractor dimension.

3.1.1 Determination of Time Delay

First, let us specify a dynamic system to elaborate traffic dynamics and its properties. In the study, traffic dynamics (including flow, speed and occupancy) is named interchangeably as traffic time series or traffic series referring to the temporal evolution of any traffic variable or its state trajectories measured in a chronological

sequence with equal time interval. Now, let *x(t)* denote the traffic series describing the time evolution in phase space, then it can be expressed by on ordinary differential equation $\dot{x}(t) = F(x(t))$, $t \in R$; or in discrete time $t = n\Delta t$ by maps of the form $x_{n+1} = f(x_n)$, $n \in \mathrm{Z}$, where *x* is a state vector that is finite dimensional $x \in R^n$, and *f* and *F* are referred to as vector fields explicitly depending on *n* and *t*. The space R^n in which *x* evolves is called a state space. A traffic time series can also be considered as a sequence of observations $\{S_t = s(x_n)\}$ performed with some measurement function $s(\cdot)$, wherein the one-dimensional traffic time series embedded into multiple dimensions reconstructed space is denoted as $S_t = (s_t, s_{t+\tau}, s_{t+2\tau} \ldots, s_{t+(m-1)\tau})$, $t = 1,2,\ldots,N$ where the parameter τ is called time delay and the integer *m* is called embedding dimension. In space, geometric objects with non-integer dimensions are called **fractals**, whereas a geometric object, which characterizes the long-term behavior of a system in the phase space, is called an attractor. Correlation dimension is a measure of the extent to which the presence of a data point affects the position of the other point lying on the attractor.

Accordingly, time delay for any traffic series can be conceptualized with Figure 3-1. In the top panel, the points of square, diamond and circle represent the value of series at time *t*; $t + \tau$ and $t + 2\tau$ respectively; in contrast to the low panel, one can find their corresponding places in the multidimensional space through reconstruction. If the time delay is different, the portrait in multidimensional space will change immediately. Thus, it is important to decide a proper time delay when one map a time series into a multidimensional space, that is the quality of reconstructed portraits for a traffic time series depended on the value of τ. For small τ, s_t and $s_{t+\tau}$ are very close to each other, whereas for a large value of τ, s_t and $s_{t+\tau}$ can be completely independent of each other, and any connection between them is random. Consequently, we need a criterion for an intermediate choice that is large enough so that s_t and $s_{t+\tau}$ are independent but not completely independent in a statistical sense.

There are two alternatives to estimate the time delay required by the embedding theorem from an observed traffic time series. The first one is calculating the linear autocorrelation function (ACF) of the data points and selecting τ as the time of its

first zero-crossing. The rationale behind this approach is that the time when ACF reaches a zero value marks the point beyond which the $s_{t+\tau}$ sample is completely de-correlated from s_t. However, this approach is suitable only for linear time series. The second one involves the calculation of data from a nonlinear autocorrelation function called average mutual information (AMI), which is proposed by Fraser and Swinney (1986) and can be expressed as θ_{ij} in Eq. (3.1):

$$\theta_{ij} = -\sum_{i,j} p_{ij}(\tau) \ln \frac{p_{ij}(\tau)}{p_i p_j} \tag{3.1}$$

where for some partition on the real numbers, p_{ij} is the probability of finding a time series value in the *i*-th interval, and $p_{ij}(\tau)$ is the joint probability that an observation falls into the *i*-th interval and an observation time τ later falls into the *j*-th interval. In theory, this expression has no systematic dependence on the size of the partition elements and can be quite easily computed. There exist good arguments that if the time delayed mutual information exhibits a marked minimum at a certain value of τ, then this is a good candidate for a reasonable time delay. In practice, one may not be interested in the absolute values of mutual information but rather in its first minimum, and thus the first minimum of AMI usually signal a proper time delay for the time series. Compared with ACF that only measures linear correlations, AMI also takes into account nonlinear correlations, therefore this paper will use the AMI approach by Fraser and Swinney (1986) to determine the proper time delay for traffic time series.

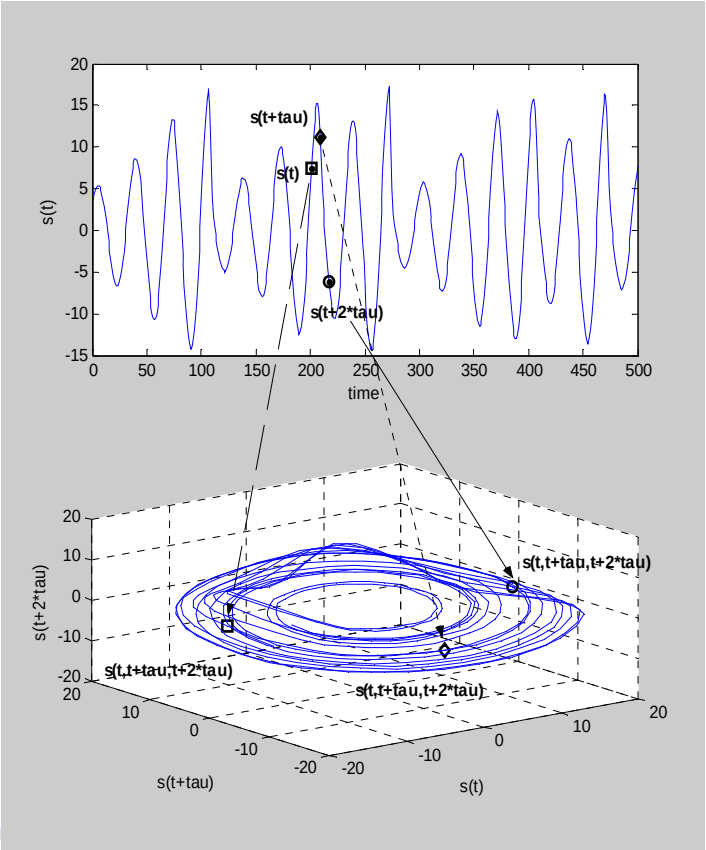

Figure 3-1 The concept of traffic series time delay in 1-D and 3-D spaces

3.1.2 Determination of Embedding Dimension

The purpose of the reconstructed state spaces is to find a Euclidean space that is large enough so that the set of points describing the attractor can be unfolded without ambiguity. Kennel *et al*. (1992) proposed a false nearest neighbor (FNN) algorithm to determine the minimal sufficient embedding dimension *m*. The FNN algorithm is to search for point s_i in the time series and to look for its nearest neighbor s_j in an *m*-dimensional space, followed by calculating the distance $\|s_i - s_j\|$ and iterating both the points, and then computing the ratio $\varepsilon_{i,j}$ of Eq. (3.2) in an *m*-dimensional space.

$$\varepsilon_{i,j} = \frac{\left|s_i^{m+1} - s_j^{m+1}\right|}{\left\|s_i^m - s_j^m\right\|}, \ldots i, j = 1,2,\ldots,N \tag{3.2}$$

If the ratio $\varepsilon_{i,j}$ exceeds a given heuristic threshold ε_t, this point s_i is marked as having a false nearest neighbor, wherein in general, the value of the threshold ε_t is

recommended as lying between 10 to 15 (Nayfeh, 1995; Abarbanel, 1996). The criterion that the embedding dimension is high enough is that the fraction of points for which $\varepsilon_{i,j} > \varepsilon_t$ is zero, or at least sufficiently small.

Figure 3-2 illustrates an example depicting the FNN algorithm. In the top panel, the square point is the nearest point to the circle point within 500 points in one-dimension, wherein their Euclidean's distance is 0.02. A simple method is used to project the square point and the circle point to the y-axis, where after it is apparent that the distance between the two circles is very close. However, the value becomes 10.01 if one calculates the Euclidean distance in a two-dimensional plane (middle panel) according to proper time delay. Because the ratio of 10.01 divided by 0.02 is greater than the threshold, ε_t, thus, the square point is a false neighbor of the circle point. If one further calculates the ratio of distances between a two-dimensional plane and a three-dimensional space (low panel), then it demonstrates that the ratio dropped drastically because the Euclidean distance is 10.4 in three-dimensional space. Since the ratio is no longer greater than the threshold, ε_t, it suggests that an embedding dimension of $m = 2$ is sufficient. After we examine every point in this time series according to the above algorithm, the proper embedding dimension can be decided. However, if there are a multitude of identical values in a realistic time series, then FNN algorithm probably cannot work precisely. In that case, the embedding dimension would be determined approximately by correlation dimension instead.

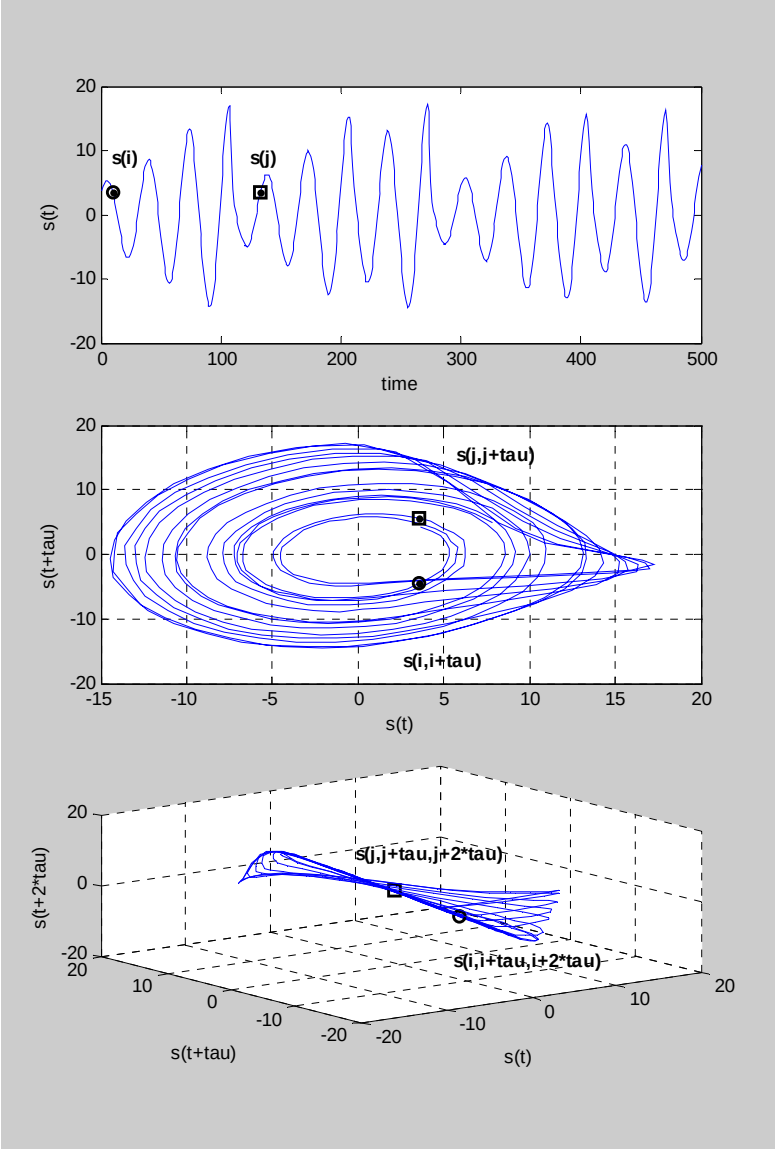

Figure 3-2 The concept of measuring the distance of traffic time series by FNN algorithm

3.2 Motions of Traffic State Trajectories

Once the appropriate time delay and embedding dimension for a traffic series are determined, one can map the one-dimensional traffic series into *m*-dimensional reconstructed spaces. After that, one is interested in knowing how traffic state trajectories moved in this space over time. Note that traffic state trajectories in this paper refer to traffic variables (flow, time-mean-speed, percent occupancy), which were tracked and recorded in reconstructed state spaces over time rather than vehicles changing their position with time evolution. This paper makes use of the Lyapunov exponent to measure the rate of expansion or contraction of traffic state trajectories and is described hereinafter.

3.2.1 Estimation of the Largest Lyapunov Exponent

If we take two points s_i and s_j in the reconstructed space, and indicate the distance between them as $|s_i - s_j| = \delta_0$, then, after a time span Δt, it is expected that the new distance δ will be equal to $\delta = \delta_0 e^{\lambda \Delta t}$, where λ is called the Lyapunov exponent. For an *m*-dimensional space, the rate of expansion or contraction of trajectories is described for each direction by one Lyapunov exponent, resulting in *m* different λs. Of the *m* different λs, the largest value λ_0 (largest Lyapunov exponent) is of main interest since it can be easily calculated even without the explicit construction of a model for the traffic time series. If λ_0 is negative, the traffic state trajectories will converge to a fixed point. If λ_0 is zero, the traffic state trajectories are periodic motions. If λ_0 is positive, the traffic state trajectories may exhibit other motions such as an aperiodically deterministic chaos or stochastic randomness (Hilborn, 2000; Kantz and Schreiber, 2004).

In theory, the largest Lyapunov exponent can be used to identify the traffic state trajectories moving in the reconstructed state spaces. However, in practice, there will be fluctuations in the calculation of the largest Lyapunov exponent due to noisy traffic data. For instance, in a true state space, distances do not always grow everywhere on the attractor at the same rate, and in fact they may even shrink locally. To minimize the influence of noisy field traffic data on calculating the largest Lyapunov exponent, one can employ an appropriate averaging statistic when computing the average exponential growth of distance. To realize this, the following procedures are proposed: (1) Choosing a point s_i of the traffic time series in the reconstructed space and select all neighbors with a distance smaller than *r*. (2) Computing the average over the distance of all neighbors to the reference part of the trajectories as a function of the relative time. The logarithm of the average distance at time *t* is some effective expansion rate over the time span Δt (plus the logarithm of the initial distance) containing all the deterministic fluctuations due to projection and dynamics. (3)

Repeating this for many values of *i*, thereby averaging out the fluctuations of the effective expansion rates. (Kantz and Schreiber, 2004)

The above procedures can be represented as Eq. (3.3), wherein the curves of stretching factor $\zeta(\Delta t)$ exhibit a robust linear increase, slope of which is an estimate of the largest Lyapunov exponent λ_0 per time step.

$$\zeta(\Delta t) = \frac{1}{N}\sum_{i=1}^{N} \ln\left(\frac{1}{\left|\Psi(s_i)\right|} \sum_{s_j \in \Psi(s_i)} \left| s_{i+\Delta t} - s_{j+\Delta t} \right| \right), i, j = 1,2,...,N \tag{3.3}$$

where $\Psi(s_i)$ is the neighborhood of s_i with diameter *r*.

Figure 3-3 demonstrates an example of Lorenz time series[1], which is known as a deterministic (chaotic) time series in estimating the largest Lyapunov exponent according to the above proposed procedures. In this figure, we observe that the dotted line, i.e., slope of bundle curves (each curve represents *m*-th dimension) is positive and the largest Lyapunov exponent is $\lambda_0 = 0.044 \pm 0.002$. Note that the curves of stretching factor in the left panel (Figure 3-3(a)) are rather steeper than those in the right panel (Figure 3-3(b)) because the distance *r* = 0.199 is smaller than *r* = 0.353. Consequently, choosing a proper distance is also essential.

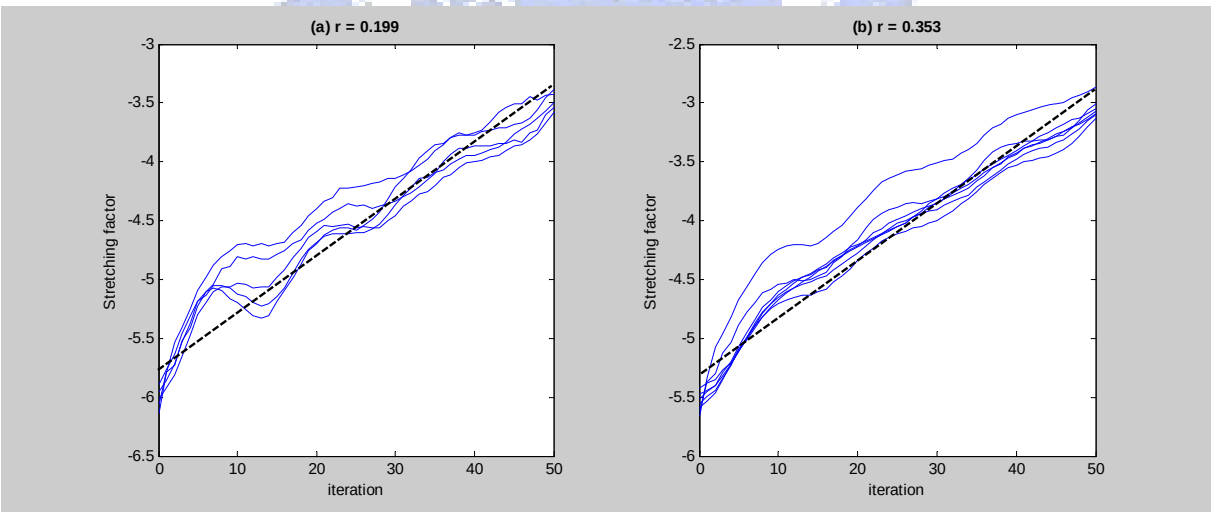

Figure 3-3 An example of estimating the largest Lyapunov exponent

[1] *dX/dt=10(Y-X); dY/dt=28X-Y-XZ; dZ/dt=XY-8Z/3*

3.2.2 Estimation of the Correlation Dimension

Correlation dimension is a measure of the extent to which the presence of a data point affects the position of other points lying on the attractor. Among the number of methods available for distinguishing between chaotic motions and stochastic motions of time-series trajectories, the correlation dimension is perhaps the most fundamental one (Shang *et al*., 2005). A seemingly irregular phenomenon arising from any deterministic time-series dynamics will have a limited number of degrees of freedom equal to the smallest number of first-order differential equations that capture the most important features of the time series. Thus, when one reconstructs spaces with increasing dimensions for an infinite data set, a point will be reached where the dimensions are equal to the number of degrees of freedom, and beyond which increasing the dimension of the representation will not have any significant effect on the correlation dimension. Under this circumstance, we view the correlation dimension of the attractor as saturated. If the attractor dimension is saturated in low-dimensions (normally, five-dimensions), then it signalizes that the time-series trajectories exhibit aperiodic motions, which is essentially deterministic chaos. In contrast, if an attractor dimension cannot reach saturation or is saturated in very high-dimensions, then the trajectories of that time series could be stochastic.

Grassberger and Procaccia (1983) showed that correlation dimension d can be evaluated by using the correlation integral $\mu(r)$, which is the probability that a pair of points (s_i, s_j) chosen randomly in the reconstructed space are separated by a distance less than r. If N is the number of points in the reconstructed vector time series S_t, the correlation integral can be approximated by the following sum in Eq. (3.4):

$$\mu_N(m,r) = \frac{2}{N(N-1)} \sum_{j=1}^{N} \sum_{i=j+1}^{N} \Theta\left(r - \left|s_i - s_j\right|\right) \tag{3.4}$$

where Θ denotes the Heaviside step function and $\left|s_i - s_j\right|$ stands for the distance between points s_i and s_j; $\Theta\left(r - \left|s_i - s_j\right|\right)=0$, if $r - \left|s_i - s_j\right| \le 0$ and $\Theta\left(r - \left|s_i - s_j\right|\right)=1$, for $r - \left|s_i - s_j\right| > 0$. In the limit of an infinite amount of data ($N \to \infty$) and for small r, we expect μ_N to scale like a power law:

$$\mu(m,r) \propto \alpha r^d \tag{3.5}$$

where α is a constant and d is the correlation dimension or the slope of the $\ln \mu(r)$ versus $\ln r$ plot given by

$$d = \lim_{r \to 0} \lim_{N \to \infty} \frac{\partial \ln \mu_N(m,r)}{\partial \ln r} \tag{3.6}$$

To observe whether a time series exhibits deterministic features, the correlation dimension (or local slope) values are plotted against the corresponding embedding dimension values. If the value of the correlation dimension is finite, low and non-integer, then the system is possibly exhibiting as low-dimensional chaos. The saturation value of the correlation dimension is defined as the correlation dimension of the attractor, or so-called attractor dimension. In general, an embedding dimension (m) is no less than double the attractor dimension ($2d$) plus one. In contrast, if the correlation dimension increases without bound with increase in the embedding dimension, then the system is considered as stochastic.

Figure 3-4 demonstrates an example of Lorenz time series by calculating its correlation dimension. The left panel (Figure 3-4(a)) is a plot of correlation integral $\mu_N(m,r)$ versus distance r on logarithmic scale; whereas the right panel (Figure 3-4(b)) is its local slope. In the right panel, the increasing curve is flat when embedding dimension is about equal to 4, suggesting that the Lorenz time series is deterministic chaos with attractor dimension (saturated value) nearly equaling 2.01.

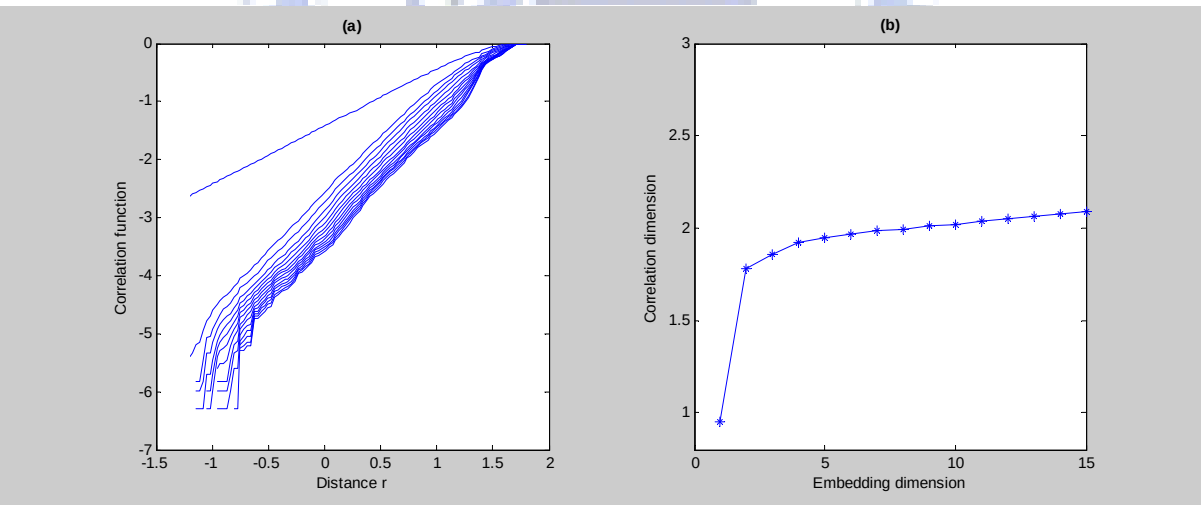

Figure 3-4 An example of estimating the correlation dimension of attractor

3.3 Linear and Simple Nonlinear Predicting Algorithms

3.3.1 Linear Prediction

After understanding algorithms of reconstructing the state spaces as well as motions of the state trajectories, let us start out from the fundamentals of linear and nonlinear predicting algorithms. Given a sequence of observations S_t, t=1,…,N, we intend to predict the outcome of the following measurements, S_{t+1}. One often wants to find the prediction $\hat{S}_{t+1}$, which minimizes the expectation value of the squared prediction error $\left\langle \left(\hat{S}_{t+1} - S_{t+1}\right)^2 \right\rangle$. When we assume the time series is stationary, we can estimate this expectation value by its average over the available measured values. If we further restrict the minimization to linear time-series models which incorporate the k last measurements, we can express this by

$$\hat{S}_{t+1} = \sum_{j=1}^{k} a_j S_{t-k+j} \tag{3.7}$$

and minimize

$$\sum_{t=k}^{N-1} \left(\hat{S}_{t+1} - S_{t+1}\right)^2 \tag{3.8}$$

with respect to the parameters a_j, j=1,…,k. Here we have assumed that the mean of the time series has already been subtracted from the measurements. By requiring that the derivatives with respect to all the a_js to be zero, we obtain the solution by solving the linear set of equations

$$\sum_{j=1}^{k} C_{ij} a_j = \sum_{t=k}^{N-1} S_{t+1} S_{t-k+i}, \qquad i = 1,...,k \tag{3.9}$$

Here C_{ij} is the $k \times k$ auto-covariance matrix

$$C_{ij} = \sum_{t=k}^{N-1} S_{t-k+i} S_{t-k+j} \tag{3.10}$$

Note that the linear relation, Eq. (3.7), is justified for harmonic as well as for linear stochastic processes. The most popular stochastic models for linear time series, autoregressive (AR) models and moving average (MA) models, either consisted of linear filters acting on a series of independent noise inputs as expressed in Eq. (3.11) or on past values of the signal itself as expressed in Eq. (3.12), while Eq. (3.13) represents the ARMA model. (Chatfield, 1996)

$$x_n = \sum_{j=0}^{M_{MA}} b_j \varphi_{n-j} \tag{3.11}$$

$$x_n = \sum_{j=1}^{M_{AR}} a_j x_{n-j} + \varphi_n \tag{3.12}$$

$$x_n = a_0 + \sum_{i=1}^{M_{AR}} a_i x_{n-i} + \sum_{j=0}^{M_{MA}} b_j \varphi_{n-j} \tag{3.13}$$

where x_n is a Gaussian random variable

a_j, b_j are parameters

M_{MA}, M_{AR} are the order of MA model and AR model

φ_n is white Gaussian noise

3.3.2 Simple Nonlinear Prediction

Nevertheless, most time series of traffic dynamics exhibited in the real world are nonlinear and more complex than the time series formulated by linear models. A local linear method in multidimensional spaces was employed to predict nonlinear time series if the data base was large and the noise level was small (Kantz and Schreiber, 2004). The original concept relevant to nonlinear prediction was used in tests for determinism by Kennel and Isabelle (1992). The resulting method is very simple. Recall the time-series expression in multidimensional spaces: $S_t = (s_t, s_{t+\tau}, ..., s_{t+(m-1)\tau})$, t=1,2,…, N, and for all measurements S_1, …,S_t, the corresponding delay vectors $(s_1, s_{1+\tau} ..., s_{1+(m-1)\tau}), \ldots, (s_t, s_{t+\tau} ..., s_{t+(m-1)\tau})$ in multidimensional spaces can be found. In order to predict a future measurement S_{t+T}, one can find the embedding vector s_{t0} closest to s_t and use s_{t0+T} as a predictor. However, owing to multiple dimensions, we have to choose the parameter ε of the order of the resolution of the measurements and form a neighborhood $\Psi_\varepsilon(s_t)$ of radius ε around the point s_t. For all points $s_{t0} \in \Psi_\varepsilon(s_t)$, i.e., all points closer than ε to s_t, look up the individual predictors s_{t0+T}. The prediction is then the average of all these individual predictors.

$$\hat{S}_{t+T} = \frac{1}{\left|\Psi_{\varepsilon}(s_t)\right|} \sum_{s_{t0} \in \Psi_{\varepsilon}(s_t)} s_{t0+T} \tag{3.14}$$

Here $\left|\Psi_{\varepsilon}(s_t)\right|$ denotes the number of elements of the neighborhood $\Psi_{\varepsilon}(s_t)$. If no neighbors closer than ε can be found, one might just increase the value of ε until some neighbors are found.

The concept of multidimensional spaces and simple nonlinear prediction for any traffic series is demonstrated in Figure 3-5. In the left top panel (a), the points of square, diamond and circle respectively represent the values of the series at time *t*; $t+\tau$ and $t+2\tau$; in contrast, in the right top panel (b), one can find their corresponding trajectories in the multidimensional spaces through reconstruction. When a proper time delay is determined, we can map the traffic series from one dimension into three dimensional spaces. On the other hand, in the left bottom panel (c), if we choose one small section part of the state trajectories in the multidimensional spaces and enlarge it as right bottom panel (d) to observe the trajectory motions, it indicates that the trajectories within radius ε, i.e., in the black circle, move towards the same direction and one can predict the square point at time (*t*+*T*) by averaging the four closed points marked start at time (*t*+*T*). That is, in this case we assume that the underlying relationship between the current observation and its nearest neighbors remains stationary with short-term time evolution, the points marked start already known their values are the neighbors of the current observation (the square point at time *t*) and then a prediction (the square point at time *t*+*T*) can be made by using the relationship and tracking the movements of the nearest neighbors.

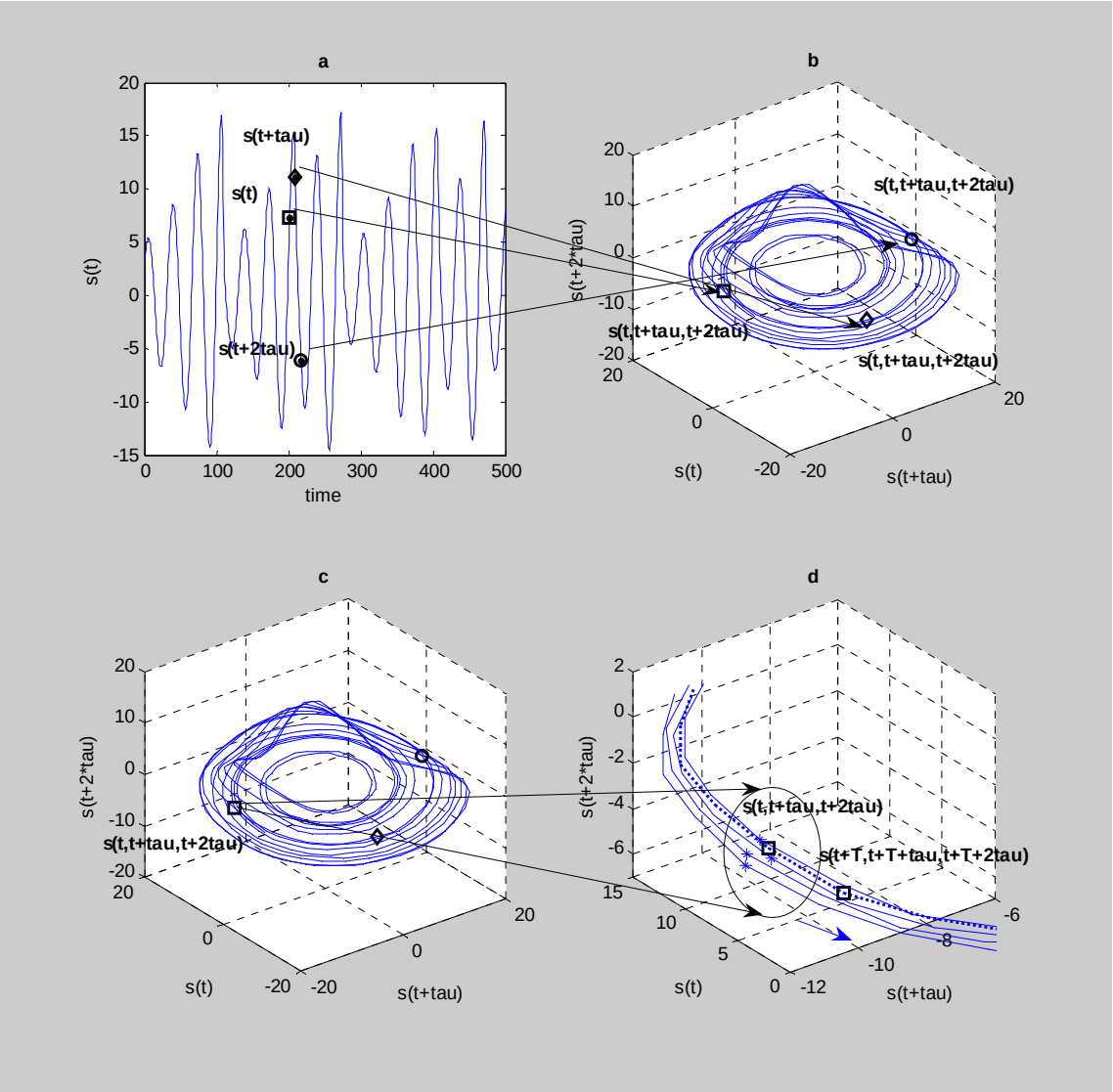

Figure 3-5 The concept of prediction for traffic series in multidimensional spaces

3.4 Rationales for RBFNN and RTRL

3.4.1 RBFNN Algorithms

Likewise, a traffic series can be considered as a sequence of observations $\{S_t = s(x_n)\}$ performed with some measurement function $s(\cdot)$, wherein an one-dimensional series embedded into multiple dimensional spaces can be transformed into $S_t = (s_{t-(m-1)\tau}, s_{t-(m-2)\tau}, ..., s_{t-\tau}, s_t),\ t = 1,2,..., N$ [2] (Lan *et al.*, 2007d). Accordingly, if input is a q-dimensional series $U_t = (u_{t-(q-1)\tau}, u_{t-(q-2)\tau}, ..., u_{t-\tau}, u_t),\ t = 1,2,..., N$ with

[2] Another type of identical expression is $S_t = (s_t, s_{t+\tau}, ..., s_{t+(m-1)\tau})$, t=1,2,…, N

corresponding output a *k*-dimensional series $Y_t = (y_{t-(k-1)\tau}, y_{t-(k-2)\tau}, ..., y_{t-\tau}, y_t),\ t = 1,2,...,N$, then Y_t can be generated by some unknown nonlinear multidimensional series of the form:

$$Y_{t+1} = f(y_{t-(k-1)\tau}, y_{t-(k-2)\tau}, ..., y_t, u_{t-(q-1)\tau}, u_{t-(q-2)\tau}, ..., u_t),\ t = 1,2,...,N \tag{3.15}$$

where $f(\cdot)$ is an unknown nonlinear function.

With using the above as a basis, a radial basis function neural network (RBFNN) can be constructed, wherein the multi-dimensional traffic series U_t is used as input to the network, and Y_t will be the corresponding output series. Formulation of network output data is accomplished through a hidden layer consisting of *M* neurons. Each of the *M* neurons in the hidden layer applies an activation function which is a function of the Euclidean distance between the input and a multiple dimensional prototype vector. Each hidden neuron contains its own prototype vector as a parameter. The output of each hidden neuron is then weighted and passed to an output layer. The outputs of the network consist of sums of the weighted hidden layer neurons. That is, formulation of output response to an input multidimensional time series is postulated as a linear combination through the hidden layer responses, and can be expressed as below:

$$y_t = w_0 + \sum_{j}^{M} w_j \cdot \phi_j\left(\left\|U_t - c_j\right\|\right)\ ,\ j = 1,2,...,M \tag{3.16}$$

where $\phi(\cdot)$ is a radial basis function (RBF) -- a response of the *j*th hidden neuron to an input multidimensional time series U_t, w_j is a weight of the *j*th hidden neuron for defining the contribution of the hidden neuron to a particular output, and w_0 is a bias term. The RBF hidden neuron responses z_j are given by

$$z_j = \phi_j\left(\left\|U_t - c_j\right\|\right) = \exp\left(-\frac{\left\|U_t - c_j\right\|}{2\sigma_j^2}\right)\ ,\ j = 1,2,...,M \tag{3.17}$$

where c_j is the center of the *j*th Gaussian function and σ_j is the width of the Gaussian.

As input traffic series are presented to the RBFNN, the network iteratively creates new center neurons to reduce its performance error (i.e. Euclidean distance). Allocation of the new hidden neurons is determined by orthogonal least squares (OLS), which employs a Gram-Schmidt algorithm and Cholesky decomposition (Chang and Chang, 2005) to create new center neurons under a given threshold. In other words, the widths and center locations of the existing hidden neurons can be adjusted during the learning process. As to the method of adjusting weight w_j, Broomhead and Lowe (1988) proposed a recursive least mean squares (LMS) algorithm to obtain an acceptable error as follows. If $d(p)$ is the pth desired value, then $y(p)$ is the pth network output. The $e(p)$ is the pth difference between the desired value and the network output. When $e(p)$ equals zero, the pth network output is thereby able to fit the pth desired value entirely. As such, the total values of $e(p)$ in network can be a minimum:

$$E = \sum_{p=1}^{N} [e(p)]^2 = \sum_{p=1}^{N} (d(p) - y(p))^2 \tag{3.18}$$

When E has a minimum value, then the gradient vector $\frac{\partial E(p)}{\partial w_j}$ is equal to zero. Substituting $\frac{\partial E(p)}{\partial w_j} = 0$ into Eq. (3.18) will obtain $W = (\phi^T \phi)^{-1} \phi^T d(p)$. The parameters w_j are iteratively updated until the learning processes stably converge. In the algorithms, because the parameters c_j, σ_j in the hidden layer have been previously determined, thus the recursive adjustment of weight w_j is capable of significantly reducing learning time when compared to error back propagation. The advantage of effectively reducing learning time is an important factor for choosing the RBF algorithm as the basis for our prediction model because in addition to capturing the traffic trend, we are also predicting the variance of traffic dynamics in the short run. If a prediction model is slow to respond to changing variables, the utility of the prediction model will be greatly restricted. Figure 3-6 depicts the typical architecture of a RBF neural network in the context of predicting traffic dynamics, collected from loop detectors.

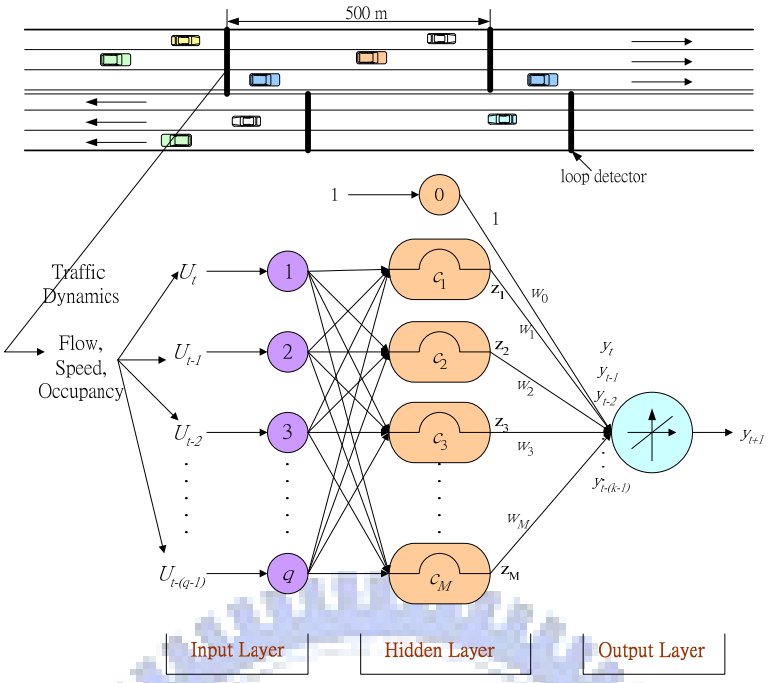

Figure 3-6 A typical RBF network and traffic dynamics from loop detectors

3.4.2 RTRL Algorithms

In contrast to the static learning algorithms, such as RBFNN, the real-time recurrent neural network (RTRNN) can be considered as a BPN with feedback loops connecting to every hidden node, which exhibits dynamical learning algorithms. The main difference compared with BPN is that the outputs are used as part of the next sequentially timed input, i.e., the output at time (t+1) is based upon the current input and previous outputs. Furthermore, the RTRNN consists of three layers: a concatenated input-output layer with (m+n) nodes, a processing (hidden) layer with n nodes and an output layer with k outputs. Let $y(t)$ denote the n-tuple of outputs of the n-processing neurons at time t and $x(t)$ the m-tuple of external inputs to the network at time t. We concatenate $y(t)$ and $x(t)$ to form the (m+n)-tuple $u(t)$, with B denoting the set of indices for the processing neurons and A the set of indices for the external inputs, so that

$$u_i(t) = \begin{cases} x_i(t) & if \quad i \in A \\ y_i(t) & if \quad i \in B \end{cases} \tag{3.19}$$

By adopting the indexing convention just described, a hidden network net_j at time t is obtained by summing up the weighted inputs with a weight matrix w. After the network is transferred by an activation function $f(\ )$, the output $y_j(t)$ is used as a

feedback input in the next time step and summing up the weighted feedback inputs with a weight matrix v is repeated. Likewise, after the transformation, the network output, $z_k(t)$, is passed to an output layer. The above said procedure can be expressed as the following equations:

$$net_j(t) = \sum_{j \in A \cup B} w_{ji}(t-1)u_i(t-1) \tag{3.20}$$

$$y_j(t) = f(net_j(t)) \tag{3.21}$$

$$net_k(t) = \sum v_{kj}(t)y_j(t) \tag{3.22}$$

$$z_k(t) = f(net_k(t)) \tag{3.23}$$

Concerning the algorithms for computing the weight matrix w, v as well as the error function, we denote $d_k(t)$ as the desired value of the k-th neuron at time t and define $e_k(t)$ to be the difference between the desired value and the network output at time t, i.e.,

$$e_k(t) = d_k(t) - z_k(t) \tag{3.24}$$

Then we define the error function, $E(t)$:

$$E(t) = \frac{1}{2}\sum_{k=1}^{K} e_k^2(t) \tag{3.25}$$

According to the steepest descent method, the amount of adjusted weight for $v_{kj}(t)$ and for $w_{mn}(t)$:

$$\Delta v_{kj}(t) = -\eta_1 \frac{\partial E(t)}{\partial v_{kj}(t)} \tag{3.26}$$

$$\Delta w_{mn}(t-1) = -\eta_2 \frac{\partial E(t)}{\partial w_{mn}(t-1)} \tag{3.27}$$

where η_1, η_2 are the learning rate,

And

$$\frac{\partial E(t)}{\partial v_{kj}(t)} = -e_k(t) f'(net_k(t)) y_j(t) \tag{3.28}$$

$$\frac{\partial E(t)}{\partial w_{mn}(t-1)} = \left[\sum_{k=1}^{K} -e_k(t) f'(net_k(t)) v_{kj}(t)\right] \frac{\partial y_j(t)}{\partial w_{mn}(t-1)} \tag{3.29}$$

According to error back propagation algorithms (Chang and Chang, 2005), a new variable with three dimension can be defined as $\pi_{mn}^{j}(t)$ which is called a dynamic

variable

$$\pi_{mn}^{j}(t) = \frac{\partial y_j(t)}{\partial w_{mn}(t)} \qquad for \quad all \quad j \in B, \quad m \in B, \quad n \in A \cup B \tag{3.30}$$

Accordingly

$$\Delta w_{mn}(t-1) = \eta_2 \left[\sum e_k(t) f'(net_k(t)) v_{kj}(t) \right] \pi_{mn}^{j}(t) \tag{3.31}$$

In brief, the steps involved in RTRL algorithms can be summarized as follows and depicted in Figure 3-7:

Step 1. Randomly initialize the weight $w_{mn}(0)$ and $v_{kj}(0)$.

Step 2. Input the $x_i(t)$ into the RTRL network and compute the $y_j(t)$, $z_k(t)$, then use $y_j(t+\tau)$ as feedback to the concatenated input-output layer together with $x_j(t+\tau)$ as new inputs.

Step 3. Compute the difference between desired value $d_k(t)$ and network output $z_k(t)$.

Step 4. Update $\Delta v_{kj}(t)$ according to Eq. (3.26).

Step 5. Update $\Delta w_{mn}(t-1)$ according to Eq. (3.27).

Step 6. Increment t by 1 and go to step 2.

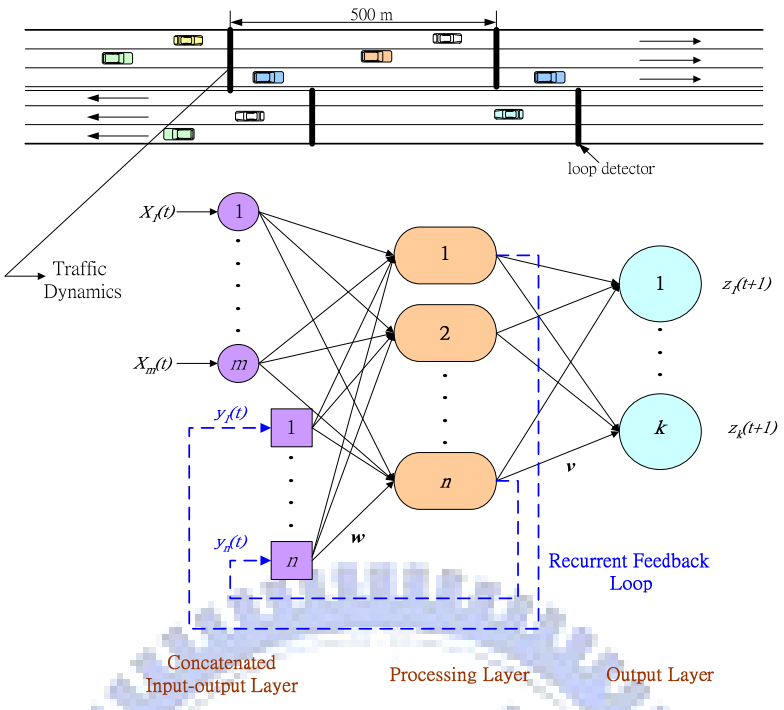

Figure 3-7 A typical RTRL network and traffic dynamics from loop detectors

CHAPTER 4 PRELIMINARY TESTING

In this study, traffic time series were directly extracted from dual-loop detectors installed at a given 3~4-lane mainline segment of the northbound Sun Yat-Sen Freeway of Taiwan, located in the northern area of Taipei County. Figure 4-1 is the sites of detector stations. In order to discover the features of traffic time series in different situations, we divided the collected raw data into three groups. Data in the first group was counted aggregately by average flow, time-mean-speed and percent occupancy per 5-minute per approach. The data was extracted from station N27.9 near station 433, collected from traffic inbounds to Taipei City. Data in the second group contained flow, time-mean-speed and percent occupancy per 20-second per lane recorded in median lane. The data was collected from stations 402, 404, 421 and 433. Stations 402 and 404 are outbound from Taipei City, whereas stations 421 and 433 are inbound to the City. Data in the third group was a processed data set, i.e., we combined ten-workday time series, which every workday time series was come from the second group data. Then, we divided the combined time series into four subgroups according to four time-of-day intervals, i.e., 00:00-03:00, 06:00-09:00, 12:00-15:00 and 18:00-21:00. The purpose of processing the traffic time series was to compare different features of traffic series between four time-of-day intervals. Similarly, in order to examine the features between traffic time series with various time scales, in the second group, we further accumulated the 20-second traffic series into longer-term data, including 1-minute, 3-minute and 9-minute series, of which, flows were directly summed from each 20-second flow, speeds were the weighted average of each 20-second time-mean-speed multiplied by its corresponding flow and occupancies were the arithmetic mean of each 20-second occupancy. Likewise, in the first group, the 5-minute approach data sets were accumulated into 15-minute, 30-minute and one hour time series via the above method. The above detailed calculations and related statistics were illustrated as the following Section 4.1.

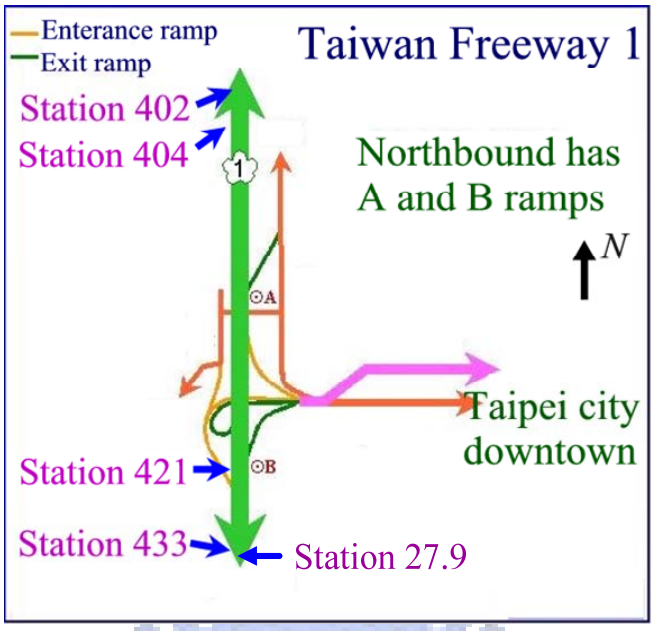

Figure 4-1 Sites of detector stations 402, 404, 421, 433 and 27.9

4.1 Calculation and Statistics of Data

As above mention, our empirical data is extracted directly from stationary sensors. The calculation and acquisition of data from stationary sensors are described as follows. When a vehicle enters the detection zone, the sensor is activated and remains so until the vehicle leaves the detection zone. We consider "0" and "1" signal to individually represent the absence of a vehicle and the presence of a vehicle. Figure 4-2(a) is the signals output from a detector during an observing time T, and Figure 4-2(b) is the plot of vehicles passing over a paired detector A and B. The on-time referred to as the vehicle occupancy time requires the i^{th} vehicle to travel a distance equivalent to its length plus the length of the detection zone. The off-time between vehicles is the time gap. Apparently, the i^{th} vehicle occupancy time and percent occupancy can be easily obtained by

$$t_{occi} = t_{Air} - t_{Aif} \quad \text{or} \quad t_{occi} = t_{Bir} - t_{Bif} \tag{4.1}$$

$$\%\ \ occ = \frac{\sum_{i=1}^{N} t_{occi}}{T} \times 100 \tag{4.2}$$

$$N = \sum_{t=0}^{T} i_{signal1} \tag{4.3}$$

where t_{occi} : the individual occupancy time (seconds)

t_{if} : the instant time that i^{th} vehicle is detected (seconds)

t_{ir} : the instant time that i^{th} vehicle is off detected (seconds)

$\%\ occ$: percent occupancy

N : number of vehicles detected in time period T

T : selected time period (seconds)

Since vehicle occupancy time is a function of vehicle speed, vehicle length and distance between two detectors as shown in the following equations:

$$\dot{x}_i = \frac{D_A + D}{t_{Bif} - t_{Aif}} \quad \text{or} \quad \dot{x}_i = \frac{D_B + D}{t_{Bir} - t_{Air}} \tag{4.4}$$

where $\dot{x}_i$: speed for vehicle i (meter per second)

D_A, D_B : length of detector A and detector B (meter)

D : distance between detector A and detector B (meter)

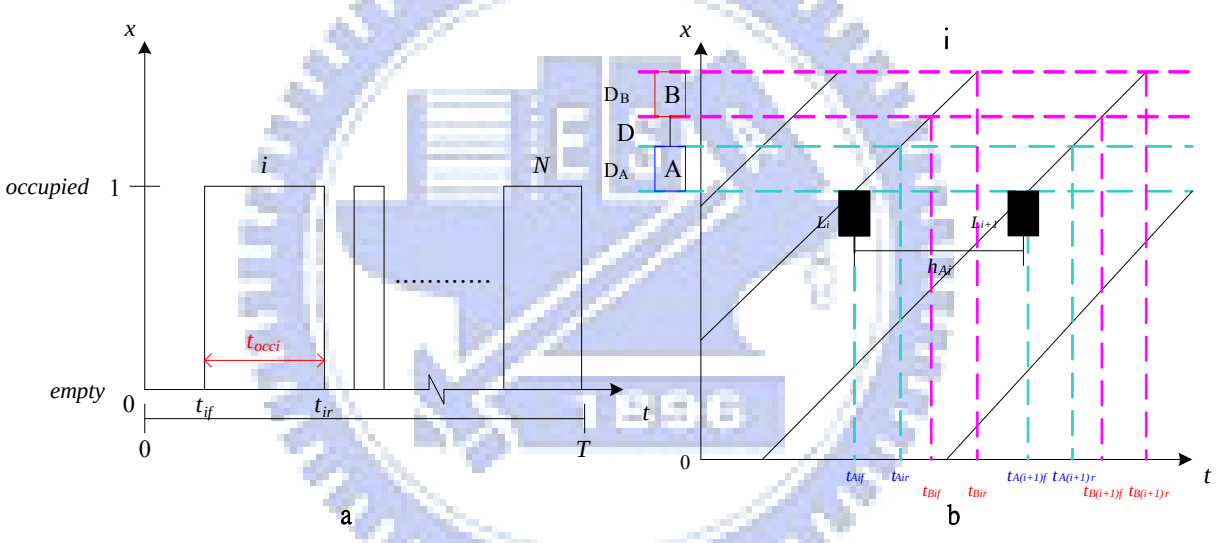

Figure 4-2 Output signals from a detector and vehicles passing over two detectors

Because the traffic raw data are measured in 20-second, one further accumulates them into 1-minute, 3-minute and 9-minute counts which can be calculated in the following equations:

$$q^T = \sum_{i=1}^{T} q_i \tag{4.5}$$

$$u^T = \frac{\sum_{i=1}^{T} (u_i * q_i)}{\sum_{i=1}^{T} q_i} \tag{4.6}$$

$$\%occ^T = \frac{\sum_{i=1}^{T} \%occ_i}{T} \tag{4.7}$$

where q_i : i^{th} flow rate (vehicles per 20-second per lane)

u_i : i^{th} time-mean-speed (kilometer per hour per lane)

$\%occ_i$: i^{th} percent occupancy time per lane

q^T : accumulated flow rate (vehicles per 20T-second per lane)

u^T : weighted time-mean-speed (kilometer per hour per lane)

$\%occ^T$: percent occupancy per lane for 20T-second time intervals

T: constant

Note: If T equals to 3, q^T means 60-second (i.e. 1-minute) volume; if T equals to 9, q^T means 180-second (i.e. 3-minute) volume, and so on…

If one would like to gather the lane quantities into approach quantities, the calculation of approach for traffic series are counted in following equations.

$$Q^T = \sum_{j}^{n} q_j^T \tag{4.8}$$

$$U^T = \frac{\sum_{j=1}^{n} (u_j^T * q_j^T)}{\sum_{j=1}^{n} q_j^T} \tag{4.9}$$

$$\%OCC^T = \frac{\sum_{j=1}^{n} \%occ_j^T}{n} \tag{4.10}$$

where q_j^T : j^{th} lane accumulated flow rate (vehicles per 20T-second)

u_j^T : j^{th} lane weighted time-mean-speed (kilometer per hour)

$\%occ_j^T$: j^{th} lane percent occupancy for 20T-second time intervals

Q^T : approach flow rate (vehicles per 20T-second per approach)

U^T : approach weighted time-mean-speed (kilometer per hour per approach)

$\%OCC^T$: approach percent occupancy for 20T-second time intervals

n: number of lanes

From our selected traffic time series, there are some invariant features noteworthy. For instance, the outbound flow rates at stations 402 and 404 in the morning peak hours (06:00-09:00) are relatively lower than the evening peak hours (18:00-21:00); while

the inbound flow rates at stations 421 and 433 in the morning peak hours are approximately equal to evening peak hours. This feature concurs with the characteristics of working trips that most suburb commuters drive into Taipei City in the morning peak hours and leave office in the evening peak hours, i.e., the temporal flow patterns at different detection stations are influenced by direction. Similarly, the speed and occupancy patterns are also affected by direction. In addition, we notice from Table 4-1(a) and (b) that the degrees of variation of traffic series depend on times of day in general. For instance, early hours (00:00-03:00) has the largest coefficient of variation (CV) while the evening peak period (18:00-21:00) has the smallest CV. The degrees of variation also decline with time scale, i.e., traffic series measured in 20-second has the largest CV, followed by 1-minute, 3-minute, and then 9-minute. Moreover, the CVs of flow and occupancy are larger than the CV of speed. Perhaps the speed limit regulation has reduced its degree of variation.

On the other hand, the mean and CV of successive traffic series at station N27.9 is listed in Table 4-1(c). From this table, one can simply notice the individual values of successive traffic series are not identical, but similar, including mean and CV. In addition, the CV of speed is the smallest, while the CVs of flow and occupancy are approximately equal. The variation degrees of successive traffic time series also decline with increasing time scale. The above consistent statistic characters illustrate that the reliability of our traffic series is (i.e., no apparent incidents). Figure 4-3 demonstrates the successive one-dimensional traffic time series measured in five minutes; while Figure 4-4 shows the traffic series measured in 1-minute scale during five workdays. Figure 4-5 displays a 24-hour traffic series exhibiting heavy traffic with various time scales on a typical workday. From Figure 4-3 and Figure 4-4, it is noted that the traffic time series, measured in 1-minute as well as 5-minute scale, vary similarly and the traffic patterns exhibit in different days, but they never exactly repeat. From Figure 4-5, we observe the fluctuation of 20-second time series is the most severe. As the measured time interval gets larger, the degrees of variation decline.

Table 4-1 The mean and coefficient of variation (CV) of traffic time series

(a) outbound

Time	Measured time interval	Flow				Speed				Occupancy			
		Station 402		Station 404		Station 402		Station 404		Station 402		Station 404	
		Mean	CV	Mean	CV	Mean	CV	Mean	CV	Mean	CV	Mean	CV
00:00 – 03:00	20-sec	2.1	0.84	0.9	1.36	92.14	0.13	98.54	0.09	2.91	0.98	1.03	1.62
	1-min	6.2	0.67	2.8	0.91	91.77	0.08	98.55	0.06	2.92	0.75	1.03	1.10
	3-min	18.6	0.57	8.3	0.70	91.23	0.05	98.54	0.04	2.93	0.62	1.03	0.81
	9-min	56.1	0.51	24.8	0.58	91.07	0.04	98.53	0.03	2.94	0.56	1.04	0.69
06:00 – 09:00	20-sec	4.8	0.64	2.8	0.94	87.03	0.11	96.28	0.08	7.47	0.69	3.28	1.04
	1-min	14.3	0.53	8.3	0.74	86.66	0.07	96.28	0.05	7.46	0.57	3.27	0.80
	3-min	42.5	0.48	25.0	0.59	86.44	0.05	96.28	0.04	7.42	0.50	3.26	0.64
	9-min	125.0	0.48	75.0	0.53	86.40	0.04	96.34	0.03	7.28	0.49	3.20	0.60
12:00 – 15:00	20-sec	5.9	0.44	3.3	0.76	81.55	0.11	94.47	0.07	9.95	0.51	3.90	0.84
	1-min	17.7	0.30	9.8	0.53	81.10	0.08	94.47	0.05	9.95	0.35	3.90	0.57
	3-min	53.1	0.21	29.3	0.40	80.86	0.05	94.48	0.03	9.95	0.24	3.90	0.41
	9-min	159.0	0.16	87.9	0.32	80.85	0.04	94.50	0.03	9.93	0.18	3.88	0.35
18:00 – 21:00	20-sec	8.2	0.38	6.4	0.57	75.05	0.12	86.41	0.10	14.47	0.45	8.93	0.63
	1-min	24.6	0.27	19.2	0.42	75.04	0.10	86.41	0.07	14.48	0.32	8.93	0.47
	3-min	74.0	0.20	57.7	0.33	75.03	0.08	86.40	0.05	14.50	0.24	8.96	0.36
	9-min	223.1	0.17	173.3	0.29	74.92	0.07	88.40	0.08	14.59	0.20	8.89	0.42

(b) inbound

Time	Measured time interval	Flow				Speed				Occupancy			
		Station 421		Station 433		Station 421		Station 433		Station 421		Station 433	
		Mean	CV	Mean	CV	Mean	CV	Mean	CV	Mean	CV	Mean	CV
00:00 – 03:00	20-sec	1.4	1.27	1.2	1.62	94.23	0.21	99.58	0.08	1.50	1.59	1.30	1.76
	1-min	4.3	1.13	3.7	1.49	94.19	0.19	99.59	0.05	1.50	1.40	1.30	1.64
	3-min	12.9	1.04	11.1	1.44	94.17	0.19	99.59	0.03	1.51	1.30	1.31	1.58
	9-min	38.6	0.96	33.1	1.39	93.34	0.18	99.61	0.02	1.50	1.18	1.30	1.53
06:00 – 09:00	20-sec	7.2	0.68	7.2	0.64	90.98	0.13	82.56	0.28	9.24	0.79	12.46	0.93
	1-min	21.6	0.62	21.5	0.58	90.66	0.12	82.62	0.27	9.22	0.72	12.42	0.88
	3-min	64.4	0.61	64.2	0.55	90.48	0.11	82.74	0.27	9.14	0.69	12.35	0.85
	9-min	188.7	0.60	189.5	0.55	90.52	0.10	83.14	0.26	8.92	0.69	12.03	0.85
12:00 – 15:00	20-sec	5.7	0.50	5.9	0.47	92.77	0.14	90.34	0.13	7.26	0.99	7.86	0.82
	1-min	17.0	0.34	17.8	0.35	92.26	0.11	90.34	0.12	7.26	0.75	7.86	0.73
	3-min	51.0	0.24	53.4	0.27	91.84	0.10	90.38	0.11	7.28	0.60	7.84	0.67
	9-min	152.5	0.19	159.8	0.22	91.76	0.09	90.38	0.11	7.26	0.49	7.81	0.65
18:00 – 21:00	20-sec	6.80	0.49	7.6	0.44	89.95	0.12	87.71	0.10	8.75	0.70	9.85	0.54
	1-min	20.3	0.36	22.7	0.33	89.30	0.10	87.69	0.08	8.75	0.58	9.86	0.43
	3-min	61.2	0.27	68.2	0.26	88.73	0.09	87.65	0.07	8.79	0.48	9.89	0.36
	9-min	185.5	0.23	205.5	0.23	88.40	0.08	87.46	0.06	8.89	0.42	10.00	0.31

Units: flow = vehicles/time interval-lane; speed = kilometer/hour; occupancy = %

(c) station N27.9

Date	Flow		Speed		Occupancy		Date	Flow		Speed		Occupancy	
	Mean	CV	Mean	CV	Mean	CV		Mean	CV	Mean	CV	Mean	CV
1th Feb.	252.3	0.529	90.97	0.035	6.17	0.562	16th Feb.	270.6	0.488	89.37	0.037	6.97	0.509
2th Feb.	244.8	0.547	87.60	0.057	6.94	0.560	17th Feb.	263.7	0.524	86.75	0.156	7.55	0.698
3th Feb.	222.0	0.553	84.00	0.073	6.99	0.571	18th Feb.	273.6	0.527	89.53	0.031	7.39	0.592
4th Feb.	220.7	0.639	83.98	0.091	6.82	0.530	19th Feb.	268.3	0.512	90.19	0.030	6.87	0.526
5th Feb.	256.5	0.540	86.85	0.048	8.05	0.870	20th Feb.	284.5	0.507	88.26	0.039	7.54	0.524
6th Feb.	285.0	0.497	88.75	0.036	7.49	0.518	21th Feb.	283.3	0.462	90.07	0.033	7.12	0.493
7th Feb.	285.1	0.486	89.60	0.037	7.04	0.522	22th Feb.	254.9	0.469	90.34	0.037	6.22	0.504
8th Feb.	261.4	0.458	89.92	0.032	6.41	0.492	23th Feb.	270.6	0.488	89.37	0.037	6.97	0.509
9th Feb.	270.4	0.491	89.00	0.043	7.09	0.510	24th Feb.	288.6	0.469	89.87	0.028	7.49	0.481
10th Feb.	265.5	0.510	88.57	0.038	6.91	0.530	25th Feb.	268.3	0.525	89.69	0.036	7.17	0.537
11th Feb.	256.0	0.530	89.21	0.063	6.84	0.535	26th Feb.	269.3	0.522	88.80	0.038	7.39	0.550
12th Feb.	260.6	0.502	88.43	0.042	6.79	0.532	27th Feb.	287.1	0.509	89.03	0.035	7.62	0.529
13th Feb.	285.0	0.497	88.75	0.036	7.49	0.518	28th Feb.	259.8	0.461	90.88	0.028	6.51	0.482
14th Feb.	285.1	0.486	89.60	0.037	7.04	0.522	29th Feb.	269.3	0.408	91.19	0.026	6.59	0.422
15th Feb.	264.6	0.453	88.76	0.033	6.41	0.492							

Units: approach flow = vehicles/5-minute time interval; approach speed = kilometer/hour; approach occupancy = %

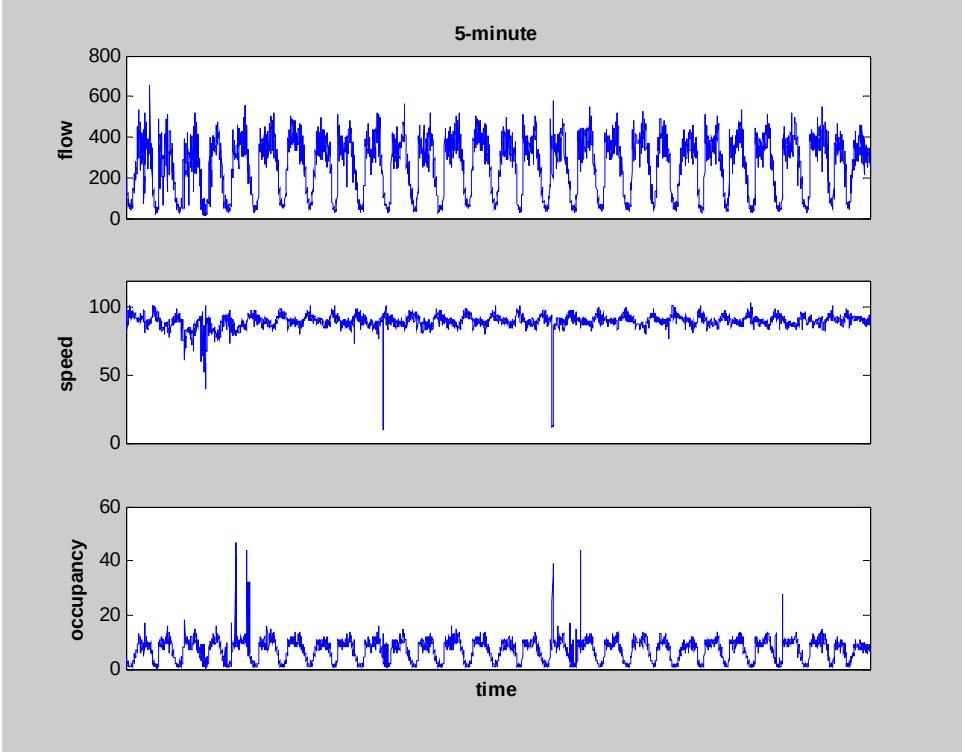

Figure 4-3 One-dimensional successive (one month) traffic time series measured in five minutes per approach (station N27.9)

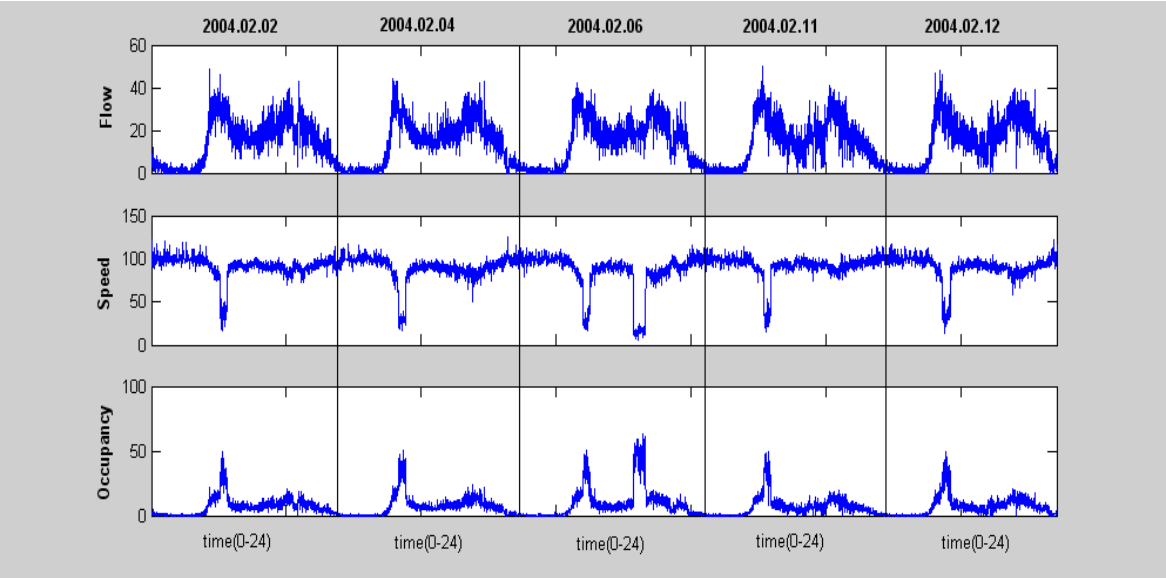

Figure 4-4 One-dimensional 1-minute traffic series for five workdays (station 433)

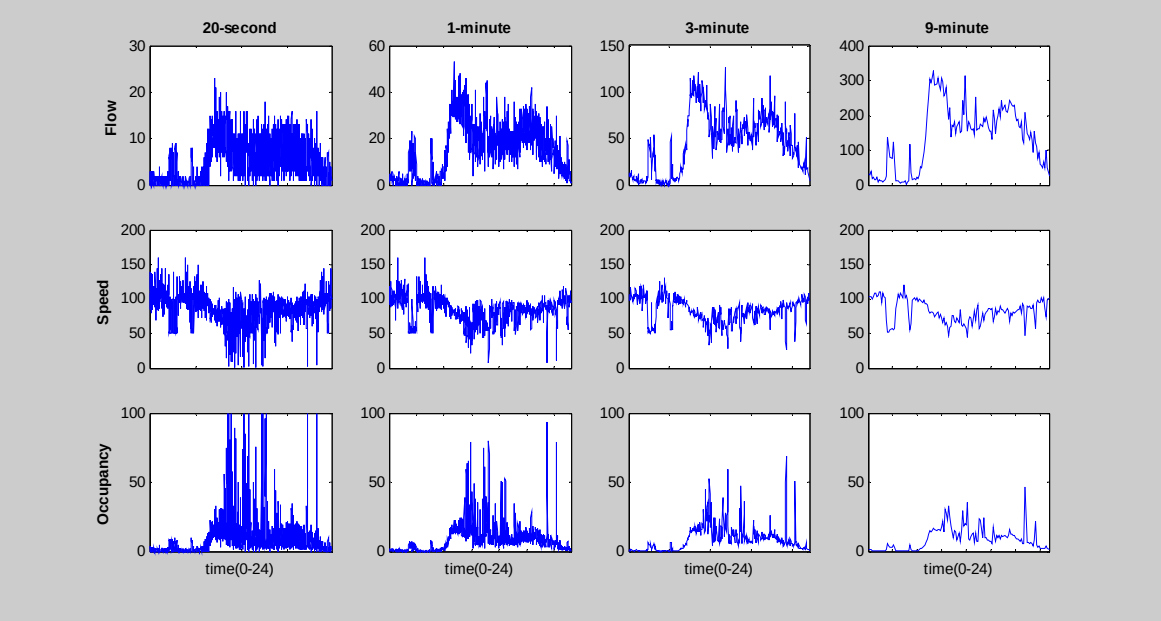

Figure 4-5 One-dimensional traffic series measured in various time scales per lane on a typical workday with congested case (station 421)

4.2 A Filtering Approach to Discriminate Features of Traffic Dynamics

Aside from research into the statistics of real traffic data, this study proposes a novel filtering approach to inspect the characteristics of real-world traffic flow dynamics. The proposed approach contains four steps as depicted in Figure 4-6. The first step is to filter out periodic/quasi-periodic trajectories by the Fourier power spectrum. The second step is to further filter out equilibrium (fixed) points by the precise largest Lyapunov exponent. The third step is to distinguish random patterns from chaotic or

stochastic patterns by comparing the iterated function system (IFS) clumpiness maps between original and surrogate data. The final step is to filter out the plausible stochasticity from chaoticity using correlation dimension. The rationales for the proposed filtering approach are explained as follows.

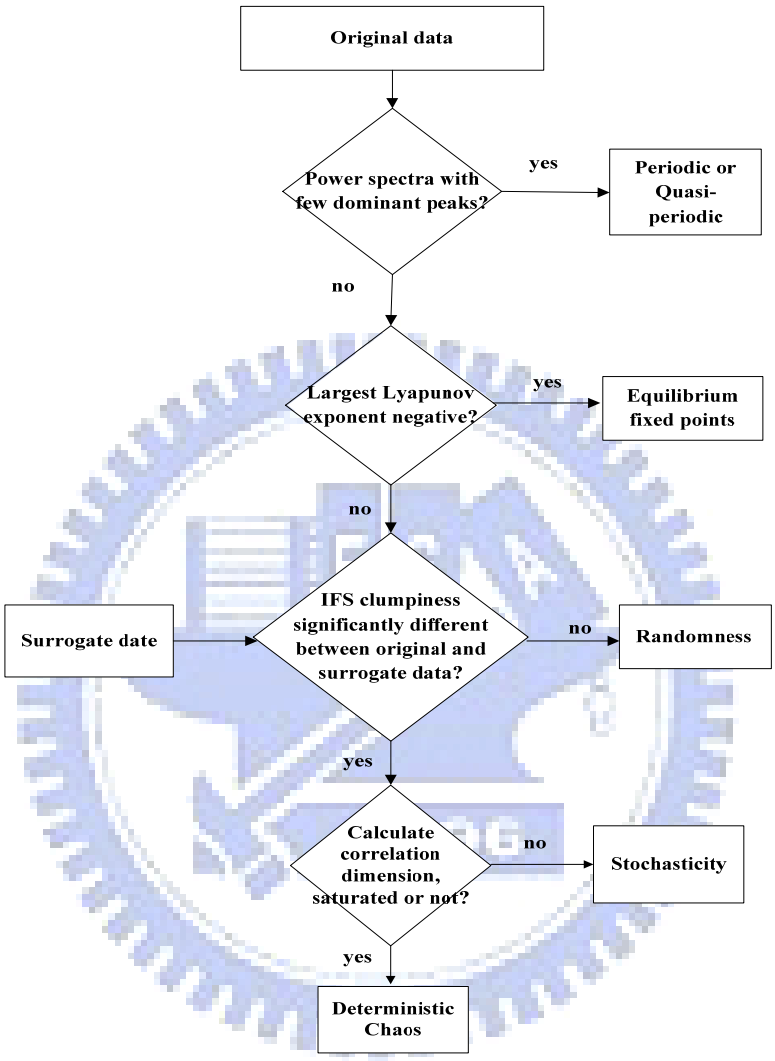

Figure 4-6 The proposed filtering approach (Lan *et al*., 2007c)

Firstly, Fourier analysis lets us determine the frequency content of some signals. If the signal is periodic or quasi-periodic, the Fourier power spectrum will consist of a sequence of "spikes" at the fundamental frequencies, their harmonics. However, if the signal is neither periodic nor quasi-periodic (for example, if it is chaotic), then the Fourier power spectrum will be continuous. Thus, the sudden appearance of a continuous power spectrum from a discrete spectrum, as some parameter of the system is changed, is viewed as an indicator of the onset of chaotic behavior (Hilborn, 2000). However, a continuous Fourier power spectrum can also arise if external noise is present. Thus, the presence of a continuous power spectrum cannot necessarily be

taken as conclusive evidence for the existence of chaos, unless that the noise is absent and that the experimental resolution is sufficient to see all the frequencies that might be present for the expected number of degrees of freedom. Sprott (2003) pointed out that a stochastic system with a non-uniform power spectrum can masquerade for chaos. Because of the noise influence, it seems easier to differentiate periodic and quasi-periodic trajectories from continuous power spectrum. Besides, the power spectrum can be affected by the noise of experimental data in such a way that a noisy deterministic chaos might not definitely have a broadband spectrum. Hence, it is suitable to distinguish periodic and quasi-periodic from chaotic trajectories, with describing "main peak with broadband noise-like" rather than just "broadband spectrum," if we infer that nonlinear trajectories exist deterministic chaoticity. The proposed filter approach will make use of the good features of power spectrum -- if the power spectrum is narrow (clear) and has only few (two or three) dominant sharp spikes, it must be periodic or quasi-periodic; if it is "main peak with broadband noise-like" spectrum, it could be chaotic; if it is stochastic, there must be many fundamental frequencies resolved with higher resolution.

Secondly, the exponential divergence of nearby trajectories in phase space is recognized as the hallmark of chaotic behaviors (Drazin, 1994). If we take two points in the phase space x_{n1} and x_{n2} and indicate their distance as $|x_{n1} - x_{n2}| = \delta_0$, then after time *t* it is expected that the new distance δ will be equal to $\delta = \delta_0 e^{\lambda t}$, where λ is called the Lyapunov exponent. In general, for an *m*-dimensional phase spaces the rate of expansion or contraction of trajectories is described for each direction by one Lyapunov exponent, resulting in *m* different λs, wherein positive value indicates expansion of the orbit; zero value indicates periodic trajectories and negative value indicates contraction. Of the *m* different λs, the main interest is to look at the largest value λ_0 since it can be easily calculated and also yields evidence for the presence of deterministic chaos in the observed data (Gencay, 1996). If λ_0 is positive, the time series can be quasi-periodic, chaotic or stochastic. If λ_0 is zero, the trajectories will eventually converge to a period-*k* sink (*k* is greater than or equal to 2); thus, the time series is periodic. If λ_0 is negative, the time series will converge toward stable sinks -- equilibrium (fixed) points. Rosenstein *et al*. (1993) proposed a method to calculate

λ_0 from an observed times series. However, since λ_0 is very sensitive to the noise of a time series, precisely estimating λ_0 is very critical. To obtain a precise value for λ_0, one needs to know in advance the proper time delay and embedding dimension. In this study, we employ average mutual information (AMI) method, proposed by Fraser and Swinney (1986), to estimate the proper time delay. Besides, we employ false nearest neighbors (FNN) algorithm, developed by Kennel *et al*. (1992), to estimate the sufficient dimension for phase space reconstruction.

Thirdly, iterated function systems provide a well-defined method to produce fractals with specific desired characteristics and appearance. It also suggests a data-analysis method (Peak and Frame, 1994). Suppose we play a game with a time series of uncorrelated random numbers $0 < X_n < 1$ on a square with moving a fraction *f* =0.5. That is, label the corners of the square ABCD clockwise from the upper left. Start anywhere in the square, such as the corner A. If the first value in the time series has $0 < X_1 < 0.25$, move half way to A; if $0.25 < X_1 < 0.5$, move half way to B, and so forth. Continue iterating until the square begins to fill in. If the values are uncorrelated, then the points will be uniformly scattered in the square. The clumpiness of the plot is an indicator of determinism, whether it may be chaos, colored (correlated) noise or white (uncorrelated) noise. Since the IFS clumpiness does not very well distinguish chaos from colored (correlated) noise. It may be necessary to further compare the properties between an original time series and its surrogates, which are designed to mimic the statistical properties of the original data, but with the determinism removed. The surrogate data can be easily generated by randomly shuffling the original data. While shuffling the sequences will preserve the same probability distribution as the original data, namely, the surrogates for any original time-series data must be random (Theiler *et al*., 1992).

Lastly, correlation dimension is a measure used to examine the phenomenon that the presence of a data point may affect the position of the other point lying on the attractor. If the value of the correlation dimension is finite, low and non-integer, the system is possibly considered as low-dimensional chaos. The saturation value of the correlation dimension is defined as the correlation dimension of the attractor, or called attractor dimension. In contrast, if an attractor dimension cannot reach saturation or is saturated in very high-dimension, then the trajectories of that time series could be stochastic (Shang *et al*. 2005). Grassberger and Procaccia (1983) showed that

correlation dimension d can be evaluated by using the correlation integral $\mu(r)$, which is the probability that a pair of points (s_i, s_j) chosen randomly in the reconstructed space are separated by a distance less than r. The details of calculating $\mu(r)$ are as the same as the Eq. (3.4) ~ (3.6).

4.3 Result of Filtering Approach

By using the proposed filtering approach, a systematic inspection on the nonlinear features of temporal flow dynamics was carried out and the results of each step were presented as follows.

Table 4-2 summaries the results of power spectra for different combinations, while Figure 4-7 illustrates the power spectrum for the one-minute flows at station 421. According to the power spectrum plots, one may find that, regardless of time intervals, all data can be deemed as continuous in the form of so-called "noise-like broadband." Neither an obvious spike nor a sequence of spikes could be identified for the traffic flow time series as periodic or quasi-periodic trajectories. However, there are still some discrepancies between different periods. For instance, during the off-peak hours, the power spectrum does not show main peaks. In other words, the traffic flow during off-peak hours has revealed random coupled with no exhibiting order or determinism. But the most important thing is that if one wishes to diagnose the characters of nonlinear dynamics more precisely, one needs further diagnosis by proceeding from the second step to the fourth step. The power spectrum in the first step is just to filter out periodic or quasiperiodic trajectories from nonlinear dynamical properties.

In the second step, we use AMI and FNN methods to determine the most appropriate time delay and embedding dimension, respectively. It should be noted that owing to the noise effect of traffic data, it is difficult to decrease the percent of FNN to zero. In this paper, we set the maximum acceptable percent of FNN as under 5%. Figure 4-8 is an example of AMI and FNN analysis at station 421. The left-hand-side plot of Figure 4-8 shows that the first low point corresponding to time delay is one time steps and the right-hand-side plot tells us if we set embedding dimension as 6, the percent of FNN will drop as low as about 3%, which is lower than 5%. Therefore, we know the proper time delay for the one-minute flows from 06:00 am to 09:00 am at station 421 is one time step (equivalent to one-minute) and the proper embedding dimension is 6.

Table 4-2 Summary of power spectra

Times of day	Measured time interval	Station 402	Station 404	Station 421	Station 433
00:00–03:00	20-sec	+	+	+	+
	1-min	+	+	+	+
	3-min	+	+	+	+
	9-min	+	+	x	x
06:00–09:00	20-sec	+	+	+	+
	1-min	+	+	+	+
	3-min	+	+	+	+
	9-min	x	x	x	x
12:00–15:00	20-sec	-	-	-	-
	1-min	x	x	-	-
	3-min	x	x	+	+
	9-min	x	x	x	x
18:00–21:00	20-sec	+	+	+	+
	1-min	+	+	-	-
	3-min	+	+	+	+
	9-min	x	x	x	x

+ represents one main peak with flat or descending noise-like
x represents peaks with noise-like
- represents flat noise-like or many fundamental frequencies

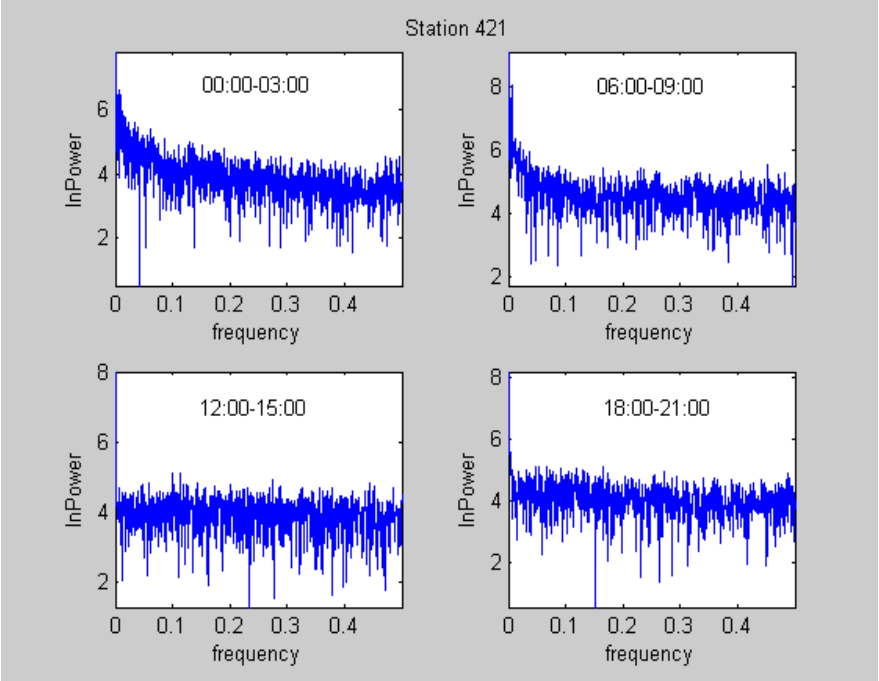

Figure 4-7 An illustration of power spectra of one-minute flows (Station 421)

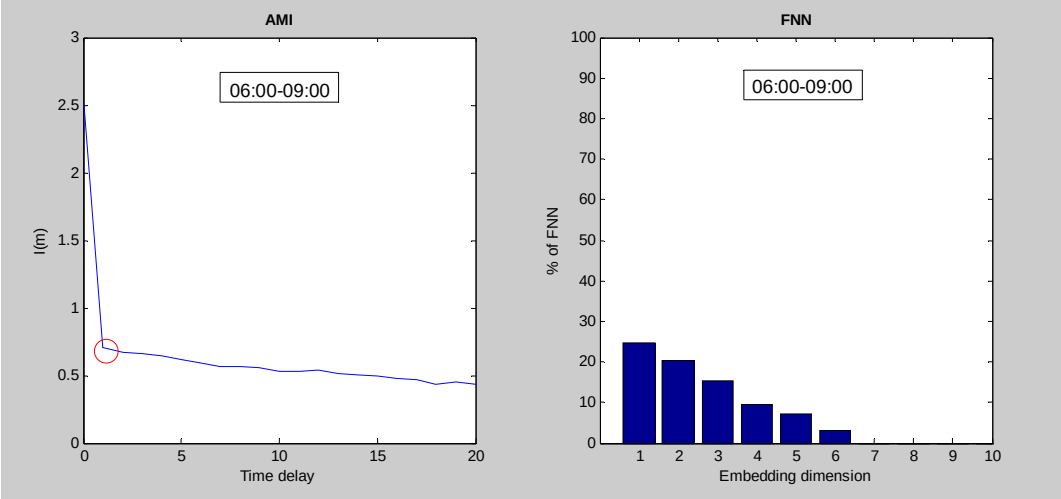

Figure 4-8 An illustration of AMI and FNN of one-minute flows (Station 421)

After choosing appropriate time delay and embedding dimension, we can then calculate the largest Lyapunov exponent λ_0. The results are summarized in Table 4-3.

It is found that the largest Lyapunov exponents are positive in most cases, indicating that the state trajectories of traffic flow in workdays would not maintain equilibrium fixed points (either zero flow or capacity flow) for a long time. The only exceptions are the data from stations 421 and 433 during the early hours (00:00 am to 03:00 am). The negative values of λ_0 for these two stations suggest that the traffic flows in early hours measured in 20-second interval are so lulled (very few travelers going into the city) that the trajectories often converge to fixed points (zero flow or near zero volume). In contrast, the positive values of λ_0 for the two outbound stations 402 and 404 during 00:00 am to 03:00 am suggest that the 20-second flows in early hours will not converge to zero. It agrees to the fact that quite a number of travelers leave Taipei city after their night activities during the midnight.

The above two steps have successfully ruled out the empirical flow patterns being periodic or quasi-periodic motions or converging to fixed points. However, we still cannot distinguish if the traffic flow patterns are chaotic, stochastic or random. As noted previously, IFS provides a well-defined method to produce fractals with specific desired characteristics and appearance. Through the comparison of traffic flow properties between an original time series data and its surrogates, one can easily distinguish randomness from nonlinear complex time series since the clumpiness plot of surrogate (randomized) data is expected to be uniformly dense and shows no

fractals at all.

Table 4-3 Summary of the largest Lyapunov exponents

Time of day	Measured time interval	Station 402	Station 404	Station 421	Station 433
00:00–03:00	20-sec	0.263	0.215	-0.115	-0.054
	1-min	0.549	0.328	0.566	0.343
	3-min	0.546	0.249	0.462	0.409
	9-min	0.416	0.243	0.438	0.341
06:00–09:00	20-sec	0.553	0.390	0.585	0.578
	1-min	0.600	0.317	0.744	0.590
	3-min	0.495	0.263	0.482	0.516
	9-min	0.539	0.348	0.356	0.395
12:00–15:00	20-sec	0.573	0.454	0.628	0.596
	1-min	0.716	0.441	0.744	0.688
	3-min	0.598	0.366	0.559	0.570
	9-min	0.410	0.376	0.413	0.487
18:00–21:00	20-sec	0.636	0.356	0.682	0.627
	1-min	0.690	0.422	0.705	0.638
	3-min	0.566	0.191	0.552	0.536
	9-min	0.432	0.184	0.501	0.418

Table 4-4 summarizes the diagnosing results for various combinations. Figure 4-9 illustrates the IFS maps for the twenty-second flows during 06:00 am - 09:00 am at station 421. The left clumpiness plot is for original data and the right plot is for surrogate data. We find that noticeable difference exists in the IFS clumpiness maps between the original data and its surrogates in periods 06:00 am - 09:00 am and 18:00 pm - 21:00 pm. However, off-peak data during 12:00 pm - 15:00 pm does not show obvious difference between two IFS clumpiness maps. As to the state trajectories of traffic flow in midnight, it is the fact that most of them are close to random because their IFS clumpiness maps between the original data and its surrogates do not show obvious difference. Such random patterns agree to the fact that most of drivers can freely drive their vehicles as long as not speeding, i.e., there is no obvious relationship between two vehicles shown in chronological order.

Table 4-4 Summary of IFS clumpiness maps

Time of day	Measured time interval	Station 402	Station 404	Station 421	Station 433
00:00–03:00	20-sec	-	-	-	-
	1-min	-	-	-	-
	3-min	-	-	-	-
	9-min	-	-	-	-
06:00–09:00	20-sec	+	+	+	+
	1-min	+	+	+	+
	3-min	+	+	+	+
	9-min	+	+	+	+
12:00–15:00	20-sec	-	+	-	-
	1-min	-	-	-	-
	3-min	+	+	+	+
	9-min	+	+	+	+
18:00–21:00	20-sec	+	+	+	+
	1-min	+	+	+	+
	3-min	+	+	+	+
	9-min	+	+	+	+

+ represents **obvious or visual** difference (original data have obvious or secret fractals but surrogates do not have; or both have fractal sets with dissimilar patterns)

- represents **no visual or secrete** difference (both original and surrogate data have no fractal sets; or original data have secret fractals but surrogates do not have)

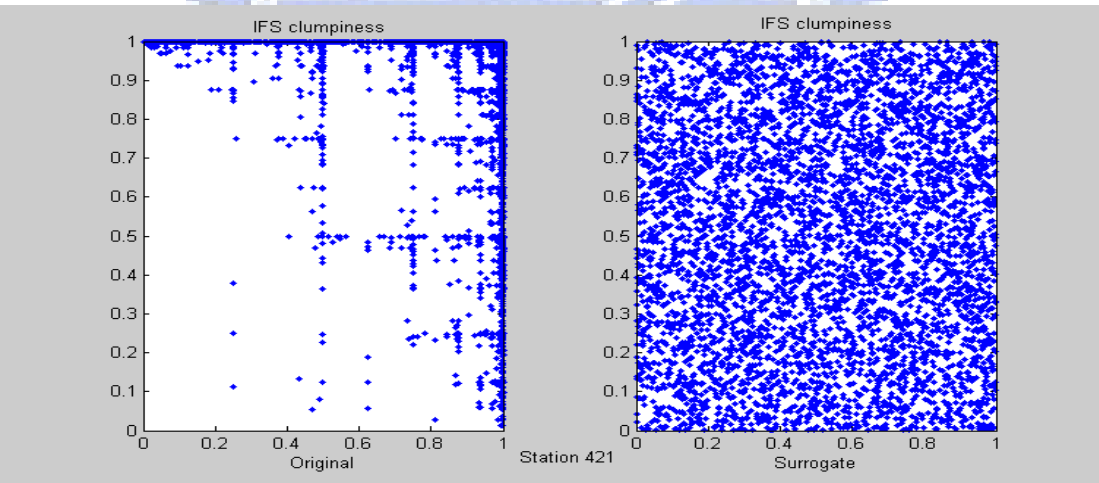

Figure 4-9 An illustration of IFS clumpiness maps of 20-second flows (06:00 am - 09:00 am, Station 421)

The final traffic flows are observed with chaotic and stochastic features after we filter out the above nonlinear patterns. Nevertheless, the external appearance of deterministic chaoticity and stochasticity are similar. It is difficult to diagnose the characteristics for such nonlinear time series by using a single figure, especially while the short-term traffic flow dynamics surging along with extreme fluctuation as well as involving with noise. In this study, a critical parameter, correlation dimension, is employed to distinguish the patterns between them. Table 4-5 reveals that state

trajectories of traffic flow during morning and evening peak-hours periods measured with coarse time intervals, such as 9-minute, exhibit more deterministic-like (chaotic) than stochastic patterns because the correlation dimensions are finite, low and non-integer. In contrast, state trajectories of traffic flow with shorter interval, such as 20-second and 1-minute, will show stochastic pattern because their attractor dimensions cannot reach saturation or converge in very high (over six) dimensions.

Table 4-5 also shows that during the off-peak period, traffic dynamics exhibit more stochastic than chaotic patterns because their attractor dimensions are higher than other corresponding time periods. Simultaneously, we notice that in the early hours (00:00-03:00) the values of correlation dimension are low and non-integer, too. It does not represent that the feature of traffic flow in the period is a deterministic chaoticity, but it shows a random phenomenon as mentioned previously instead. An in-depth inspection to the raw data clarifies that during the midnight the state trajectories of traffic flow associated with copious zero- and identical volumes reconstructed in multidimensional spaces will masquerade as a low attractor dimension. Fortunately, the parameter of IFS clumpiness maps helps filter out the random pattern during the early hours.

Table 4-5 Summary of the correlation dimension

Time of day	Measured time interval	Station 402	Station 404	Station 421	Station 433
00:00–03:00	20-sec	3.3	3.7	3.3	3.3
	1-min	3.2	3.5	3.2	3.3
	3-min	2.9	3.3	2.8	3.1
	9-min	2.7	3.2	2.5	2.6
06:00–09:00	20-sec	-	-	-	-
	1-min	5.4	5.2	5.6	5.6
	3-min	4.5	4.6	4.4	4.3
	9-min	3.3	3.6	3.2	3.2
12:00–15:00	20-sec	-	-	-	-
	1-min	-	-	-	-
	3-min	5.4	5.1	5.4	5.3
	9-min	4.6	4.6	4.9	4.7
18:00–21:00	20-sec	-	-	-	-
	1-min	5.7	5.7	5.8	5.7
	3-min	4.8	4.9	4.7	4.5
	9-min	3.7	3.9	3.5	3.4

- represents an attractor dimension cannot reach saturation over six dimensions

In this section, a novel filtering approach was proposed to analyze the features of nonlinear traffic flow time-series data directly extracted from four detector stations on Taiwan Freeway. Different nonlinear patterns have been found, depending on the measured time intervals, times of day and locations. During the peak hours, the temporal flows measured in larger time intervals are in general close to chaotic-like (deterministic) patterns; but they are close to stochastic-like patterns if measured in shorter time intervals. During the off-peak period, the temporal flows are close to stochastic-like patterns, too. At midnight, most temporal flows reveal random patterns; some measured in 20-second interval even converge into equilibrium (fixed) points when most of travelers depart downtown after their night activities during the midnight.

4.4 Testing for Predictability of Various Techniques

In addition to the proposed filtering approach, in this section we further describes the main procedures and testing results for the predictability of various techniques depicted in Chapter 3. We generated two time-series data categories including linear stochastic time series and nonlinear deterministic time series in advance of prediction therein. The stochastic time series derived from a linear equation was adopted to compare the predictability between the linear autoregressive method and the RTRL algorithms while the nonlinear time series derived from a first-order differential-delay equation was used to compare the predictability between the simple nonlinear method and the RTRL algorithms. Details about the preliminary test procedures are described as follows:

First, an AR(1) time series, $(x_{t+1} - 0.4) = 0.75(x_t - 0.4) + e_t$ with $e_t \overset{i.i.d}{\sim} N(0,1)$ was used to compare the predictability between the linear model and the RTRL algorithms. In the AR(1) linear time series, two hundred independent points e_t, which conformed to Gausian distribution, were created and an initial x_t was picked to iterate two hundred times together with e_t. Then we set the order of the above model be equal to one to compute the average prediction error and residuals for each time step. After computation, we learned that the root-mean-square error (*RMSE*) was equal to 1.03. Employing the same time series x_t as an input as well as x_{t+1} as output, we adopted the RTRL algorithms to train a network and calculated the *RMSE*, which equaled 0.979 for one trained data set and 0.93 for another test data set. In order to train the AR(1) model, in the RTRL neural network, six nodes were used to process the recurrent feedbacks and the learning rate was set to 0.1. The goal of the RTRL network we set was either

that the *RMSE* equals 0.01 or the training times reached 700 times, whereupon the training iterations would stop. In Figure 4-10, the panel (a) represents the difference between the outputs of the AR(1) model and desired values; while the panel (d) represents the difference between the outputs of the RTRL network and desired values. It's obvious to indicate that for a stochastic time series, the accuracy of prediction by adopting RTRL algorithms is superior to adopting linear prediction both from observing the difference in figure and comparing the values of *RMSE*.

Second, a first-order differential-delay equation, which is the famous Mackey-Glass equation: $\frac{dx(t)}{dt} = \frac{0.2x(t-\tau)}{1+x^{10}(t-\tau)} - 0.1x(t)$, was used to compare the predictability between the simple nonlinear method and the RTRL algorithms. This equation represents a physiological responsive system, which can be used as an index to examine the features of a nonlinear time series (Mackey and Glass, 1977). For instance, the series displays periodic motions when τ is a relatively small value, whereas for τ larger than 17, it displays a chaotic phenomenon. We employed an average mutual information (AMI) approach and a false nearest neighbor (FNN) algorithm to search for the proper time delay and to determine the minimal sufficient embedding dimension. Once the appropriate time delay and the sufficient dimension were determined, we were able to map the one-dimensional differential equation into multidimensional spaces and make use of the neighboring measurements in multidimensional spaces to predict future points. In accordance with this approach, a time series which contained five hundred data points was reconstructed into multidimensional spaces and was forward predicted five hundred time steps. The panel (b) in Figure 4-10 represents the predicting results showing the difference between output of the simple nonlinear technique and desired values. The *RMSE* was equal to 0.1268. Similarly, we adopted the RTRL algorithms to train a network, in which the input and output are the as same as the above time series, to predict the first-order differential-delay equation. In the RTRL network, twelve nodes were used to process the recurrent feedbacks and the learning rate was set to 0.1. The goal of the RTRL network we set was either that the *RMSE* equals 0.07 or the training times reached 2,000 times, whereupon the training iterations would stop. The panel (e) in Figure 4-10 represents the prediction results, showing the difference between output of RTRL algorithms and desired values. The *RMSE* was equal to 0.07. From Figure 4-10 and *RMSE*, again we learned that for a deterministic equation, the accuracy of prediction by adopting RTRL algorithms is superior to adopting the simple nonlinear technique.

Note that if further observing the top panel in Figure 4-10(b), we will find that the errors of prediction by using the simple nonlinear technique are not the same as time evolves, but rather the differences are getting larger, i.e., the accuracy of prediction is getting low as time evolves. By contrast, the errors of prediction by using the RTRL algorithms do not exhibit such a situation, but show large differences during the first steps. The right panels of Figure 4-10 display the difference between the model output and desired values by adopting the simple nonlinear technique (see panel c) and adopting the RTRL network (see panel d) in the first twenty time steps. It can be clearly seen that in the panel (c), the curve marked in red depicting the simple nonlinear technique and the curve marked in blue depicting the desired values match quite closely. The *RMSE* of short time steps (e.g., 20 steps) is equal to 0.0035, which is greatly superior to the average *RMSE* of whole steps (e.g., the average *RMSE* of 500 time steps is equal to 0.1268). In other words, if one would like to forward predict a nonlinear time series resulting from a deterministic function in short steps, then the simple nonlinear technique is quite a good method to adopt. By contrast, in the panel (f), the curve marked in red depicting RTRL algorithms and the curve marked in blue depicting the desired values don't match well in the beginning but converge gradually. It indicates that the RTRL algorithms is suitable to train a network to predict, and the eventually average predictability compared with other techniques is satisfactory; however, training time of the neural network is comparably long and is a factor that should be taken into account in practice. Consequentially, in accordance with the different purposes to be achieved, the predicting techniques with their particulars serve various functions. In terms of the purpose of improving the accuracy of prediction in this case, the RTRL network is a suitable technique because the results of training and testing have revealed that the method can not only successfully simulate a linear time series with stochastic characteristics, but also can capture the nonlinear dynamic trajectories resulting from a deterministic function.

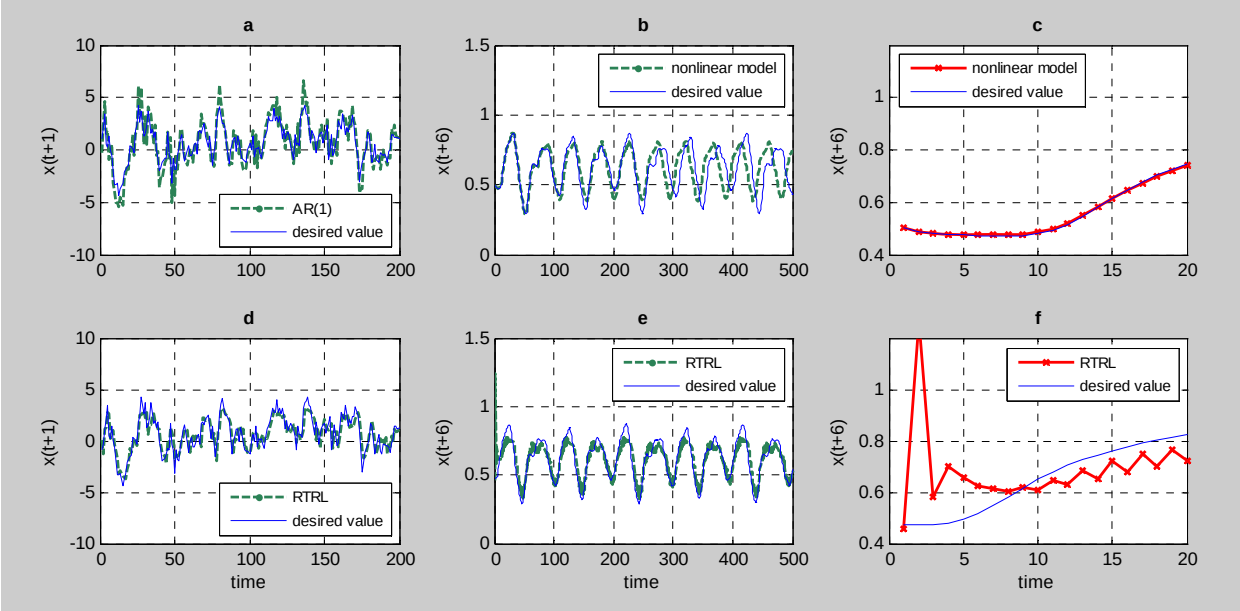

Figure 4-10 The difference between model output and desired values by adopting linear method, simple nonlinear method and RTRL algorithms

Furthermore, the prediction power of RBFNN was calibrated simultaneously. Two deterministic functions were illustrated: one is a *sincos* mathematical function and the other is a first-order differential-delay equation being as same as the above equation. Firstly, in a *sincos* mathematical function, we test $f(x, y) = \cos(3x)\sin(2y)$, wherein the boundary of variable x and variable y is between -1 and 1. Four hundred (x, y) points are created, of which three hundred points are used as the training sets and the remaining one hundred points are used as the testing sets. Tolerance is set equal to 0.8. Following the rules of RBFNN, we employ the OLS algorithm to determine centre neurons and employ the LMS algorithm to modify weighted vectors. Figure 4-11(a) presents the training results, which illustrate the difference between network outputs and desired values in three dimensions. The *RMSE* (root-mean-square error) is equal to 0.0321.

Secondly, in a first-order differential-delay equation, we also employ the famous Mackey-Glass equation. A vector [$x(t\text{-}18)$, $x(t\text{-}12)$, $x(t\text{-}6)$, $x(t)$] is further used as input and a vector $x(t+6)$ is used as output, then the RBF network is applied to train the model and the tolerance is set as 0.9. Five hundred vectors are used as both the training and testing sets. Likewise, OLS algorithm is employed to determine the centre neurons and LMS algorithm is used to modify the weighted vectors. Figure 4-11(b) presents the test results showing the difference between network outputs and desired values in three dimensions. The *RMSE* is equal to 0.0263. Figure 4-11(c) displays directly the difference between network outputs and desired values in one dimension for this

first-order differential-delay equation. The training and testing results have revealed that the RBFNN is able to successfully simulate a mathematical function as well as capture the dynamic trajectories of a nonlinear time series.

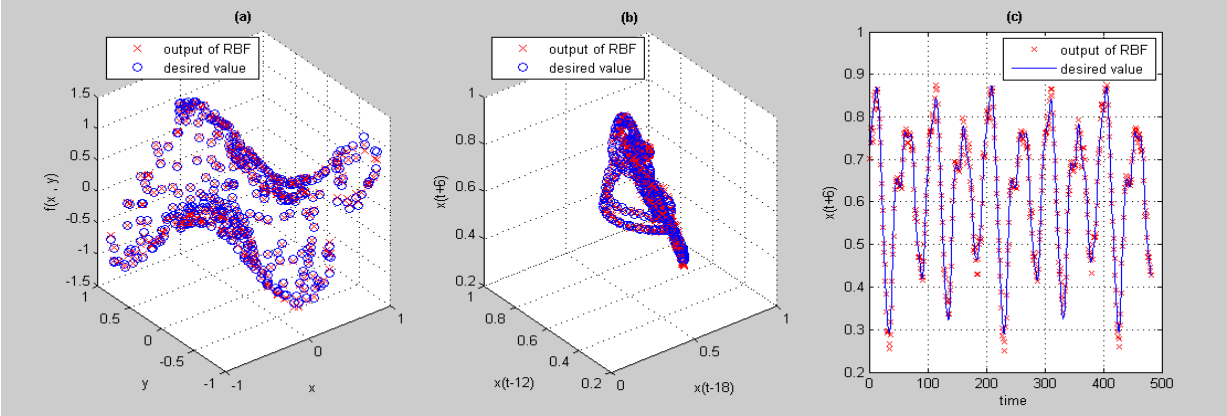

Figure 4-11 The results of training and testing RBFNN with two deterministic functions

CHAPTER 5 EMPIRICAL STUDY

To illustrate the potential advantages of proposed models in analyzing and predicting traffic dynamics, an empirical study and a sensitivity analysis are conducted individually, where the main procedures and analytical results together with discussions are provided as follows.

5.1 Temporal Traffic Patterns and State Trajectory Evolution in Multi-dimensional Spaces

The following demonstrates more interesting features of our empirical traffic series mapped in a reconstructed state space. First, the 20-second traffic series for a typical workday at station 433 is reconstructed into two and three-dimensional state spaces with appropriate time delays. Figure 5-1 compares the same traffic series plotted in 1-D, 2-D and in 3-D spaces. With reference to time delay, it can be seen that points in 1-D numerically change with time evolution, while in the 2-D diagram points not only change with time evolution but also composed of s_t and $s_{t+\tau}$. Similarly, in the 3-D diagram every point is composed of s_t, $s_{t+\tau}$ and $s_{t+2\tau}$. Consequently, variations in 1-D correspond to the degree of spread in 2-D and 3-D spaces, in addition, the steep fluctuations in 1-D correspond to different areas in 2-D or in 3-D spaces. On the other hand, the state trajectories in the 2-D and 3-D diagrams change with time enabling the state trajectories to move back and forth. However, the curves always move forward with time.

Figure 5-2 presents the three-dimensional 1-minute traffic series for five workdays at station 433. The different features of traffic series in three-dimensional space from day

to day are similar but not exactly the same. To see the effect of time scale, Figure 5-3 demonstrates the traffic patterns in three-dimensional reconstructed state spaces measured in 20-second, 1-minute, 3-minute and 9-minute intervals respectively for one workday at station 433. It is noticed that the traffic features become more explicit as the time scale gets coarser. Figure 5-4 further compares the features of 20-second traffic series over 24 hours and within various times of day arranged from midnight to evening peak-hour period, i.e., 00:00-03:00, 06:00-09:00, 12:00-15:00 and 18:00-21:00. Investigating the dynamical behaviors at different times of day, one can find that the conspicuous dynamics of traffic state trajectories come mainly from periods 06:00-09:00 and 18:00-21:00. In the early hours, when traffic is very calm, the occupancy trajectories shrink to very low values, but the speed trajectories can vary rather significantly, which fully explains heterogeneous driver characteristics. Under free flow conditions, some aggressive drivers may move very fast while some conservative drivers may not, causing the wide diversity of speed dynamics. In contrast, during the morning peak-hour period, speed trajectories tend to shrink to some low values while flow trajectories can vary largely in a wide-range domain.

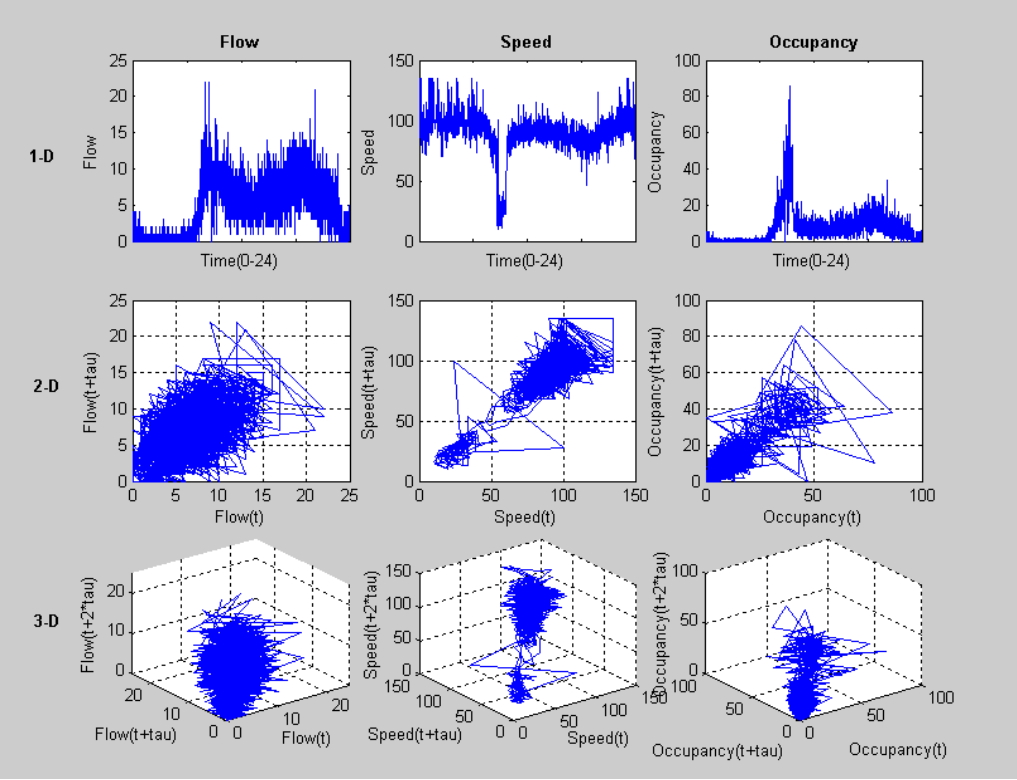

Figure 5-1 Comparison of 1-D, 2-D and 3-D 20-second traffic series on a typical workday (station 433)

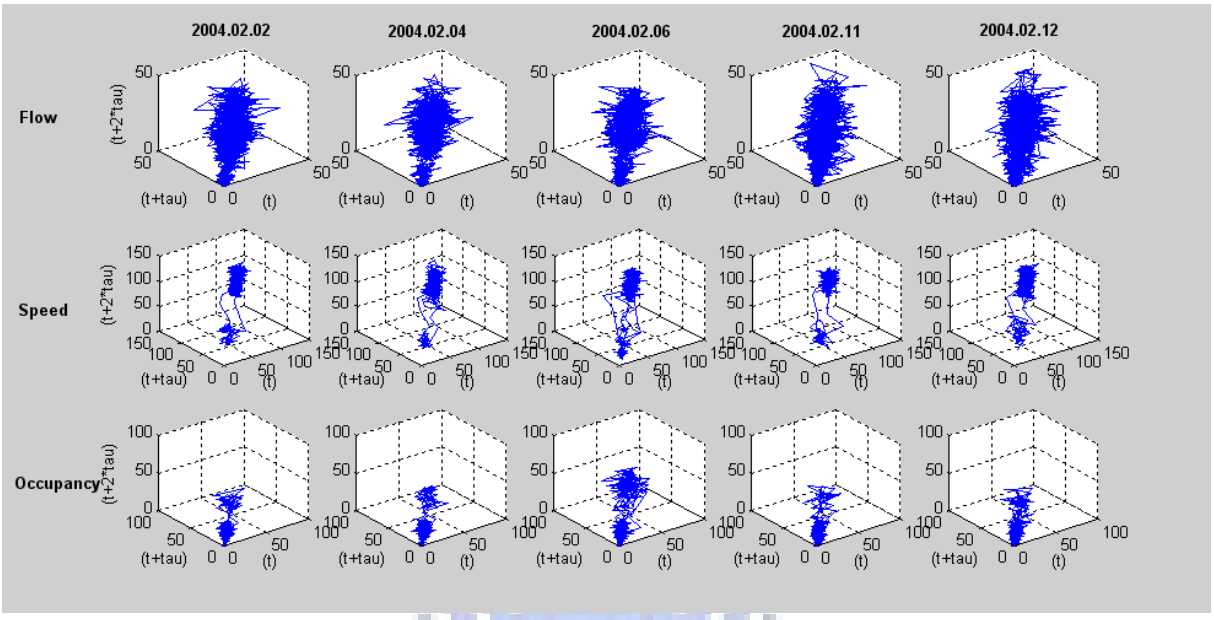

Figure 5-2 Three-dimensional 1-minute traffic series for five workdays (station 433)

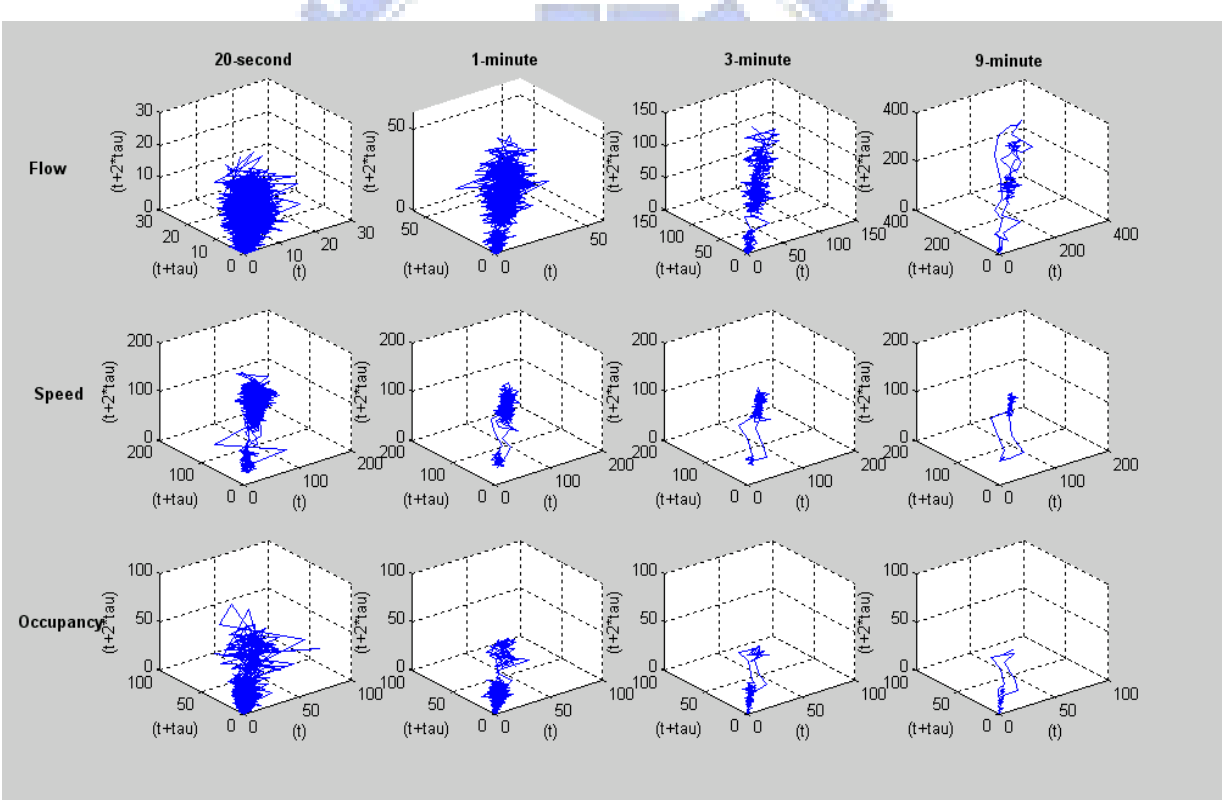

Figure 5-3 Three-dimensional traffic series measured in various time scales (station 433)

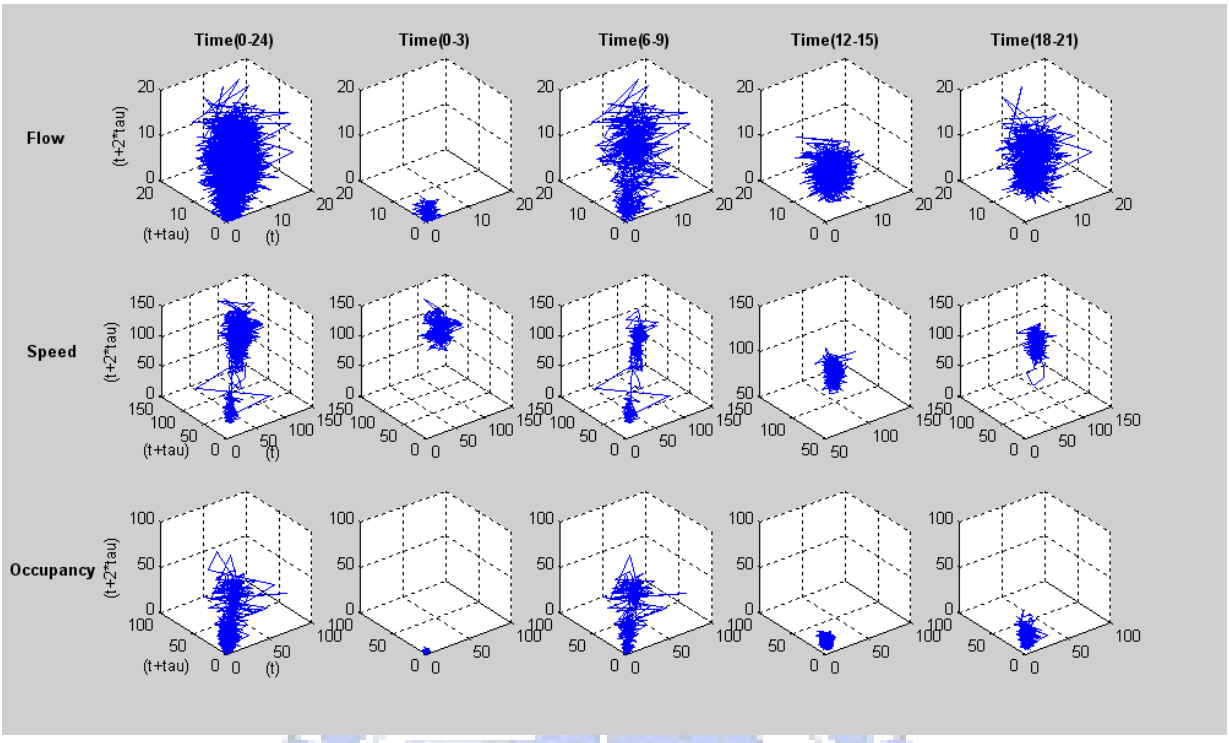

Figure 5-4 Three-dimensional 20-second traffic series in different times of day (station 433)

Let us take the 9-minute traffic series as an example to further explore the dynamical behaviors of trajectories in more detail. In order to trace the sequential order, we only illustrate a limited number of points of the dynamics, as shown in Figure 5-5, which clearly indicates the dynamical behaviors of state trajectories in the reconstructed spaces. For a typical workday, the flow state trajectories move around the lowest corner, i.e., at the coordinate (0, 0, 0) with less fluctuation at midnight (00:00-03:00). In the morning peak hours (06:00-09:00), however, the state trajectories advance along the diagonal direction and sometimes move back and forth as time evolves, which continue to advance until the later morning peak hours. During off-peak hours (12:00-15:00), the state trajectories fluctuate in the middle of the 3-D spaces. After evening peak hours (18:00-21:00), the state trajectories move back to the original place. The whole sequence of features of the traffic flow series within a day are demonstrated in Figure 5-6, which similarly shows that the motion of occupancy trajectories advances along the diagonal direction from bottom to top in the reconstructed space. The difference between the occupancy and flow state trajectories is that the range of motion for occupancy is smaller than that for flow. Compared with flow and occupancy, the direction of motion for speed state trajectories is just the opposite, i.e., from top to bottom. It can be concluded that the direction of traffic state trajectories in multidimensional spaces corresponds to that of the traffic series in 1-D

space, especially when the data is measured on a coarse scale.

Figure 5-7 shows a comparison between 1-D and 3-D spaces for successive traffic flow series. In the top panel, the flow series goes from left to right with time evolution while the direction of traffic state trajectories goes anti-clockwise with time evolution in reconstructed space. Four data points have been selected and marked with Arabic numerals 1, 2, 3, and 4 in the top panel, wherein time delays between paired points i.e., point 1 vs. point 2; point 3 vs. point 4, are equal. After reconstruction, the four points were projected into the bottom panel and correspondingly marked with the same Arabic numerals 1, 2, 3, and 4. From Figure 5-7, it's found that, in the top panel, the difference in flow between points 1 and 2 is lower than between points 3 and 4, therefore, in the bottom panel the distance between points 3 and 4 is larger than between points 1 and 2. In addition, in the bottom panel, one circle distance of trajectories going around the space approximately equals the variety of flow from 00:00 to 24:00 in the top panel. However, it's noticed that not every circle moves smoothly, but heads for one direction with variation and the degrees of variation increase by the time scale shortening.

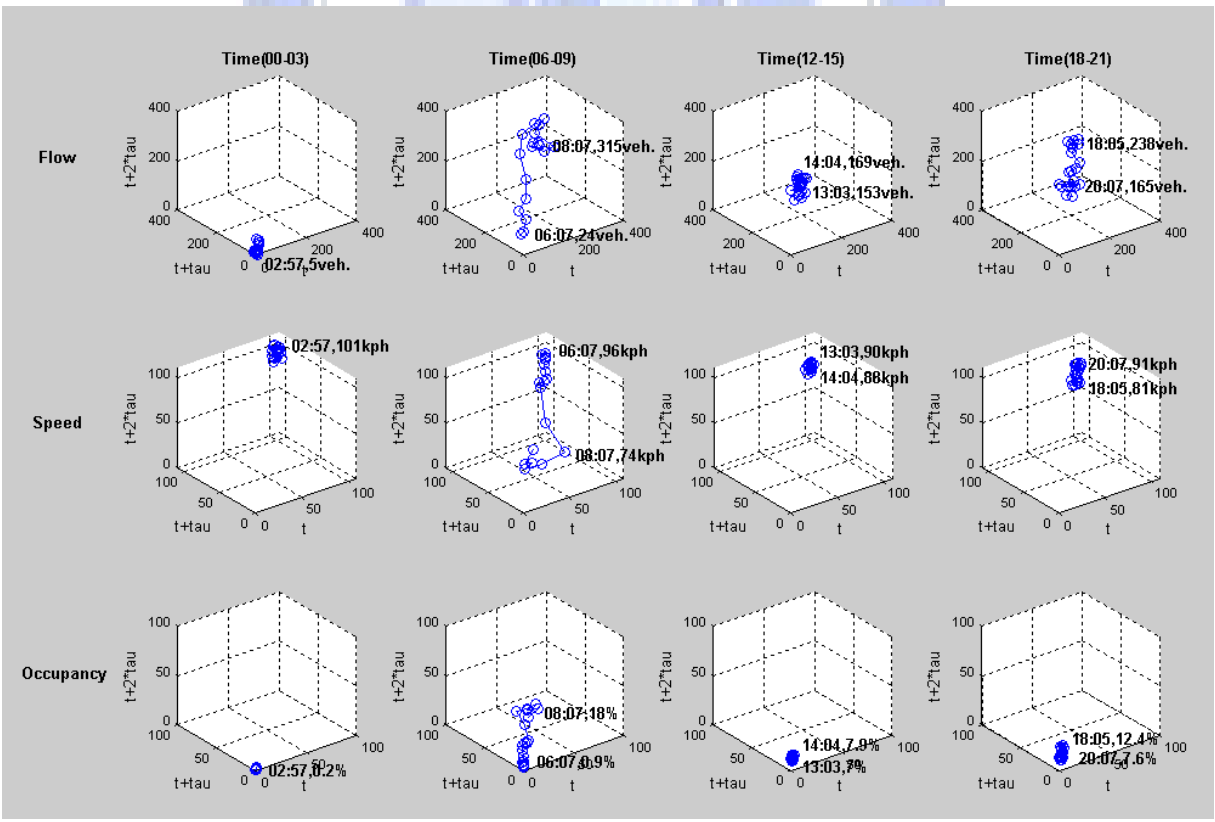

Figure 5-5 The dynamics of 9-minute traffic trajectories in various time-of-day in 3-D space (station 433)

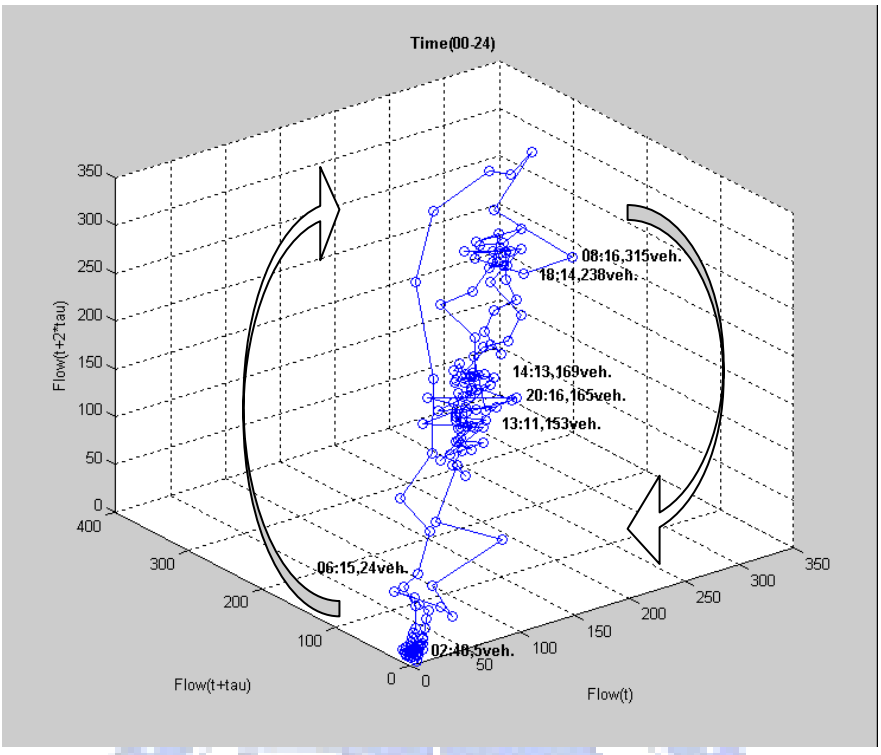

Figure 5-6 The whole-day dynamics of 9-minute flow trajectories in 3-D spaces (station 433)

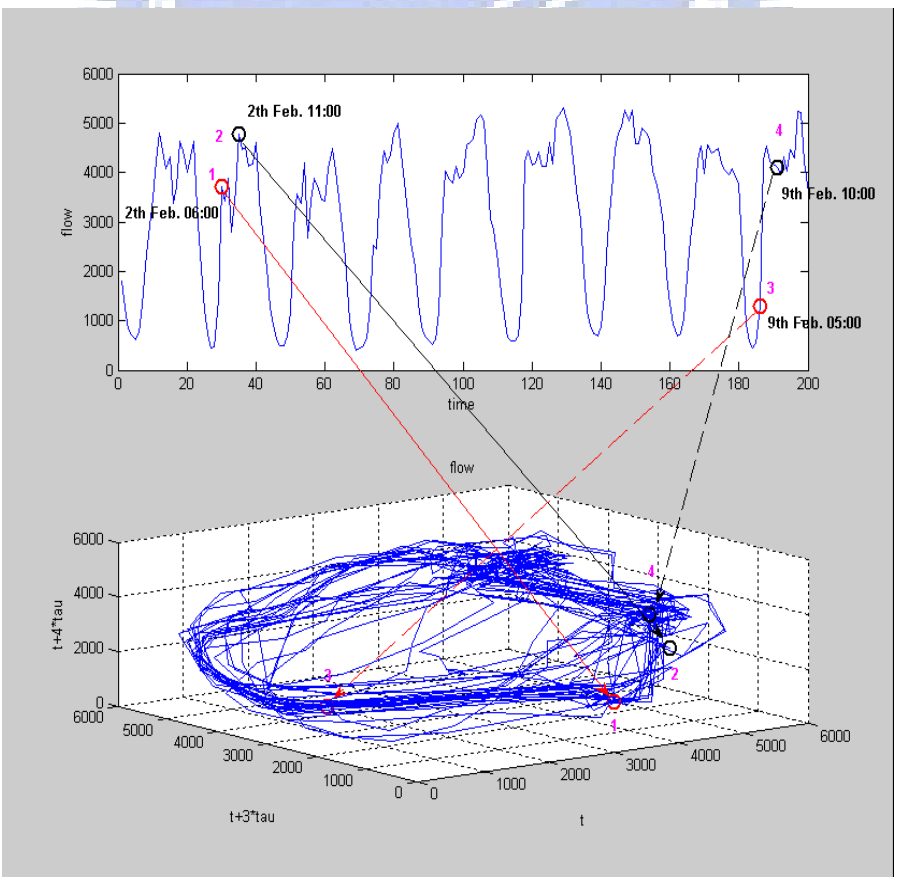

Figure 5-7 Successive flow time series in 1-D and its trajectories in 3-D reconstructed spaces (flow: vehicles per hour per approach)

5.2 Diverse Temporal Patterns in Multidimensional Spaces

In this section, we employ the methodologies introduced in Chapter 3 to further compute the related parameters that can disclose the features of traffic series. The results are summarized in Table 5-1 – Table 5-5. From Table 5-1, it is found that the relationship between time delay and time interval is an inverse proportion. The values of embedding dimension are five or six, which illustrate that the successive traffic series are not composed of a disorder data set, but rather, some state trajectories are dominated by an intrinsic attractor, which may be called as a "deterministic-like" feature. Furthermore, the numerals in the last column (correlation dimension) represent attractor dimension changing with embedding dimension increasing. Further observing the tendency for correlation dimension, it's easily noticed that the slope of curve is much smoother with increasing embedding dimension, and as the time scale gets larger, the degree of smoothness becomes more obvious. In addition, although the largest Lyapunov exponents are positive; however, they are almost nearly equal to zero, which means that the successive traffic series, reconstructed in reconstructed spaces, should be periodic trajectories or they recur regularly day after day.

From Table 5-2 – Table 5-4, it's found that the proper embedding dimensions for 20-second flow, speed and occupancy state trajectories are around 9 and 10, which are rather high. It suggests that these 20-second traffic state trajectories exhibit much more stochastic motions than deterministic-like motions, if observed within a typical workday. Furthermore, the reason that the time delays of traffic series on different workdays, stations and time scales are always equal to one is that the AMI exhibits a fairly low value at (t+1) step, then the value doesn't drop down to zero abruptly at following steps but gradually decrease. In other words, the time delays at (t+1), (t+2),…,(t+m-1) steps are relatively small corresponding to the time delay at t = 0, thus the time delays (Table 5-1) can be considered as "one". From Table 5-3, however, it is found that the proper embedding dimensions for 1-minute flow, speed and occupancy state trajectories are reduced to 6 and 7, lower than those of 20-second measurements, in addition, in Table 5-4 the proper embedding dimensions have further reduced to 3 or 4 for the 9-minute traffic state trajectories, which indicates that an initial deterministic-like pattern would have been observed if the measured time interval gets longer.

From Table 5-5, the time delays of flow and occupancy, in contrast to those of a typical workday, are no longer equal to one. Instead, like successive time series, they

show different values with various time scales. In addition, the time delay declines with increasing time scale. Such change in time delays from one to specific values indicates that the pattern of traffic series has probably changed. For instance, road users can drive freely in the early hours as long as they don't speed, i.e., the speed state trajectory is random so that the time delay of speed-series is equal to one; embedding dimension is larger than five; the largest Lyapunov exponent is positive and correlation dimension is not saturated. However, aside from midnight (00:00-03:00), in the morning peak hours 06:00-09:00, for example, commuters' speeds are mainly confined by heavy traffic volumes, thereby the time delay is no longer equal to one, instead diverse time delays are exhibited and there is evidence for other parameters. Hence, we are convinced that the random features must have disappeared.

Apart from time delay, Table 5-5 also provides additional details regarding embedding dimension. According to the various embedding dimension in Table 5-5, the characteristics of very short-term traffic time series (e.g., 20-sec and 1-min) seemingly should be stochastic because of relatively high dimensions. Finally, like the successive traffic time series, parts of the curve for correlation dimension in Table 5-5 gradually become smooth with increasing embedding dimension, which indicates that an initial attractor has been developing to make correlation dimension be saturated. In addition, the negative values of λ_0 for flow and occupancy in the early hours suggest that flows and occupancy at such times measured in 20-second intervals should be equivalent to fixed point under steady state. Such pattern could result from the fact that traffic flow and occupancy are so lulled (very few travelers going into City) that the state trajectories eventually converge to fixed points in reconstructed state spaces.

Table 5-1 Four parameters of successive one-month traffic series

Traffic Variable	Time scales	Time delay (τ)	Embedding dimension (m)	The largest Lapunov exponent	Correlation dimension (d)
Flow	5-min	61	6	0.002	(0.87, 1.64, 2.12, 2.56, 2.85, 3.01, 3.28, 3.36, 3.64, 3.89)
	15-min	20	6	0.002	(0.87, 1.62, 2.06, 2.46, 2.80, 3.17, 3.60, 3.59, 3.87, 3.72)
	30-min	10	5	0.005	(0.88, 1.66, 2.22, 2.72, 2.83, 3.16, 3.44, 3.46, 3.59, 3.72)
	60-min	5	5	0.005	(0.88, 1.65, 2.10, 2.40, 2.46, 2.74, 2.71, 2.86, 2.74, 2.78)
Speed	5-min	84	6	0.001	(0.76, 1.49, 2.17, 2.74, 3.11, 3.33, 3.53, 3.76, 3.96, 4.13)
	15-min	27	6	0.001	(0.79, 1.53, 2.15, 2.58, 3.14, 3.14, 3.18, 3.42, 3.65, 3.89)
	30-min	13	5	0.005	(0.85, 1.64, 2.30, 2.65, 3.02, 3.13, 3.45, 3.72, 3.52, 3.70)
	60-min	6	5	0.005	(0.86, 1.65, 2.17, 2.59, 2.62, 2.75, 2.87, 3.01, 3.16, 3.17)
Occupancy	5-min	61	6	0.002	(0.52, 0.99, 1.38, 1.73, 2.03, 2.25, 2.37, 2.42, 2.45, 2.48)
	15-min	20	6	0.002	(0.70, 1.32, 1.84, 2.23, 2.48, 2.74, 3.14, 3.01, 3.01, 3.11)
	30-min	10	6	0.003	(0.81, 1.51, 2.12, 2.69, 2.55, 2.91, 3.19, 3.05, 3.25, 3.41)
	60-min	5	5	0.005	(0.79, 1.50, 2.07, 2.21, 2.45, 2.43, 2.67, 2.61, 2.76, 2.67)

Table 5-2 Parameters of 20-second traffic trajectories at different stations on a typical workday

Station	Variable	Time delay (τ)	Embedding dimension (m)	The largest Lyapunov exponent	Correlation dimension (d)
402	Flow	1	10	0.104	Not saturated
	Time-mean-speed	1	9	0.044	Not saturated
	Percent occupancy	1	9	0.101	Not saturated
404	Flow	1	9	0.085	Not saturated
	Time-mean-speed	1	9	0.097	Not saturated
	Percent occupancy	1	9	0.085	Not saturated
421	Flow	1	10	0.112	Not saturated
	Time-mean-speed	1	9	0.066	Not saturated
	Percent occupancy	1	9	0.036	Not saturated
433	Flow	1	10	0.081	Not saturated
	Time-mean-speed	1	9	0.039	Not saturated
	Percent occupancy	1	9	0.021	Not saturated

Table 5-3 Parameters of 1-minute traffic trajectories for five workdays (station 433)

Date	Variable	Time delay (τ)	Embedding dimension (m)	The largest Lyapunov exponent	Correlation dimension (d)
2004.02.02	Flow	1	7	0.108	Not saturated
	Time-mean-speed	1	6	0.076	Not saturated
	Percent occupancy	1	6	0.067	Not saturated
2004.02.04	Flow	1	7	0.121	Not saturated
	Time-mean-speed	1	6	0.085	Not saturated
	Percent occupancy	1	6	0.057	Not saturated
2004.02.06	Flow	1	7	0.134	Not saturated
	Time-mean-speed	1	6	0.085	Not saturated
	Percent occupancy	1	6	0.073	Not saturated
2004.02.11	Flow	1	7	0.127	Not saturated
	Time-mean-speed	1	6	0.077	Not saturated
	Percent occupancy	1	6	0.075	Not saturated
2004.02.12	Flow	1	6	0.164	Not saturated
	Time-mean-speed	1	6	0.078	Not saturated
	Percent occupancy	1	6	0.062	Not saturated

Table 5-4 Parameters of traffic trajectories measured with various time scales on a typical workday (station 433)

Time scale	Variable	Time delay (τ)	Embedding dimension (m)	The largest Lyapunov exponent	Correlation dimension (d)
20-second	Flow	1	10	0.081	Not saturated
	Time-mean-speed	1	9	0.039	Not saturated
	Percent occupancy	1	9	0.021	Not saturated
1-minute	Flow	1	7	0.121	Not saturated
	Time-mean-speed	1	6	0.085	Not saturated
	Percent occupancy	1	6	0.057	Not saturated
3-minute	Flow	1	4	0.198	Not saturated
	Time-mean-speed	1	4	0.201	Not saturated
	Percent occupancy	1	4	0.120	Not saturated
9-minute	Flow	1	4	0.216	Not saturated
	Time-mean-speed	1	3	0.320	Not saturated
	Percent occupancy	1	3	0.273	Not saturated

Table 5-5 Parameters of ten-workday traffic trajectories measured in various time scales and intervals (station 433)

	Time interval	Time scale	Time delay	Embedding dimension (m)	λ_0	Correlation dimension
flow	00:00-03:00	20-sec	234	(6~7)	-0.002	(0.4,0.9,1.3,1.7,2.1,2.6,3.0,3.3,3.3,3.3)
		1-min	77	(6~7)	0.003	(0.4,0.8,1.2,1.6,2.0,2.4,2.5,2.8,3.1,3.5)
		3-min	26	(5~6)	0.005	(0.5,0.9,1.3,1.7,2.1,2.6,2.7,2.9,3.0,3.1)
		9-min	9	4	0.009	(0.5,0.9,1.2,1.5,1.6,1.8,1.9,2.1,2.4,2.5)
	06:00-09:00	20-sec	129	(10~11)	0.004	(0.8,1.5,2.1,2.7,3.3,3.8,4.3,4.5,4.9,5.5)
		1-min	42	(8~9)	0.006	(0.8,1.6,2.2,2.8,3.4,3.8,4.0,4.5,4.7,4.8)
		3-min	14	5	0.009	(0.8,1.5,2.1,2.4,2.6,2.8,2.8,3.0,3.2,3.4)
		9-min	4	4	0.010	(0.8,1.4,1.9,2.0,2.4,2.6,2.7,2.8,3.1,3.3)
	12:00-15:00	20-sec	246	(12~13)	0.002	(0.7,1.4,2.0,2.6,3.3,3.9,4.6,5.1,5.4,6.0)
		1-min	82	(10~11)	0.005	(0.8,1.6,2.3,2.8,3.3,3.6,4.4,4.7,4.8,5.3)
		3-min	28	(8~9)	0.011	(0.8,1.6,2.4,3.1,3.9,4.0,4.4,4.6,4.7,4.9)
		9-min	10	(8~9)	0.014	(0.9,1.8,2.6,3.2,3.6,3.9,4.1,4.1,4.2,4.4)
	18:00-21:00	20-sec	182	(10~11)	0.005	(0.7,1.5,2.2,2.9,3.3,4.0,4.3,4.5,5.1,5.6)
		1-min	62	(10~11)	0.007	(0.8,1.6,2.4,3.1,3.6,4.3,4.6,4.8,5.2,5.3)
		3-min	21	7	0.009	(0.9,1.7,2.2,2.5,2.8,2.9,3.2,3.3,3.6,3.7)
		9-min	7	6	0.012	(0.8,1.5,2.0,2.2,2.5,2.7,2.8,3.1,3.3,3.5)
speed	00:00-03:00	20-sec	1	12	0.02	Not saturated
		1-min	1	8	0.08	Not saturated
		3-min	1	6	0.04	Not saturated
		9-min	1	5	0.05	Not saturated
	06:00-09:00	20-sec	115	8	0.006	(0.6,1.2,1.7,2.3,2.8,3.3,3.8,4.1,4.4,4.5)
		1-min	38	6	0.007	(0.6,1.1,1.6,2.1,2.6,3.1,3.4,3.5,3.6,3.9)
		3-min	13	5	0.008	(0.6,1.1,1.5,2.0,2.4,2.7,2.8,2.9,3.0,3.0)
		9-min	5	5	0.009	(0.6,1.0,1.3,1.6,1.9,2.1,2.2,2.2,2.2,2.2)
	12:00-15:00	20-sec	92	10	0.001	(0.5,0.9,1.4,1.8,2.3,2.8,3.2,3.6,4.0,4.6)
		1-min	32	7	0.003	(0.5,0.9,1.3,1.7,2.2,2.6,3.0,3.3,3.7,4.0)
		3-min	10	6	0.005	(0.4,0.7,1.0,1.4,1.7,2.0,2.3,2.6,2.7,2.8)
		9-min	5	5	0.006	(0.3,0.6,0.8,1.1,1.3,1.5,1.6,1.9,2.1,2.2)
	18:00-21:00	20-sec	149	10	0.009	(0.7,1.4,2.1,2.8,3.5,4.1,4.8,5.0,5.6,5.8)
		1-min	60	8	0.013	(1.0,1.4,2.1,2.8,3.6,4.2,4.7,5.0,5.2,5.6)
		3-min	20	4	0.028	(0.8,1.6,2.4,3.2,3.8,4.1,4.6,4.9,5.2,5.5)
		9-min	8	4	0.029	(0.8,1.8,2.7,3.5,3.7,4.1,4.,0,4.1,4.2,4.2)
occupancy	00:00-03:00	20-sec	231	(7~8)	-0.001	(0.6,0.9,1.5,1.9,2.2,2.7,3.2,3.2,3.2,3.2)
		1-min	77	(7~8)	0.003	(0.5,0.8,1.4,1.7,2.1,2.5,3.0,3.2,3.5,3.7)
		3-min	26	(6~7)	0.004	(0.5,0.8,1.4,1.7,2.3,2.6,3.1,3.2,3.5,3.9)
		9-min	9	5	0.010	(0.5,0.8,1.4,1.6,2.2,2.8,2.9,3.1,3.4,3.8)
	06:00-09:00	20-sec	115	(8~9)	0.004	(0.8,1.6,2.2,2.6,3.3,3.7,4.1,4.3,4.6,4.9)
		1-min	39	(7~8)	0.006	(0.8,1.6,2.2,2.8,3.4,3.8,3.9,4.3,4.7,4.8)
		3-min	13	6	0.011	(0.8,1.5,2.4,2.7,3.2,3.3,3.3,3.4,3.5,3.6)
		9-min	5	5	0.013	(0.7,1.4,1.8,2.2,2.5,2.8,3.0,3.0,3.1,3.3)
	12:00-15:00	20-sec	89	(8~9)	0.002	(0.7,1.4,1.7,2.2,2.3,2.8,3.4,3.7,3.9,4.0)
		1-min	30	(6~8)	0.004	(0.8,1.5,1.8,2.2,2.4,2.6,3.2,3.4,3.4,3.5)
		3-min	10	5	0.009	(0.8,1.4,1.7,2.1,2.3,2.5,2.6,2.8,3.1,3.4)
		9-min	5	4	0.010	(0.6,0.8,1.6,1.8,2.3,2.4,2.6,2.6,2.6,2.7)
	18:00-21:00	20-sec	182	(9~10)	0.009	(0.7,1.5,2.2,2.5,3.2,3.4,3.6,3.8,3.9,4.2)
		1-min	60	6	0.011	(0.8,1.5,1.8,2.4,2.6,2.8,3.4,3.6,3.8,3.9)
		3-min	20	5	0.02	(0.8,1.6,1.9,2.3,2.5,2.7,3.2,3.3,3.6,3.7)
		9-min	7	5	0.02	(0.6,1.3,1.6,1.8,2.2,2.5,2.6,2.8,2.8,2.9)

5.3 Some Observed Details for Paired- and Three-variable Traffic Evolutions

The above empirical study has not only demonstrated the traffic patterns by mapping the 1-D traffic series into 3-D state spaces, but has also estimated the most appropriate time delay and embedding dimensions for real-world traffic series. Apart from these, the present study further compares the paired (speed-flow, speed-occupancy, and flow-occupancy) traffic features with and without relation to the sequential order. Figure 5-8 illustrates the 9-minute paired-traffic features on a typical workday (station 421). From the upper panel (without sequential order), one can at most figure out the relationships between speed-flow, speed-occupancy and flow-occupancy. However, these relationships do not explain the detailed evolution of traffic behaviors. From the lower panel (with sequential order), in contrast, we can trace the detailed evolution of traffic behaviors. Obviously, sequential order is taken into consideration and more detailed information on traffic evolution dynamics can be found, which could help understand the possible causes of formation of congested traffic phase in such a way that one could propose more effective traffic managements, e.g., regulation of low-speed vehicles in free-flow phase, determination of start-up for ramp metering, and so on.

To illustrate the more detailed information, we trace some selected points to elucidate the daily evolution of the 9-minute paired-traffic by observing the chronological order of speed-flow diagram. We start with the first point in the early hours at time 01:12 (flow: 7 vehicles/9-min, speed: 101 kph) at the upper left corner indicating a free traffic phase. As time evolves, the dynamics of speed-flow advances along a southeast direction to the second point in the morning peak hours at time 08:25 (289 vehicles/9-min, 80 kph), which moves southbound to the third point near noon at time 11:58 (313 vehicles/9-min, 60 kph) indicating a congested traffic phase. After that, the dynamics moves back and forth in the middle of diagram, representing phase transitions, during the day-time off-peak hours, e.g., the fourth point at time 15:12 (129 vehicles/9-min, 87 kph). After the afternoon peak hours the dynamics of speed-flow returns to the original upper left corner (free traffic phase); e.g., the fifth point at time 23:08 (48 vehicles/9-min, 97 kph).

In the light of the sequential order of speed-flow dynamics, we can see that congestion or near congestion can easily formulate as traffic switches from a high-speed, low-volume free-flow phase to an irregular moderate-speed, moderate-volume synchronized phase or the low-speed, low-volume congested phase. In reality, the

transition occurs whenever the occupancy has exceeded a critical level. Once the traffic dynamics enters the congestion phase, it takes a long time for traffic to return to free-flow, and meanwhile delay accumulates. We also notice that from Figure 5-8 there is a sixth point in the early hours at time 02:22 (136 vehicles/9-min, 53 kph) which indicates a relatively slow traffic flow, an outlier for free flow. It could have arisen from erratic driver behaviors, heterogeneous vehicle performances, any other incident or all at the same time. In contrast to Figure 5-8, the paired-traffic in Figure 5-9 seems to be quite fluent. From the locations at station 433 and station 421, one can definitely know that commuters regularly drive vehicles to work from their origin through station 433 to the destination (station 421) in the morning peak-hour. Such situations have caused congestion or near congestion traffic phase at station 421. Although a congestion traffic phase, i.e., high volume (235 vehicles/9-min), low speed (30 kph), high occupancy (33.1%) can also be seen at station 433 at rush hour, the congested traffic phase disappears after morning peak-hours. Compared with station 433, the congested traffic phase at station 421 doesn't disappear instantaneously but get worse because of the tremendous number of vehicles continuously coming from on-ramps. Hence, for seriously congested locations, such as station 421, had a rapid detection system successfully diagnosed the recurring congestions and a smart control measure actuated accordingly, the congestions have been immediately mitigated or alleviated.

In a similar way, three-variable traffic (flow-speed-occupancy) dynamics in three-dimensions is shown in Figure 5-10. The trajectory moves from the coordinate (flow = 0, speed = 100, occupancy = 0), advances along a diagonal direction, i.e., coordinate (flow = 350, speed = 40, occupancy = 50) till morning peak hours, when it moves back and forth as time evolves. Finally, similar to the one-day dynamics, the trajectory moves back to the original coordinate. In order to understand the progression in traffic dynamics, the dotted lines in Figure 5-10 represent those speeds less than 70 kph, and they appear intermittently among the straight lines which speed is over than 70 kph. It suggests that the quality of traffic flow progresses in a moderately dense platoon, in which traffic cannot move smoothly, but moves in a stop and go motion. If traffic data is collected from upstream ahead of a bottleneck, some trajectories of dotted lines would probably not appear intermittently, but show together in some part of space. Obviously, from traffic control and management practice perspectives depicting traffic characteristics with three variables simultaneously and with sequential order in three dimensional spaces is more subtle than just presenting any of these three variables in one-dimensional space.

Summarizing, the speed-flow dynamical graphs with sequential order can not only interpret the conventional speed-flow relationship but also present details of traffic phase-transition, which could provide more useful information for management and control purposes. Similarly, Figure 5-8 and Figure 5-9 have been used to compare graphical data for the dynamics of speed-occupancy and flow-occupancy without sequential order and with sequential order. From the above observations, we have learned that there are various traffic phases under normal circumstance: a free flow phase, which typically takes place in the early hours; a moving jam phase, which typically happens in the peak periods; and a synchronized traffic phase, a repeated back and forth transition, which more likely coexists with a moving jam.

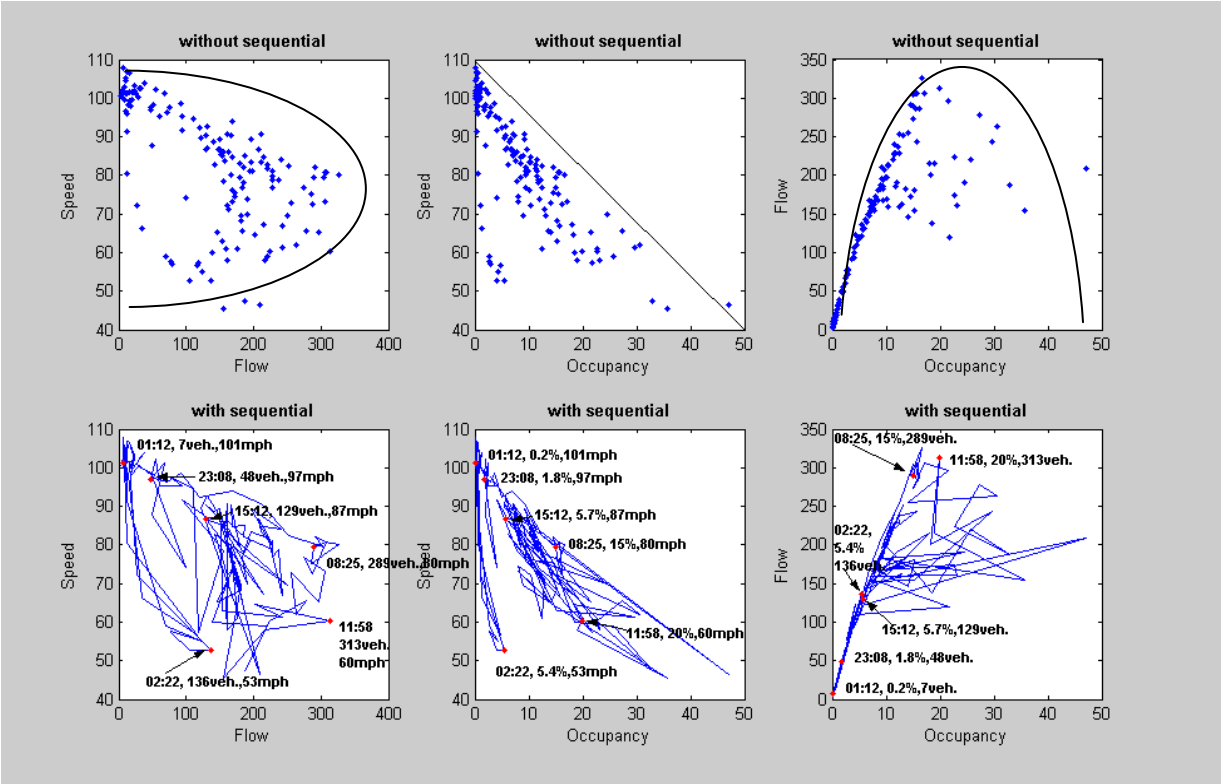

Figure 5-8 The paired-traffic relationship and dynamics (station 421, 2004.02.04)

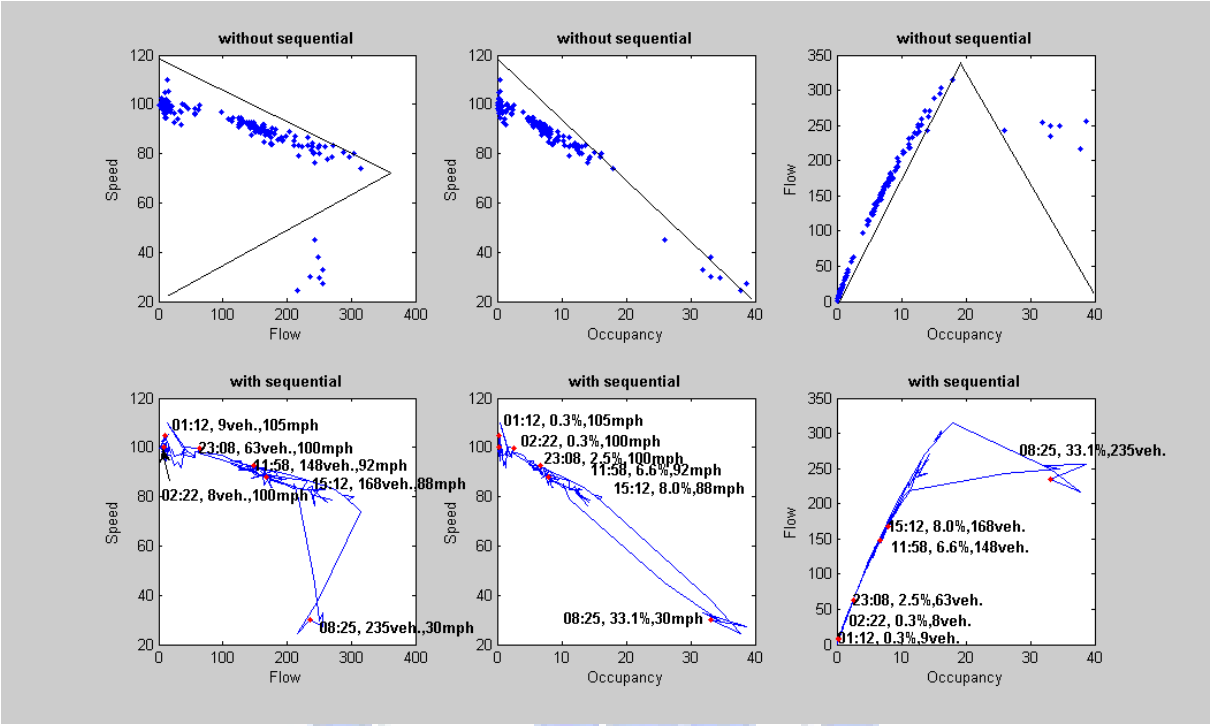

Figure 5-9 The paired-traffic relationship and dynamics (station 433, 2004.02.04)

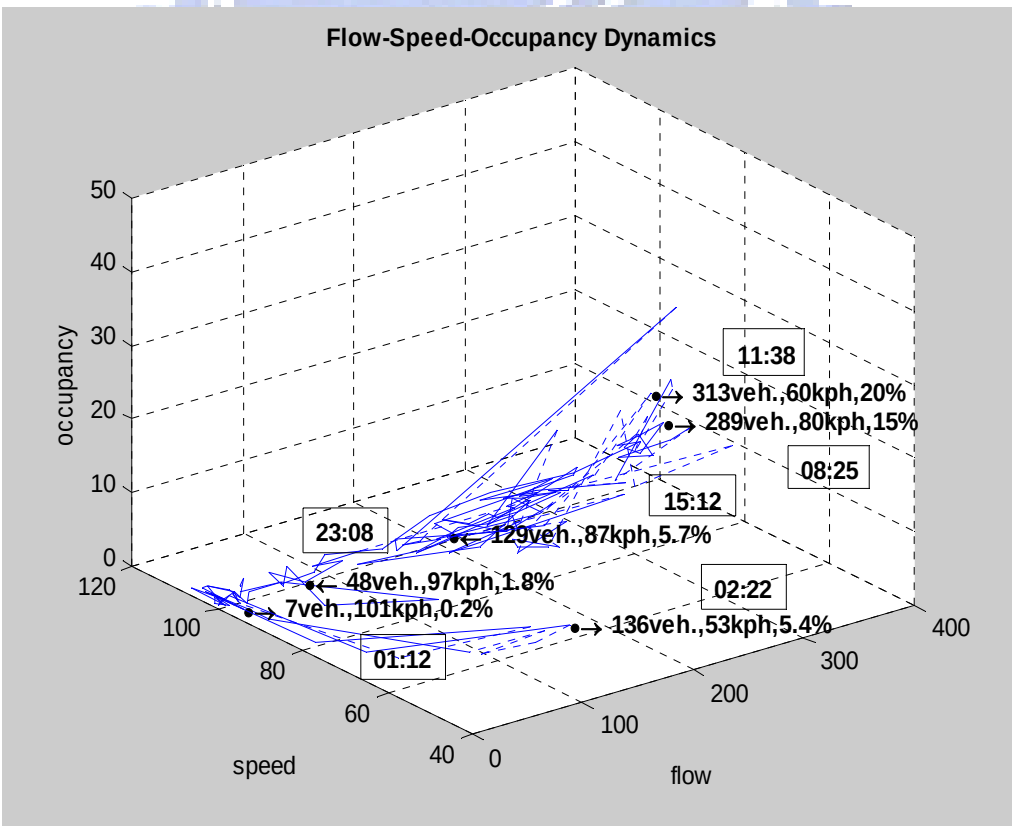

Figure 5-10 The flow-speed-occupancy dynamics in three-dimensions

5.4 Sensitivity Analysis for Short-term Prediction

After entirely elucidating the temporal features of traffic dynamics in multi-dimensional spaces as well as the paired- and three-variable traffic evolutions, we would like to further take advantage of the analytic results to obtain better accuracy on predicting the future short-term traffic dynamics. Here, we adopted two techniques, radial basis function neural network (RBFNN) and real-time recurrent learning (RTRL) algorithm, to execute sensitivity analysis with manipulating different time intervals, time lags and times of day. The main reason for choosing the RBF neural network as well as RTRL algorithm to train a nonlinear traffic dynamics is that both of the RBF and RTRL algorithms can iteratively modify performance errors and update its weighted parameters to meet the characteristics of traffic dynamics, which is neither deterministic nor complete random series but exhibits various features with times of day instead. In addition, many disadvantages pertaining to original techniques, such as determining center neurons randomly in the beginning of iterations and undesirable convergence characteristics, have also been improved. Therefore, among the neural network techniques, the RBFNN and RTRL algorithms are effective tools available to predict nonlinear time series, both for long-interval and short-interval traffic dynamics.

Since flow, speed and occupancy time series carry different units and cover a diverse range, it makes no sense to compare their relative predictive accuracies by the criterion of *RMSE*. For comparison purposes, therefore, all the traffic data studied were standardized using Eq. (5.1).

$$\widetilde{x}_i = \frac{x_i - x_{\min}}{x_{MAX} - x_{\min}}, \quad i = 1,2,\ldots, N \tag{5.1}$$

where x_i is the i^{th} observed data point; x_{min} is the minimum in observed points; x_{MAX} is the maximum in observed points; $\widetilde{x}_i$ is the i^{th} standardized data point. The prediction results for flow, speed, and occupancy series measured in different time intervals, time lags, and times of day, are detailed as follows.

5.4.1 Various Intervals

Before a network is trained, it's necessary to clarify the input and output of the neural network. For RBFNN, according to Lan *et al* (2007d) the traffic series measured with time lag (=1) in three-dimensional state spaces provides a satisfying training effect. Namely, the input vector is $[\widetilde{x}(t-3), \widetilde{x}(t-2), \widetilde{x}(t-1)]$; output vector is $\widetilde{x}(t)$, where

$\tilde{x}(t)$ represents the standardized traffic data at time *t*. For RTRLNN, the input vector is $\tilde{x}(t-1)$ and the output vector is $\tilde{x}(t)$, wherein the network output at time *t* consists of the current input vector $\tilde{x}(t-1)$ and network outputs of the previous layer. At station 433, the number of lane-base data points to be analyzed were 1,440 and 480 respectively, for 1-minute and 3-minute traffic series, thus a 24-hour workday (2004.02.04) data set was selected for training and another 24-hour workday (2004.02.12) data set for testing. At station N27.9, we also used 1,440 and 480 approach-base data points for 5-minute and 15-minute traffic series, respectively, thus a consecutive five-workday (2004.02.09 ~ 2004.02.13) data set was selected for training and another consecutive five-workday (2004.02.16 ~ 2004.02.20) data set for testing.

The results of prediction are summarized in Table 5-6 and Table 5-7. From the tables, all of the *RMSE*s are sufficiently small to show that both the RTRL and RBFNN model are highly satisfactory in predicting the real-world short-term traffic series. Figure 5-11 and Figure 5-12 depict the difference between network outputs and observed values by adopting RTRL algorithms, in which a portion of the data points are picked deliberately to clearly depict the differences in the lower panel. However, it is noted that in Figure 5-13 the curve of difference using the RTRL model oscillates up and down more significantly than the curve of difference using the RBF model for the first fifteen steps or even longer period. Such oscillations are similar to our preliminary testing demonstrated in the above chapter. In addition, due to the convergent ability of the RTRL network, the average predictability for RTRL networks and for RBFNN is about the same. Further comparing the *RMSE*s in more detail, we find that for both RTRL networks and RBF networks, the $RMSEs_{(3\text{-min})}$ are smaller than the $RMSEs_{(1\text{-min})}$; similarly, the $RMSEs_{(15\text{-min})}$ are smaller than the $RMSEs_{(5\text{-min})}$. The findings suggest that the predictive accuracy for traffic dynamics measured in longer time intervals is better than those measured in shorter intervals.

Table 5-6 Prediction results of traffic series measured in different time intervals (station 433)

Time interval	Traffic variable	Time lag τ	RTRL-*RMSE*		RBF- *RMSE*	
			train (2004.02.04)	test (2004.02.12)	train (2004.02.04)	test (2004.02.12)
1-minute	flow	1	0.0943	0.1049	0.0851	0.0907
	speed	1	0.0510	0.0600	0.0556	0.0678
	occupancy	1	0.0566	0.0600	0.0433	0.0477
3-minute	flow	1	0.0787	0.0800	0.0593	0.0734
	speed	1	0.0500	0.0600	0.0547	0.0555
	occupancy	1	0.0510	0.0557	0.0392	0.0458

Table 5-7 Prediction results of traffic series measured in different time intervals (Station N27.9)

Time interval	Traffic variable	Time lag τ	RTRL-*RMSE*		RBF-*RMSE*	
			train (2004.02.09-2004.02.13)	test (2004.02.16-2004.02.20)	train (2004.02.09-2004.02.13)	test (2004.02.16-2004.02.20)
5-minute	flow	1	0.0671	0.0686	0.0819	0.0623
	speed	1	0.0574	0.0640	0.0624	0.0587
	occupancy	1	0.0806	0.0500	0.0494	0.0549
15-minute	flow	1	0.0663	0.0648	0.0620	0.0602
	speed	1	0.0449	0.0574	0.0590	0.0575
	occupancy	1	0.0755	0.0475	0.0428	0.0513

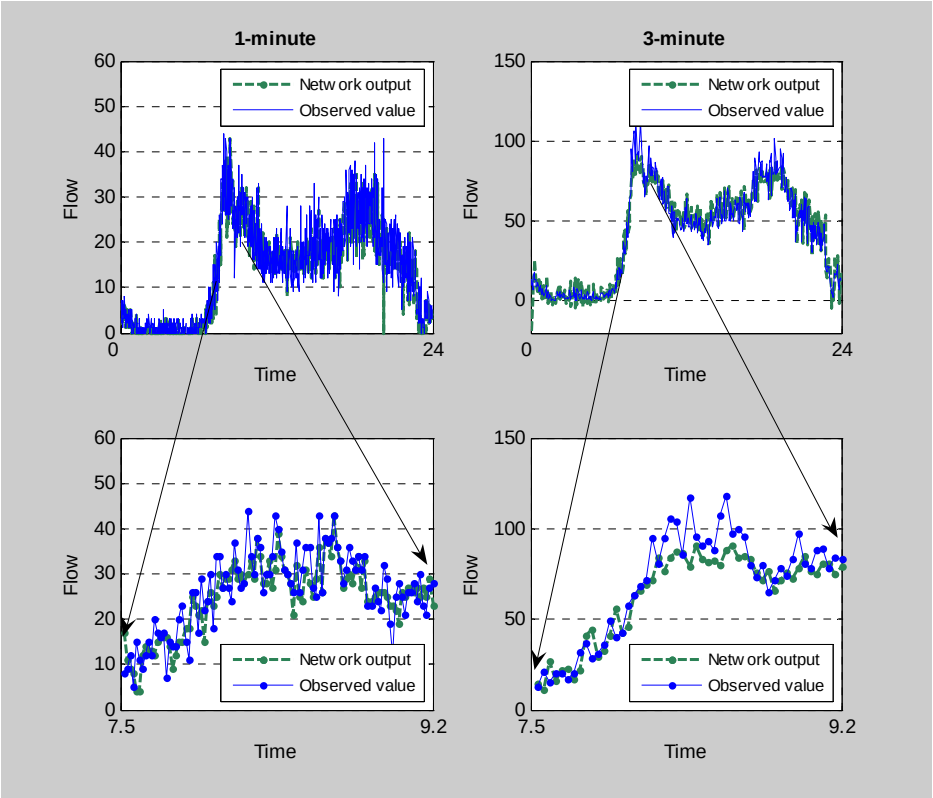

Figure 5-11 The RTRL network outputs and observed values of flows measured in different time intervals (Station 433)

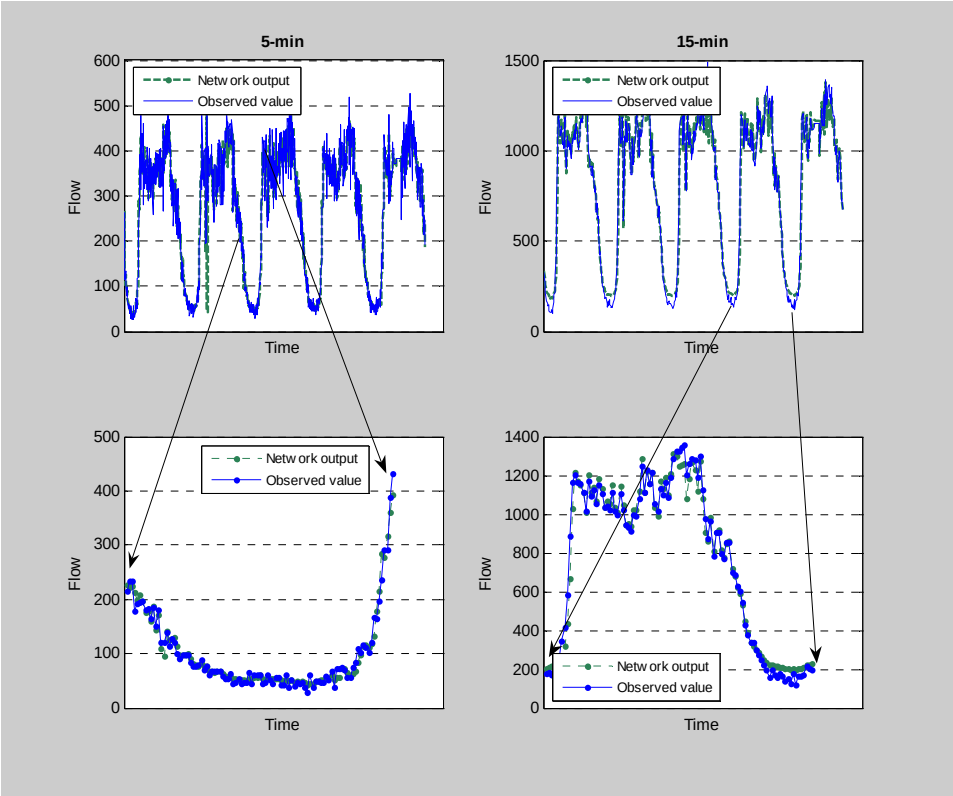

Figure 5-12 The RTRL network outputs and observed values of flows measured in different time intervals (Station N27.9)

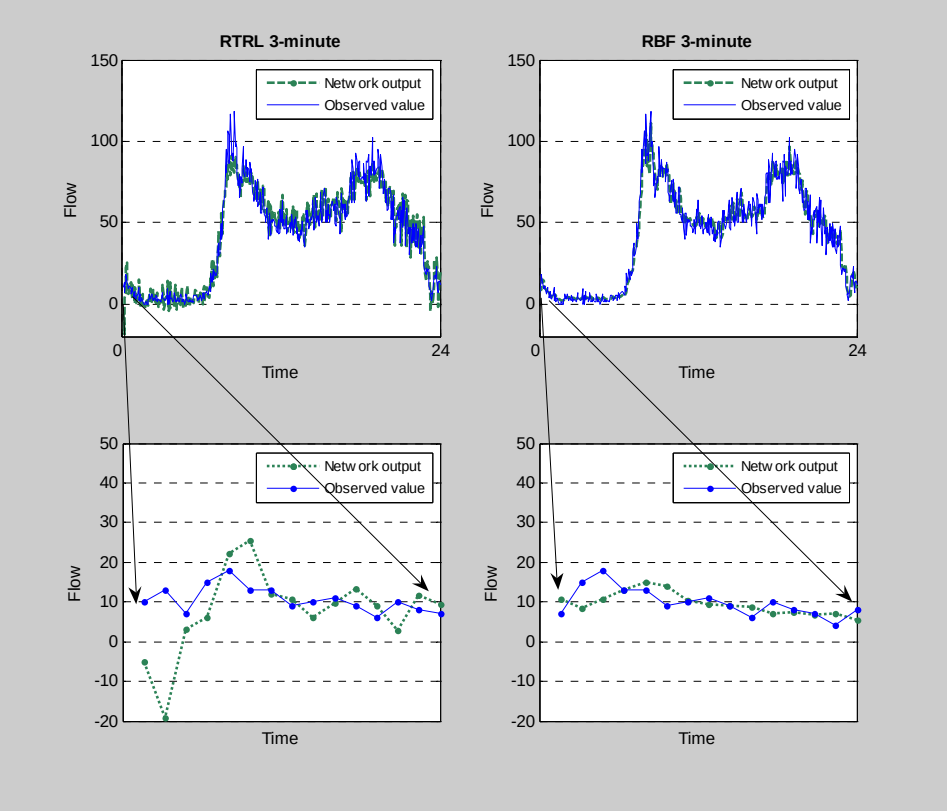

Figure 5-13 The RTRL and RBF network outputs and observed values of flows measured in 3-minute intervals for the first 15 steps

5.4.2 Various Lags

As mentioned previously, it is important to determine a proper time lag τ when analyzing time series, especially when the time series in one-dimension is mapped into multidimensional spaces. For the RTRL algorithms and RBFNN, it is postulated that the training process is a sequential learning scheme and that the traffic time series at time t and at time (t+1) have relevant dependence, i.e., the time series is a first-order process or Markov process. Therefore, in this study, when considering the vector $[x(t-(q-1)\tau),...,x(t-\tau)]$ as inputs and using the input vector to predict the desired value, $x(t)$, we set $\tau = 1$. Nevertheless, would the accuracy of prediction be better if we used other time lags? For instance, for a deterministic function, using the Mackey-Glass equation with a time lag $\tau = 6$ would produce the best accuracy of prediction compared with adopting other time lags.

Accordingly, Table 5-8 shows the prediction results for various time lags. For traffic data sets with 1-minute and 3-minute intervals, we find that the prediction accuracy declines with increasing time lags for both RTRL algorithms and RBFNN, i.e., $RMSE_{(\tau=1)} < RMSE_{(\tau=2)} < RMSE_{(\tau=3)}$. Likewise, for traffic data sets with 5-minute and 15-minute intervals, the prediction accuracy also declines with increasing time lags, i.e., $RMSE_{(\tau=1)} < RMSE_{(\tau=\frac{1}{2}\text{ time delay})} < RMSE_{(\tau=\text{time delay})}$, except for one RBF case marked in gray ($RMSE$_flow_15-minute$_{(\tau=\text{time delay})} <$ $RMSE$_flow_15-minute$_{(\tau=\frac{1}{2}\text{ time delay})}$).

Table 5-8 Prediction results of traffic dynamics for various time lags using RTRL and RBF

Time interval	Traffic variable	Time lag	*RMSE*		Time lag	*RMSE*		Time lag	*RMSE*	
			RTRL	RBF		RTRL	RBF		RTRL	RBF
1-minute (one workday, station 433)	flow	1	0.0943	0.0851	2	0.0968	0.0960	3	0.0979	0.1074
	speed	1	0.0510	0.0556	2	0.0632	0.0606	3	0.0669	0.0655
	occupancy	1	0.0566	0.0433	2	0.0612	0.0458	3	0.0677	0.0466
3-minute (one workday, station 433)	flow	1	0.0787	0.0593	2	0.0790	0.0659	3	0.0792	0.0679
	speed	1	0.0500	0.0547	2	0.0547	0.0666	3	0.0727	0.0754
	occupancy	1	0.0510	0.0392	2	0.0599	0.0471	3	0.0662	0.0576
5-minute (five workdays, station N27.9)	flow	1	0.0686	0.0623	30	0.1897	0.0911	60	0.1947	0.1023
	speed	1	0.0640	0.0587	42	0.0984	0.1484	84	0.0998	0.1718
	occupancy	1	0.0500	0.0549	30	0.0870	0.0951	60	0.0895	0.1009
15-minute (five workdays, station N27.9)	flow	1	0.0648	0.0602	10	0.2011	0.093	20	0.2829	0.0898
	speed	1	0.0574	0.0575	13	0.1024	0.0903	27	0.1062	0.1266
	occupancy	1	0.0557	0.0513	10	0.1171	0.0748	20	0.1384	0.0763

The above results seem to indicate that the characteristics of short-interval traffic dynamics extracted from real world detectors measured within 15-minute intervals and involving numerous noises are more stochastic than deterministic; therefore, in the prediction of nonlinear short-interval traffic dynamics, stochastic characteristics can be stronger than deterministic characteristic which is similar to the famous Mackey-Glass equation. Nevertheless, the only one exception for RBF model in Table 5-8 reveals that the 15-minute flows have shown a slight tendency towards deterministic characteristics, so a better accuracy of prediction for 15-minute flows using a proper time lag (i.e., time delay) occurs, compared to using half time delay. However, with regard to RTRL, owing to its real-time recurrent algorithms, the prediction accuracy significantly declines with increasing time lags. Figure 5-14 presents the differences between RTRL network outputs and observed values of flows for various time lags. In this Figure, the same training data as Chapter 4 was employed; but only a portion of data points are picked deliberately to clearly depict the differences.

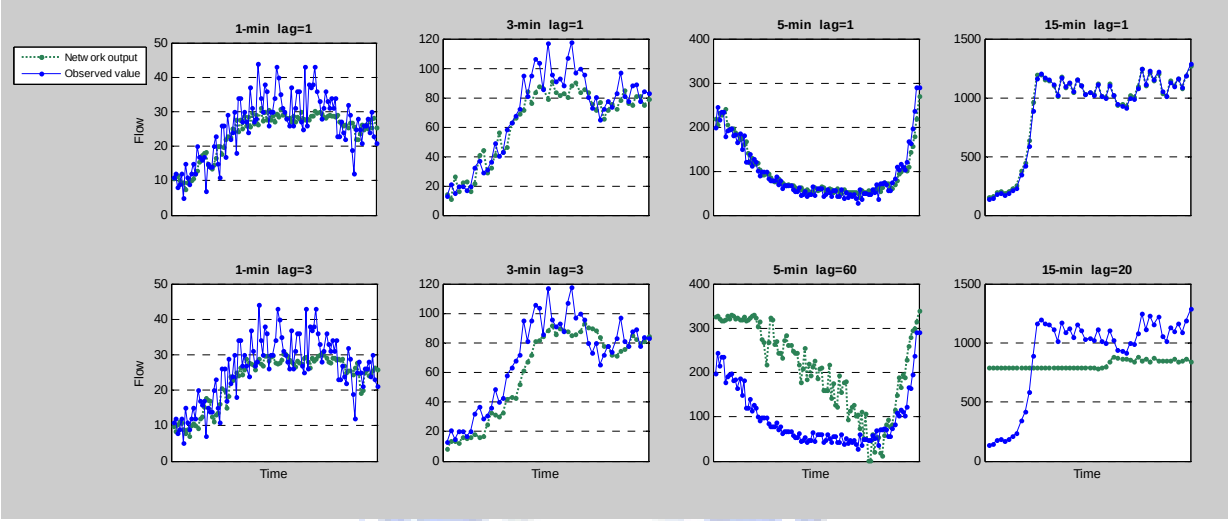

Figure 5-14 The RTRL network outputs and observed values of flows for various time lags

5.4.3 Various Times of Day

Although different time intervals and time lags have been investigated above, the most interesting aspects applicable for practical prediction of traffic dynamics are to detect when the most necessary time-of-day is to predict and how to improve their accuracy. In general, doing efforts on precise prediction of traffic dynamics in the real world should solve more important issues, such as the daily recurrent congestions during rush hours. In other words, in view of efficient management, what we mostly need to predict is a “critical” span that may cause serious traffic jams rather than prediction for a long period of time, such as twenty-four hours. Based on this, in this subsection, we

attempt to identify the most critical times-of-day for prediction and how to improve the prediction accuracy. Accordingly, we tested the proposed algorithms using different data sets collected in times of day. Table 5-9 provides the corresponding prediction results. Observed from this table, we find that the values of *RMSE* in four time periods are different. In terms of 1-minute flow, for RBFNN, the results are $RMSE_{(18:00\text{-}21:00)} > RMSE_{(06:00\text{-}09:00)} > RMSE_{(12:00\text{-}15:00)} > RMSE_{(00:00\text{-}03:00)}$. Likewise, other 3-minute traffic variables, speed and occupancy, also have different *RMSE* values, depending on various time periods. Corresponding results for an RTRL network are $RMSE_{(18:00\text{-}21:00)} > RMSE_{(06:00\text{-}09:00)} > RMSE_{(00:00\text{-}03:00)} > RMSE_{(12:00\text{-}15:00)}$ which compared with the values of *RMSE*, it's noted that the order of $RMSE_{(00:00\text{-}03:00)}$ and $RMSE_{(12:00\text{-}15:00)}$ are reversed. This is because an oscillation often occurs during the beginning steps whenever one adopts the RTRL algorithms to train a network, hence the $RMSE_{(00:00\text{-}03:00)} > RMSE_{(12:00\text{-}15:00)}$. Such results may reveal that in general the morning and evening peak-hour periods remain the most critical for accurate prediction compared to other periods because serious jams are constantly incurred during such periods. Figure 5-15 illustrates the difference between RTRL outputs and observed values of flows during various periods of time in a workday (2004.02.04) at station 433.

To improve the accuracy of prediction during peak-hours, a feasible method is to train a network that only consists of historical data for a specific time period, e.g., 06:00 – 09:00 or 18:00 – 21:00, in other words, to predict traffic dynamics at the same time period rather than to train a whole-day network to predict a specific time period of traffic dynamics. Table 5-10 illustrates the improved prediction results using this feasible method. It indicates that the prediction performance obtained from the network of historical data at specific time periods is better than that obtained from a whole-day network, that is $RMSE_{(8days\_1\text{-}min\_06:00\text{-}09:00)} < RMSE_{(1day\_1\text{-}min\ 00:00\text{-}24:00)}$ and $RMSE_{(8days\_3\text{-}min\_06:00\text{-}09:00)} < RMSE_{(1day\_3\text{-}min\ 00:00\text{-}24:00)}$.

Table 5-9 Prediction results of traffic dynamics during different time periods (Station 433)

Time period	Traffic variable	Time lag	*RMSE*(1-min)		*RMSE*(3-min)	
			RTRL	RBF	RTRL	RBF
00:00-03:00	flow	1	0.0653	0.0322	0.0548	0.0213
	speed	1	0.0510	0.0479	0.0493	0.0395
	occupancy	1	0.0411	0.0101	0.0338	0.0082
06:00-09:00	flow	1	0.1187	0.0954	0.1022	0.0755
	speed	1	0.0533	0.0673	0.069	0.0603
	occupancy	1	0.0864	0.0538	0.0851	0.0499
12:00-15:00	flow	1	0.0693	0.0941	0.0532	0.0582
	speed	1	0.0405	0.0391	0.0286	0.0305
	occupancy	1	0.0401	0.0414	0.0315	0.0298
18:00-21:00	flow	1	0.1258	0.1142	0.1059	0.0812
	speed	1	0.0638	0.059	0.0558	0.0586
	occupancy	1	0.0732	0.0647	0.0647	0.0527

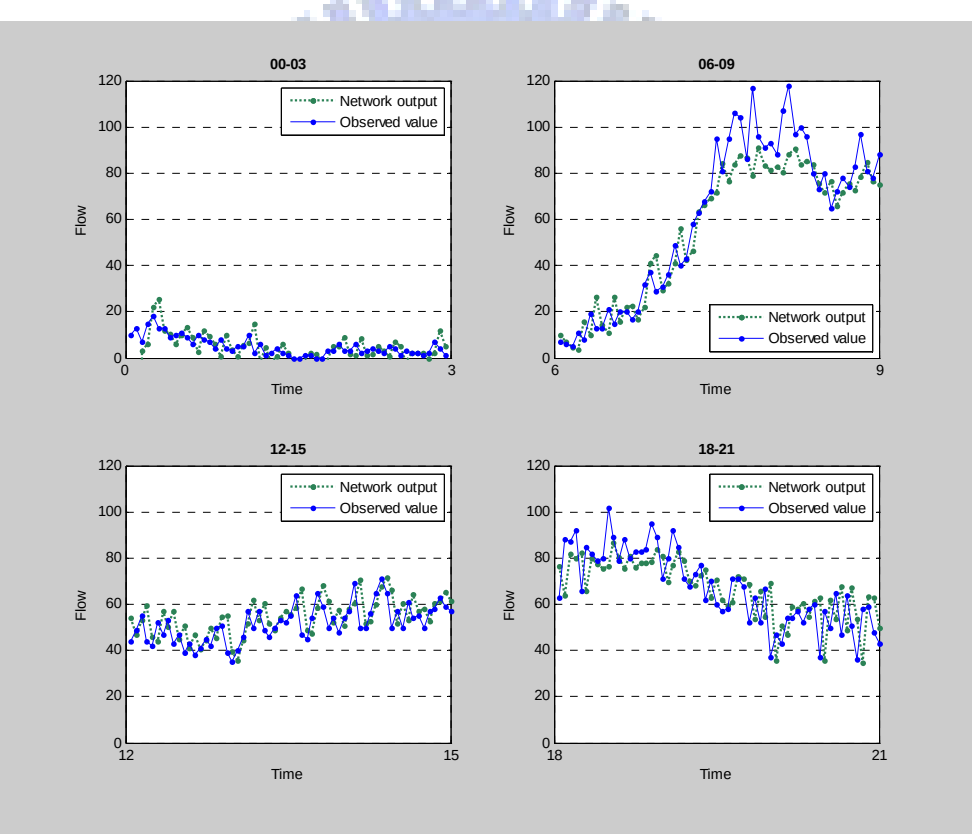

Figure 5-15 The difference between RTRL network outputs and observed values of flows during various time periods (station 433)

Table 5-10 Prediction results based only on peak-hours traffic data for network training

Time period	Traffic variable	Time lag	*RMSE* (1-day,1-min)		*RMSE* (1-day,3-min)		*RMSE* (8-days,1-min)		*RMSE* (8-days,3-min)	
			RTRL	RBF	RTRL	RBF	RTRL	RBF	RTRL	RBF
06:00	flow	1	0.1187	0.0954	0.1022	0.0755	0.0908	0.0742	0.0845	0.0645
-	speed	1	0.0533	0.0673	0.0690	0.0603	0.0501	0.0667	0.0461	0.0568
09:00	occupancy	1	0.0864	0.0538	0.0851	0.0499	0.0694	0.0531	0.0674	0.0414
18:00	flow	1	0.1258	0.1142	0.1059	0.0812	0.1006	0.0812	0.0882	0.0711
-	speed	1	0.0638	0.0590	0.0558	0.0586	0.0594	0.0511	0.0501	0.0485
21:00	occupancy	1	0.0732	0.0647	0.0647	0.0527	0.0562	0.0366	0.0510	0.0334

5.4.4 Various Dimensions

The above analyses are based on input vectors of three dimensions and output vectors of one dimension to examine the prediction results of traffic dynamics measured in various time intervals for various time lags. In reality, more information can be obtained by mapping the traffic time series into higher-dimensional spaces (see, for example, Lan, *et al.*, 2007c), thus varying the input dimensions is also attempted in the present study. Table 5-11 summarizes the variety of prediction results for RBFNN with various input dimensions. According to the *RMSE*s in this table, it is found that the smallest *RMSE* for traffic dynamics with 1-minute and 3-minute intervals is located on input vectors of four dimensions, while the smallest *RMSE* for flow and percent occupancy with 5-minute and 15-minute intervals is located on input vectors of three dimensions. This finding provides us with a useful rule that, in general, the traffic time series measured in shorter intervals (e.g., 1-minute and 3-minute) would need higher dimensional inputs to train in order to acquire a good prediction; in contrast, longer-interval traffic time series (e.g., 5-minute and 15-minute) would produce a good prediction as long as lower dimensional inputs are used if the RBF algorithm was adopted to train a network.

In sum, in terms of RBFNN, for short-interval (within 15-minute) traffic dynamics, multidimensional inputs of at least two dimensions are needed. Depending on the purposes or objectives the researchers would like to achieve, if high accuracy of prediction is desired with no concern for the training time, high-dimensional inputs (say, four or five dimensions) are recommended for short-interval traffic dynamics. Yet, if one hopes to consider both the accuracy and training time, lower-dimensional inputs (say, three dimensions) are acceptable. Certainly, if the traffic dynamics are measured in long intervals (e.g., 30-minute or longer), two-dimensional inputs are enough to produce a good prediction.

Table 5-11 Prediction results of traffic dynamics embedded in various dimensions

Time interval	Traffic variable	Time lag	*RMSE* (1-D)	*RMSE* (2-D)	*RMSE* (3-D)	*RMSE* (4-D)
1-minute (one day, station 433)	flow	1	0.1276	0.1236	0.0851	0.0706
	speed	1	0.0919	0.0888	0.0556	0.0493
	occupancy	1	0.0755	0.0576	0.0433	0.0392
3-minute (one day, station 433)	flow	1	0.0756	0.0735	0.0593	0.0576
	speed	1	0.0614	0.0573	0.0547	0.0538
	occupancy	1	0.0562	0.0424	0.0392	0.0363
5-minute (five workdays, station N27.9)	flow	1	0.0813	0.0634	0.0623	0.0634
	speed	1	0.0772	0.0690	0.0587	0.0616
	occupancy	1	0.0594	0.0573	0.0549	0.0556
15-minute (five workdays, station N27.9)	flow	1	0.0695	0.0603	0.0602	0.0619
	speed	1	0.0697	0.0655	0.0575	0.0688
	occupancy	1	0.0606	0.0556	0.0513	0.0538

CHAPTER 6 CONCLUSIONS AND SUGGESTION

In this study, real world traffic variable (flow, speed, and occupancy) patterns extracted from isolated detecting stations have been characterized with varied trends and drastic fluctuations in reconstructed state spaces. Meanwhile, some traffic evolutions for paired- and three-variable were observed. In addition, sensitivity analysis was implemented for short-term (within 15-minute) prediction of traffic dynamics with various time intervals, time lags, times of day and dimensions. After comparing the diverse features of traffic time series in reconstructed state spaces and predictability of various techniques, we summarize some important findings and explain their nature here.

6.1 Temporal and Spatiotemporal Patterns

We have conceptualized the reconstruction of traffic series by creating appropriate embedding spaces to investigate the temporal traffic patterns. From the four indexes, time delay, embedding dimension, the largest Lyapunov exponent and correlation dimension, we would like to stress that traditional methods of time series analysis are mainly concerned with decomposing the variation in a series into trend, seasonal variation, other cyclic changes, and the remaining “irregular” fluctuations. However, recent research claimed that random input is not the only possible source of irregularity in a system’s output. A nonlinear dynamics (e.g., chaotic system) can produce very irregular data with purely deterministic equations of motion in an autonomous way. Therefore, a complex system, such as traffic dynamics, requires a nonlinear approach to detecting whether the apparently irregular behaviors are purely random or not. Such requirement is exactly the core rationales for adopting the four

proposed parameters to investigating our current study topics. We believe this study will be most valuable in presenting a systematical nonlinear approach to exploring more information of temporal traffic dynamics as of now.

According to the parameters of successive one-month versus one-day traffic time series, the former state trajectories, which exhibit distinct time delay, unchangeable embedding dimension, near zero largest Lyapunov exponent and saturated correlation dimension, are characterized as having periodic-like patterns, which is as anticipated. In contrast, the latter state trajectories of very short times (i.e., 20-second and 1-minute) display random motions, and since their time delay is equal to one, embedding dimension is larger with increasing quantity of data, and correlation dimension is not saturated. Both state trajectories exhibit nonlinear dynamic features, one is periodic-like dynamic and the other is random dynamic. Following the above, we investigated a ten-workday traffic time series at various times of day and inspected their parameters. The diversity of patterns which contain fixed point, deterministic-like patterns and stochastic patterns were explored. In other words, different nonlinear phenomena were found to emerge depending on the measured time scales, time-of-day and history data. However, the chaotic feature was not obtained in traffic time series extracted from dual-loop detectors. Perhaps, further inspecting spatiotemporal features of congested traffic patterns can answer the question about chaotic or other complex behavior traffic characteristic.

We regard those traffic patterns attributed to deterministic-like dynamics as having some intrinsic rules governing the regularity. What do the real meanings or phenomena imply for such intrinsic rules in our daily life? We may assume that most trip makers get to work by 9 am and finish work at 5 pm on workdays, that is, they leave their homes or work places at approximately the same times, using the same modes, and/or choosing the same routes everyday. Such macroscopic regularities have caused “similar but not exactly the same” trends (i.e., slight fluctuations still exist) from day to day. Moreover, due to the constraints of travel demand, roadway capacity, speed limit, and so on, the observed traffic flows would not go beyond two extreme values: zero (free or jam) flow and maximum (capacity) flow. The speed and occupancy dynamics are also bounded within two extreme values (from free-flow speed or near zero occupancy to near zero speed or jammed occupancy). Thus, if we investigate the traffic time series on successive days, many recurrent curves are expected to be exhibited in 1-D plot, and cyclic patterns would appear in 3-D spaces. The macroscopic regularities indeed dominate the shape (trend) of such deterministic-like traffic patterns.

However, it's noticed that not every driver is completely confined by such macroscopic regularities. The majority of drivers always control his/her vehicle at a desired speed and safe spacing and clearance so as to best interact with roadway environments and neighboring vehicles. The presence of human behavior is perhaps a key factor making traffic dynamics more complicated than many other physical systems that do not involve human behavior. Besides, roadway traffic is essentially composed of heterogeneous vehicles with diverse powers or maneuver capabilities. Hence, due to the heterogeneity across drivers and vehicles, the microscopic traffic dynamics will always fluctuate and surge along with the macroscopic traffic trend. Namely, the heterogeneity of drivers and vehicles not only elucidates the random feature of one-workday traffic series but also explains the phenomenon of "similar but not exactly the same" patterns for successive (many-workday) traffic series.

Although our research attempt only aimed at characterizing the evolutional trajectories of time-varying traffic features, we also probed the traffic phases between upstream and downstream stations in this paper. For example, we found congested traffic at station 421 in the morning peak-hour. According to three-phase traffic theory, congested traffic occurs most at freeway bottlenecks where can be a result of road-works, on- and off-ramps, a decrease in the number of freeway lanes, road curves and road gradients, etc. For an isolated bottleneck, there are two types of patterns in congested traffic: "synchronized flow pattern (SP)" and "general pattern (GP)." The GP is a congested pattern, which consists of synchronized flow upstream of an effectual bottleneck and wide moving jams that emerge spontaneously in that synchronized flow. For two or more adjacent bottlenecks, then an expanded congested pattern (EP) can be formed. In the EP, a synchronized flow phase or a complex interactive process among various moving jams could be anticipated. However, conventional theories, such as shock wave theory and queuing theories, and those models based on the fundamental diagram approach or a few results simulated by cellular automata (CA) models are hampered by lack of capability of predicting fundamental empirical features of phase transitions and spatiotemporal congested pattern features of real traffic. This is because spatiotemporal solutions of these models are in a fundamental qualitative contradiction with empirical (measured) traffic breakdown and the resulting congested patterns. Only the main spatiotemporal pattern features are fully understood, additional study of some nonlinear pattern features can be performed (Kerner, 2004).

By contrast, in the example of our paired-traffic features, speed and flow can transform from a free-flow phase in the early hours to a synchronized or congested phase in the morning peak-hours, during which the 9-minute lane-flow rates can range from 7 vehicles to 289 vehicles and the corresponding time-mean-speed can drop from 101 kph to 80 kph. This suggests that an influx of vehicles in the morning peak-hour pushes the occupancy over a critical level, forcing the free-traffic phase into the moving jam or synchronized phase. The onset of traffic congestion is accompanied by a sharp drop in average vehicle speed, known as "the breakdown phenomenon." Even near noon, the flow rates remain high and the congested traffic does not disappear until around 14:00 PM. Unfortunately, the afternoon peak-hour arrives quickly thereafter thus the traffic state does not return to free-flow. Such irregular back-and-forth speed-flow features in the real world indicate that the synchronized traffic phase and the moving jams are alternative, which is similar to general pattern (GP). For such recurrent congestion, if a smart ramp metering instantaneously holds back the incoming vehicles in such a way that occupancy is kept below its critical value, traffic would flow freely and congestion could be avoided altogether. In sum, our observed paired- and three-variable traffic evolutions at the isolated detectors in effect provide evidence in support of Kerner's three-phase traffic theory and tackle the field problems.

6.2 Temporal Features and Short-term Prediction

In this study, four techniques, including a linear method, simple nonlinear prediction, RTRL algorithms and a RBFNN model were employed to compare their predictability. Wherein, a first order autoregressive model and a first-order differential-delay equation were used to test the predictability between the linear method, simple nonlinear prediction and RTRL algorithms. After validating the prediction power of RTRL algorithms, we further implemented the sensitivity analysis by employing the short-term (within 15-minute) traffic series, including flow, speed and occupancy measured with various time intervals, time lags and times of day. In accordance with the above investigation, we summarize some important findings as follows.

From the comparison between different techniques, we have learned that it is very important to take into account the characteristics of traffic series before prediction. Without a prerequisite analysis, it is hasty to claim or determine which technique is better or able to precisely predict a nonlinear time series because different characteristics of the time series could greatly affect the accuracy of prediction. For instance, we have learned that the traffic flows in the midnight measured in very short

intervals are so lull that most drivers can freely drive their vehicles, i.e., the features of traffic dynamics is a random pattern and even the trajectories converge to some fixed points. If we want to predict such a random pattern in the midnight, then it is not suitable to adopt the simple nonlinear algorithms, since the postulation of simple nonlinear algorithms are in effect mainly based on the theory that different time series with equal states may exhibit equal futures and similar states, while such a postulation is not exhibited for random patterns. Furthermore, it is less important compared with predicting traffic volume for other times of day, since the volume in the midnight is low. Even if an incident occurs in this period, the impact to traffic flow will quickly dissipate with the light traffic. In contrast to the random pattern exhibited during midnight, the intrinsic structures of successive traffic dynamics during morning and evening peak hours may show deterministic-like patterns. Such deterministic features or deterministic-like features with slight noises could be predicted using simple nonlinear algorithms. In regard to the stochastic features or deterministic-like features with considerable noises, iterative learning algorithms, such as RBFNN or RTRL algorithms would become a candidate to predict such features.

In addition, different methods of prediction may only provide a certain function for a specific purpose rather than being capable of error-free predicting including all aspects. For example, the simple nonlinear technique can immediately learn the intrinsic rules of the dynamics to precisely catch the trajectories in multidimensional spaces within a few time steps. However, the requirement is that the underlying dynamics be deterministic or a time series with slight noises. Likewise, we successfully predict the short-term nonlinear traffic dynamics extracted from the dual-loop detectors by employing RTRL algorithms as well as RBFNN. Nevertheless, at the present time, the problems of how to decide the proper hidden neurons, hidden layers and training time can only be solved by a trial and error method. Consequently, in terms of prediction, characteristic analysis of a time series is important and is a prerequisite for prediction. Furthermore, what we would like to do in practice is to select a technique that permits predicting the short-term traffic dynamics to meet the requirements of ATMS rather than arbitrarily searching for a method for perfect prediction without any errors.

Aside from the above statements, the traffic time series measured in different time intervals (1-minute, 3-minute, 5-minute, 15-minute), with different time lags (time lag=1, one-half *time delay*, 1-*time delay*) and during different times of day (00:00 – 03:00, 06:00 – 09:00, 12:00 – 15:00, 18:00 – 21:00) have been trained to predict traffic dynamics. According to our field study, several findings have been illustrated to support the accuracy of prediction when influenced by various time intervals, time lags

and time periods. We have found that the accuracy of predicting traffic dynamics for longer-intervals (15-minute) is better than for shorter-intervals (5-minute); likewise, 3-minute is better than 1-minute. In addition, a deterministic model with a proper time delay can precisely predict the dynamic state, for instance, $\tau = 6$ is a good time delay for the Mackey-Glass equation. In contrast, a stochastic time series for short time-lag (e.g., $\tau = 1$) will produce a better prediction than adopting other time lags. Short-interval traffic dynamics extracted from detectors are very likely close to stochastic patterns, thus the training results of adopting time lag being equal to one produce optimum prediction compared to adopting other time lags. Furthermore, we have also found that traffic dynamics in the morning and evening peak-hours are the most difficult to predict compared to other time periods, but this situation can be improved by training a historical network using the traffic data composed of only the same time periods, i.e., gathering several historical data at the same time periods will produce a better training network to predict traffic dynamics. Nevertheless, it is noticed that one has to carefully select proper historical data when adopting the above approach to train a neural network, wherein the "proper historical data" means to pick similar historical data that emulates the trend and variance as the future traffic dynamics. Improper historical data (e.g., that involving serious incidents, bad weather, etc.) may contribute to unexpected inaccuracy in prediction.

6.3 Extensive Applications

The current research outcomes can be employed to tackle the field problems like recurrent congestions and non-recurrent congestions that exist ubiquitously in various transport systems in our daily life (Lan *et al.*, 2007a). Theoretically, for recurrent congestion, what we can do is altering the service process more closely matching the arrival patterns; making the arrival process more closely matching the service capacity; or imposing proper service disciplines to cut down the overall delay costs or the size of delays. The main challenge is to determine proper time and intensity for actuating the control mechanism. For non-recurrent congestion, what we need to do is expediting the system capacity retrieval and the main challenge is to diagnose and remove the incidents as soon as possible, as delay is proportional to square of the incident duration.

As we have emphasized, more information of state trajectories of traffic dynamics can be obtained via converting the conventional traffic series (flow, speed, occupancy) in 1-D space into reconstructed multidimensional spaces. We can take advantages of outstanding multidimensional parameters of traffic series for management and control

purposes. Here we further present two examples. In the paper "Diagnosis of Freeway Traffic Incidents with Chaos Theory," Lan *et al.* (2003a) attempted to use the change of multidimensional parameters for flow series, including largest Lyapunov exponent, capacity dimension, correlation dimension, relative complexity, Kolmogorov entropy, delay time, and Hurst exponent to examine the existence of traffic incident. Through a deliberately-arranged incident experiment in Taiwan Freeway No. 1, they found that the largest Lyapunov exponent parameter of flow series has presented much more sensitive than the change in flow rate, a conventional expression of flow in 1-D space. Thus, the largest Lyapunov exponent was used for incident detection and the off-line tests showed that overall average detection rate can reach 93.75%, better than that by the conventional incident detection algorithms (fuzzy neural network, with detection rate ranging from 80% to less than 90%) using 1-D flow information.

In addition, in the example of our paired-traffic features, speed and flow transit from free-flow phase in the midnight to synchronized- or jammed- phase in the morning peak-hours. This indeed suggests that an influx of vehicles in the morning peak-hours has pushed the occupancy over a critical level, forcing the free-traffic into the phase of congestion or synchronization. Then, we can anticipate that there could be heavy delays for a long time on each typical workday. For such recurrent congestions, if a smart ramp metering could instantaneously hold back the incoming vehicles in such a way that occupancy is kept below its critical value, traffic would flow more freely in most occasions and the congestion size would be downsized altogether.

As another example, Lan *et al*. (2003b) argued that a self-organization phenomenon might exist when the phase shifts from non-congested to congested state within a system. They employ cellular automaton (CA) traffic simulator to investigate the self-organization forming process as the occupancy grows. Real traffic data are used to examine whether the power law, an indicator of self-organization phenomenon, exists or not. The empirical evidence on a two-lane freeway shows that self-organization phenomenon appears when the occupancy exceeds 45%; however, the edge of chaos is at a level of occupancy 33.8%, which should be the starting control point (e.g., ramp metering) for the recurrent congestions.

The above two examples may support that the proposed method and concept in this study can be used to develop traffic management schemes which are practically applicable in dynamic control.

6.4 Follow-up

According to our empirical results, the proposed analytical method permits extracting more information on traffic series in reconstructed state spaces, particularly, unfolding the motions of flow, speed, and occupancy state trajectories, which could converge, diverge, or perform periodic motions. In addition, the analytical results in terms of flow, speed, and occupancy time series as well as their paired data have illustrated various traffic phases and traffic stream characteristics. They would help understand the possible causes of formation of recurrent congested traffic phase in such a way that one could propose more effective traffic management. However, in contrast with temporal traffic patterns that occur only in time at specific locations, spatiotemporal traffic patterns that occur in both time and space can also be investigated with various perspectives. Different methodologies having certain advantages may achieve some purposes and thus we intend to further investigate more spatiotemporal patterns in future research.

Nevertheless, cellular automaton (CA) simulation has been widely used to explicate the behaviors of traffic flows. These modification models, however, mainly devoted efforts to introduce more realistic CA rules that can better govern the maneuvers of vehicles or drivers. The main bottleneck of this study that the traffic series extracted from “isolated” stations can only provide us to explore the temporal patterns of traffic dynamics may be conquered by modified CA model. The interface which transforms spatiotemporal features depicted in CA model to temporal state trajectories mainly remains investigation how to calibrate the traffic data derived from CA model and measure the position of vehicles using mathematical equations. More fundamentals of traffic dynamics associated with microscopic models as well as macroscopic models will be explored when the temporal features and spatiotemporal patterns are disclosed then.

Apart from the above issues being of investigative value, a few new topics associated with pattern recognition need to be tackled and mulled over. For example, from the results of our empirical study, it is stated that different nonlinear traffic patterns could emerge depending on the observed time-scale, history data and time-of-day. However, do the different patterns of traffic dynamics exhibit a distinct boundary? If so, what are these boundaries? Or, one may be curious to know whether different traffic patterns could transform into each other without distinct boundaries under a certain situation or during a specific time period. All the above subjects are worth further investigation.

In addition, this study places its emphasis on sequential order. However, another issue we hope to understand is whether or not the sequential order also possesses intrinsic rules/naturals depending on the observed times of day. For instance, the sequential order of traffic dynamics in the midnight should be different from that in the peak hours. The former may regularly change their positions because of light traffic while the latter could dramatically alter their trajectories and even stay for a while with the increasing volume. As the traffic parameters involving with sequential order are several traffic variables (speed, flow, occupancy) in multi-dimensions, we can take advantage of these parameters and adequately dominate the traffic dynamics. Namely, if the naturals of sequential order can be investigated well, we could more precisely diagnose the causes of formation of congestion and promptly deal with the incidents, thereby reinforcing the scheme of traffic management.

Moreover, we have claimed that different characteristics of the time series could greatly affect the accuracy of prediction; however, recently more novel techniques or hybrid methods, such as rough set theory, gray theory and artificial neural networks combined with genetic algorithms have been developed to predict short-term traffic dynamics. Future research can make use of the new approaches to predict short-term traffic dynamics while considering both accuracy and “real time” factors, but also to take advantage of the characteristics of traffic dynamics to effectively implement management in practice. In addition, it is recommended to add a naïve model or other available models in the future study for comparison purposes. Furthermore, attempt of other proper indexes to elucidate the prediction error, such as RMSPE, deserves further exploration.

Finally, it remains difficult to reproduce the multi-dimensional traffic time series by mathematical forms, which serve dynamic traffic forecasting in a shorter time scale, such as 20-sec and 1-min. Therefore, another challenge for further study is to develop rationales for modeling and predicting the traffic dynamics in the multi-dimensional reconstructed spaces. Development of effective traffic management and control tactics by utilizing such processed traffic information from the reconstructed spaces may also warrant more exploration.

BIBLIOGRAPHY

Abarbanel, H. D. I. (1996), *Analysis of observed chaotic data*, Springer-Verlag, New York.

Ansley, C. F., Spivey, W. A. and Wrobleski, W. J. (1977), "On the structure of moving average processes," *Journal Econometrics*, Vol. 6, No. 1, pp. 121-134.

Barlović, R., Santen, L., Schadschneider, A. and Schreckenberg, M. (1998), "Metastable states in cellular automata for traffic flow," *European Physical Journal B*, Vol. 5, pp. 793–800.

Bham, G. H. and Benekohal, R. F. (2004), "A high fidelity traffic simulation model based on cellular automata and car-following concepts," *Transportation Research Part C*, Vol. 12, No. 1, pp. 1-32.

Box, G. E. P., Hillmer, S. C. and Tiao, G. C. (1976), "Analysis and modeling of seasonal time series," *N. B. E. R.- Census Conference on Seasonal Time Series*, Washington D.C.

Box, G. E. P. and Jenkins, G. M. (1970), *Time series analysis, forecasting and control*, San Francisco: Holden-Day (revised edn published 1976).

Broomhead, D. S. and Lowe, D. (1988), "Multivariable functional interpolation and adaptive networks," *Complex Systems*, Vol. 2, pp. 321-355.

Chang, F. J., Chang, L. C. and Huang, H. L. (2002), "Real time recurrent neural network for stream flow forecasting," *Hydrological Processes*, Vol. 16, No. 13, pp. 2577-2588.

Chang, F. J. and Chang, L. C. (2005), *Neural Network*, Tung Hua, Taiwan.

Chang, J. L. and Miaou, S. P. (1999), "Real-time prediction of traffic flows using dynamic generalized linear models," *Transportation Research Record*, Vol. 1678, pp. 168-178.

Chang, W. F. and Mak, M. W. (1999), "A conjugate gradient learning algorithm for recurrent neural networks," *Neurocomputing*, Vol. 24, No. 1-3, pp. 173-189.

Chatfield, C. (1996), *The analysis of time series*, 5th edition, Chapman & Hall, Landon UK.

Chen, F. C., Cowan, C. F. N. and Grant, P. M. (1991), "Orthogonal least squares learning algorithm for radial basis function networks," *IEEE Transportation on Neural Networks*, Vol. 2, No. 2, pp. 302-309.

Chen, H. and Grant-Muller, S. (2001), "Use of sequential learning for short-term traffic flow forecasting," *Transportation Research Part C*, Vol. 9, No. 5, pp. 319-336.

Chowdhury, D., Wolf, D. E. and Schreckenberg, M. (1997), "Particle-hopping models for two-lane traffic with two kinds of vehicles: effects of lane-changing rules," *Physica A*, Vol. 235, No. 3-4, pp. 417-439.

Clark, S. D., Dougherty, M. S. and Kirby, H. R. (1993), "The use of neural networks and time series models for short-term traffic forecasting: a comparative study," In: Transportation Planning Methods, *Proceedings of the PTRC 21st Annual Summer Meeting*, Manchester.

Clarke, B. R. (1983), "An algorithm for testing goodness of fit of ARMA (P,Q) models," *Applied Statistics*, Vol. 32, No. 3, pp. 335-344.

Dendrinos, D. S. (1994), "Traffic-flow dynamics: a search for chaos," *Chaos, Solitons & Fractals*, Vol. 4, No. 2, pp. 605-617.

Disbro, J. E. and Frame, M. (1989), "Traffic flow theory and chaotic behavior," *Transportation Research Record*, No. 1225, pp. 109-115.

Dochy, T., Danech-Pajouh, M. and Lechevallier, Y. (1996), "Short-term road traffic forecasting using neural network," *RTS English Issue*, 11.

Dougherty, M. and Cobbett, M. (1997), "Short-term inter-urban traffic forecasts using neural networks," *International Journal of Forecasting*, Vol. 13, No. 1, pp. 21-31.

Drazin, P. G. (1994), *Nonlinear Systems*, Cambridge University Press, New York.

Fraser, A. M. and Swinney, H. L. (1986), "Independent coordinates for strange attractors from mutual information," *Physical Review A*, Vol. 33, No. 2, pp. 1134-1140.

Gardiner, C. W. (1997), *Handbook of stochastic methods: for physics, chemistry and the natural sciences*, 2nd edition, Springer series in synergetics: Springer, Berlin.

Gencay, R. (1996), "A statistical framework for testing chaotic dynamics via Lyapunov exponents," *Physica D*, Vol. 89, No. 3-4, 261-266.

Goh, S. L. and Mandic, D. P. (2003), "Recurrent neural networks with trainable amplitude of activation functions," *Neural Networks*, Vol. 16, No. 8, pp. 1095-1100.

Granger, C. W. J. and Newbold, P. (1976), "Forecasting transformed series," *Journal Royal Statistical Society, Series B*, Vol. 38, No. 2, pp. 189-203.

Grassberger, P. and Procaccia, I. (1983), "Measuring the strangeness of strange

attractors," *Physica D*, Vol. 9, No. 1-2, pp. 189-208.

Ham, F. M. and Kostanic I. (2001), *Principles of Neurocomputing for Science and Engineering*, McGraw-Hill: New York, NY.

Haykin, S. (1999), *Neural networks: A comprehensive foundation*, Englewood Cliffs, NJ: Prentice-Hall.

He, G. and Ma, S. (2002), "A study on the short-term prediction of traffic volume based on wavelet analysis," *The IEEE 5th International Conference on ITS*.

Hilborn, R. C. (2000), *Chaos and Nonlinear Dynamics: An Introduction for Scientists and Engineers*, 2nd edition, Oxford University Press, New York.

Hsu, C. C., Lin, Z. S., Chiou, Y. C. and Lan, L. W. (2007), "Exploring traffic features with stationary and moving bottlenecks using refined cellular automata," *Journal of the Eastern Asia Society for Transportation Studies*, Vol. 7, in CD-ROM.

Iokibe, T., Kanke, M. and Yasunari, F. (1995), "Local fuzzy reconstruction model for short-term prediction on chaotic time series," *Fuzzy Set*, Vol. 7, No. 1, pp. 186-194.

Jenkins, G. M. and Alavi, A. S. (1981), "Some aspects of modeling and forecasting multivariate time series," *Journal of Time Series Analysis*, Vol. 2, pp. 1-47.

Kalman, R. E. (1960), "A new approach to linear filtering and prediction problems," *Tranasactions of the ASME-Journal of Basic Engineering*, Series D, Vol. 82, pp. 34-45.

Kants, H. and Schreiber, T. (2004), *Nonlinear Time Series Analysis*, Cambridge University Press, Cambridge, UK.

Kecman, V. (2001), Learning and Soft Computing: Support Vector Machines, Neural Networks, and Fuzzy Logic Models, Cambridge, MA: MIT press.

Kennel, M. B. and Isabelle, S. (1992), "Method to distinguish possible chaos from colored noise and to determine embedding parameters," *Physical Review A*, Vol. 46, No. 6, pp. 3111-3118.

Kennel, M. B. and Brown R., Abarbanel, H. D. I. (1992), "Determining embedding dimension for phase-space reconstruction using a geometrical construction," *Physical Review A*, Vol. 45, pp. 3403 -3411.

Kerner, B. S. (1998), "A Theory of Congested Traffic Flow," *In: Proceedings of the 3rd Symposium on Highway Capacity and Level of Service*, Vol. 2, pp. 621-642.

Kerner, B. S. (1999), "Congested Traffic Flow: Observations and Theory," *Transportation Research Record*, No. 1678, pp. 160-167.

Kerner, B. S. (2002a), "Synchronized flow as a new traffic phase and related problems for traffic flow modeling," *Mathematical and Computer Modeling*, Vol. 35, No. 5, pp. 481-508.

Kerner, B. S. (2002b), "Empirical macroscopic features of spatial-temporal traffic patterns at highway bottlenecks," *Physical Review E*, Vol. 65, No. 4, 046138 (30 pages).

Kerner, B. S. and Klenov, S. L. (2002), "A microscopic model for phase transitions in traffic flow," *Journal of Physics A: Mathematical and General*, Vol. 35, No. 3, pp. L31-L43.

Kerner, B. S., Klenov, S. L. and Wolf, D. E. (2002), "A cellular automata approach to three-phase traffic theory," *Journal of Physics A: Mathematical and General*, Vol. 35, No. 47, pp. 9971-10013.

Kerner, B. S., Rehborn, H., Aleksic, M. and Haug, A. (2004), "Recognition and tracking of spatial-temporal congested traffic patterns on freeways," *Transportation Research Part C*, Vol. 12, No. 5, pp. 369-400.

Kerner, B. S. (2004), *The Physics of Traffic*, Springer, Berlin, New York.

Kerner, B. S., Klenov, S. L. and Hiller, A. (2006), "Criterion for traffic phase in single vehicle data and empirical text of three-phase traffic theory," *Journal of Physics A: Mathematical and General*, Vol. 39, No. 9, pp. 2001-2020.

Kirby, H., Dougherty, M. and Watson, S. (1997), "Should we use neural networks or statistical models for short term motorway traffic forecasting?" *International Journal of Forecasting*, Vol. 13, No. 1, pp. 43-50.

Knospe, W., Santen, L., Schadschneider, A. and Schhreckenberg, M. (2000), "Towards a realistic microscopic description of highway traffic," *Journal of Physics A*, Vol. 33, No. 48, pp. 477-485.

Lam, W. H. K., Chan, K. S. and Shi, J. W. Z. (2002), "A traffic flow simulator for short-term travel time forecasting," *Journal of Advanced Transportation*, Vol. 36, No. 3, pp. 265-291.

Lam, W. H. K., Tang, Y. F. and Tam, M. L. (2006), "Comparison of two non-parametric models for daily traffic forecasting in Hong Kong," *Journal of Forecasting*, Vol. 25, No. 3, pp. 173-192.

Lan, L. W. and Lin, S. Y. (2001), "Prediction of short-term traffic dynamics--phase space local approximation method," *Proceedings of the 16th Annual Conference for the Chinese Institute of Transportation*, pp. 477-486.

Lan, L. W., Lin, F. Y. and Kuo, A. Y. (2003a), "Testing and prediction of traffic flow dynamics with chaos," *Journal of the Eastern Asia Society for Transportation Studies*, Vol. 5, pp. 1975-1990.

Lan, L. W., Lin, F. Y. and Wang, Y. P. (2003b), "Self-organized phenomenon and the edge of Chaos in traffic flow dynamics," *Proceedings of the 5th International Conference of Eastern Asia Society for Transportation Studies*, Vol. 4, pp. 574-582.

Lan, L. W., Sheu, J. B. and Huang, Y. S. (2007a), "Features of Traffic Time-series on Multi-dimensional Space," *Journal of the Chinese Institute of Transportation*, in press. (Accepted)

(2007b), "Investigation of temporal freeway traffic patterns in reconstructed state

spaces," *Transportation Research Part C*, in press. (Accepted)

(2007c), "The characteristics of temporal traffic flow dynamics," *Journal of the Eastern Asia Society for Transportation Studies*, Vol. 7, in CD-ROM.

(2007d), "Prediction of short-interval traffic dynamics in multidimensional spaces," *Journal of the Eastern Asia Society for Transportation Studies*, Vol. 7, in CD-ROM.

Lárraga, M.E., del Río, J.A. and Alvarez-lcaza, L. (2005), "Cellular automata for one-lane traffic flow modeling," *Transportation Research Part C*, Vol. 13, No. 1, pp. 63-74.

Lee, S. and Fambro, D. B. (1999), "Application of subset autoregressive integrated moving average model for short-term freeway traffic volume forecasting," *Transportation Research Record*, Vol. 1678, pp. 179-188.

Li, S. (2002), "Nonlinear combination of travel-time prediction model based on wavelet network," *The IEEE 5th International Conference on ITS*.

Lingras, P., Sharma, S. C. and Osborne, P. (2000), "Traffic volume time-series analysis according to the type of road use," *Computer-Aided Civil and Infrastructure Engineering*, Vol. 15, No. 5, pp. 365-373.

Liu, L. M. and Lin, M. W. (1991), "Forecasting residential consumption of natural gas using monthly and quarterly time series," *International Journal of Forecasting*, Vol. 7, No. 1, pp. 3-16.

Mackey, M. C. and Glass, L. (1977), "Oscillation and chaos in physiological control systems," *Science*, Vol. 197, No. 4300, pp. 287-289.

Mak, M. W., Ku, K. W. and Lu, Y. L. (1999), "On the improvement of the real time recurrent learning algorithm for recurrent neural networks," *Neurocomputing*, Vol. 24, No. 1-3, pp. 13-36.

Maravall, A. (1983), "An application of nonlinear time series forecasting," *Journal Business Economic Statistics*, Vol. 1, No. 1, pp. 66-74.

May, A. D. (1990), *Traffic Flow Fundamentals*, Prentice Hall, New Jersey.

Nagel, K. (1996), "Particle-hopping models and traffic flow theory," *Physical Review E*, Vol. 53, No. 5, pp. 4655-4672.

Nagel, K. (1998), "From particle-hopping models to traffic flow theory," *Transportation Research Record*, Vol. 1644, pp. 1-9.

Nagel, K., Wolf, D. E., Wagner, P. and Simon, P. (1998), "Two-lane traffic rules for cellular automata: A systematic approach," *Physical Review E*, Vol. 58, No. 2, pp. 1425-1437.

Nayfeh, A. H. and Balachandran, B. (1995), *Applied Nonlinear Dynamics*, John Wiley & Sons, Inc., New York.

Oller, L. E. (1985), "Macroeconomic forecasting with a vector ARIMA model: A case

study of the Finnish economy," *International Journal of Forecasting*, Vol. 1, No. 2, pp. 143-150.

Peak, D. and Frame, M. (1994), *Chaos under Control: the Art and Science of Complexity*, Freeman, New York.

Rickert, M., Nagel, K., Schreckenberg, M. and Latour, A. (1996), "Two lane traffic simulations using cellular automata," *Physica A*, Vol. 231, No. 4, pp. 534-550.

Ragwitz, M. and Kantz, H. (2000), "Detecting nonlinear structure and predicting turbulent gusts in surface wind velocities," *Europhys. Lett.*, Vol. 51, No. 6, pp. 595-601.

(2002), "Markov models from data by simple nonlinear time series predictors in delay embedding spaces," *Physical Review E*, Vol. 65, No. 5, 056201 (12 pages).

Rosenstein, M. T., Collins, J. J. and Deluca, C. J. (1993), "A practical method for the calculating largest Lyapunov exponents from small datasets," *Physica D*, Vol. 65, No. 1-4, pp. 117-134.

Sakawa, M., Kosuke, K. and Ooura, K. (1998), "A deterministic nonlinear prediction model through fuzzy reasoning using neighborhoods' difference and its application to actual time series data," *Fuzzy Set*, Vol. 10, No. 2, pp. 381-386.

Shang, P., Li, X. and Kamae, S. (2005), "Chaotic analysis of traffic time series," *Chaos, Solitons & Fractal*, Vol. 25, No. 1, pp. 121-128.

Sheu, J. B., Chou, Y. H. and Chen, A. (2004), "Stochastic modeling and real-time prediction of incident effects on surface street traffic congestion," *Applied Mathematical Modelling*, Vol. 28, No. 5, pp. 445-468.

Smith, B. L. and Demetsky, M. J. (1997), "Traffic flow forecasting: comparison of modeling approaches," *Journal of Transportation Engineering*, Vol. 123, No. 4, pp. 261-266.

Smith, B. L., Williams, B. M. and Oswald, R. K. (2002), "Comparison of parametric and nonparametric models for traffic flow forecasting," *Transportation Research Part C*, Vol. 10, No. 4, pp. 303-321.

Soltani, S. (2002), "On the use of the wavelet decomposition for time series prediction," *Neurocomputing*, Vol. 48, No. 1-4, pp. 267-277.

Sprott, J. C. (2003), *Chaos and Time-Series Analysis*, Oxford University Press, New York.

Sprott, J. C. and Rowlands, G. (1995), Chaos data analyzer: the professional version. Physics Academic Software, Raleigh, NC.

Stathopoulos, A. and Karlaftis, M. G. (2003), "A multivariate state space approach for urban traffic flow modeling and prediction," *Transportation Research Part C*, Vol. 11, No. 2, pp. 121-135.

Takens, F. (1981), Detecting strange attractors in turbulence. Dynamical systems and

turbulence. Lecture Notes in Mathematics 898, Springer, New York.

Tam, M. L., Lam, W. H. K. and Tang, Y. F. (2004), "Short-term prediction of hourly traffic flows in Hong Kong," *Proceedings of the 9th Conference of Hong Kong Society for Transportation Studies*, Hong Kong, pp. 360-369.

Theiler, J., Eubank, S., Longtin, A., Galdrikian, B. and Farmer, J. D. (1992), "Testing for nonlinearity in time series: the method of surrogate data," *Physica D*, Vol. 58, No. 1-4, pp. 77-94.

Varaiya, P. (2005), What we've learned about highway congestion. Access 27, pp. 2-9.

Wedding II, D. K. and Cios, K. J. (1996), "Time series forecasting by combining RBF networks, certainty factors, and the Box-Jenkins model," *Neurocomputing*, Vol. 10, No. 2, pp. 149-168.

Williams, B. M. (2001), "Multivariate vehicular traffic flow prediction: an evaluation of ARIMAX modeling," *Transportation Research Board Annual Meeting*, Washington, D.C., No. 80, pp. 194-200.

Williams, B. M. and Hoel, L. A. (2003), "Modeling and Forecasting Vehicular Traffic Flow as a Seasonal ARIMA Process: Theoretical Basis and Empirical Results," *Journal of Transportation Engineering*, Vol. 129, No. 6, pp. 664-672.

Williams, R. J. and Zipser, D. (1989), "A learning algorithm for continually running fully recurrent neural networks," *Neural Computation*, Vol. 1, pp. 270-280.

Zhang, X. and Jarrett, D. F. (1998), "Chaos in a dynamic model of traffic flows in an origin-destination network," *Chaos*, Vol. 8, No. 2, pp. 503-513.

APPENDIX A TERMINOLOGIES

Correlation dimension: Correlation dimension is a measure of the extent to which the presence of a data point affects the position of other points lying on the attractor.

Deterministic time series: To measure values x_1, x_2,…x_n,… at time t_1,t_2,…,t_n,… of a time dependent random variable $x(t)$, the existence and uniqueness of solutions of x_n are ensured.

Dynamics: A dynamical system whose state evolves (changes) with time t.

Embedding dimension: A sequence of observations $\{S_t = s(x_n)\}$ performed with some measurement function $s(\cdot)$, wherein the one-dimensional traffic time series embedded into multiple dimensions reconstructed space is denoted as $S_t = (s_t, s_{t+\tau}, s_{t+2\tau}..., s_{t+(m-1)\tau})$, $t = 1,2,..., N$ where the parameter integer m is called embedding dimension.

Fixed point: For a system described by a set of first-order differential equations, a point in the state space for which all of the time derivatives of the state space variables are 0 is said to be a fixed point.

Linear dynamics: Time series can be represented by linear equations of motions.

Markov process: A time series is a purely random process with mean zero and variance σ^2. The process is said to be an autoregressive process of first order or Markov process when the order equals one.

Nonlinear dynamics: Time series can be represented via nonlinear Eqs. of motion, e.g., differential Eqs, iteration of maps, etc.

Periodic trajectory: The trajectories show that the sequence of peaks is periodic-2, periodic-3,…, and so on.

Quasi-periodic trajectories: A type of motion occurring in three-dimensional state space has two different frequencies associated with it.

Random data: In general, if the data obtained from the experiment are not repeatable with the bounds of the experimental error under identical conditions, then the

corresponding system can be called a random system. The data obtained from a random system is called random data.

Reconstructed spaces: Map the one-dimensional traffic series into *m*-dimensional reconstructed spaces via the determination of appropriate time delay and embedding dimension.

Spatiotemporal traffic features: Traffic variables (flow, time-mean-speed, percent occupancy) vary transversely across the highway between lanes and direction of travel, and longitudinally along the highway or street as time evolution.

State space/Phase space: In the nonautonomous case, the equations are of the form $\dot{x} = F(x,t)$, where x is finite dimension, $x \in R^n$, $t \in R$ and F explicitly depends on *t*. The vector *x* is called a state vector and the space R^n in which *x* evolves is called a state space.

State trajectory: Traffic variables (flow, time-mean-speed, percent occupancy), which were tracked and recorded in reconstructed state spaces over time.

Stochastic processes: To measure values x_1, x_2,…x_n,… at time t_1,t_2,…,t_n,…,a set of probability distribution denoting that at time t_n the value x_n can be found.

Temporal traffic features: Traffic variables (flow, time-mean-speed, percent occupancy) vary over time at specific locations in a highway system.

Time delay: A sequence of observations $\{S_t = s(x_n)\}$ performed with some measurement function $s(\cdot)$, wherein the one-dimensional traffic time series embedded into multiple dimensions reconstructed space is denoted as $S_t = (s_t, s_{t+\tau}, s_{t+2\tau}..., s_{t+(m-1)\tau})$, $t = 1,2,...,N$ where the parameter τ is called time delay.

Traffic dynamics/ Traffic time series: The evolution or temporal variation of any traffic variables (flow, time-mean-speed, percent occupancy) measured in a sequential (chronological) order.

Traffic patterns: Those characteristics of vehicle groups pass a point or short segment during a specified span or traveling over longer sections of highway.

APPENDIX B NOTATIONS

τ	Time delay
m	Embedding dimension
λ	The Lyapunov exponent
λ_0	The largest Lyapunov exponent
d	Correlation dimension/Attractor dimension
r	Distance
θ_{ij}	Average mutual information (AMI)
p_{ij}	The probability of finding a time series value in the *i*-th interval.
$p_{ij}(\tau)$	The joint probability that an observation falls into the *i*-th interval and an observation time τ later falls into the *j*-th interval.
$\varepsilon_{i,j}$	The ratio of false nearest neighbor (FNN)
s_i^m	A point s_i is located in an *m*-dimensional space.
s_j^m	A point s_j is located in an *m*-dimensional space which is a considerable near neighbor of s_i^m.
$\zeta(\Delta t)$	Stretching factor: an estimate of the largest Lyapunov exponent λ_0 per time step.
$\Psi(s_i)$	The neighborhood of s_i with diameter *r*
$\mu(r)$	The correlation integral.
Θ	Heaviside step function
x_n	Gaussian random variable
M_{MA}	The order of MA model
M_{AR}	The order of AR model
s_t	The embedding vector at time *t*
s_{t0}	A predictor of s_t
s_{t0+T}	The embedding vector s_{t0} at future time (*t*+T)
$\phi(\cdot)$	Radial Basis Function (RBF)

U_t	An input multidimensional time series of RBFNN
Y_t	An output multidimensional time series of RBFNN
w, v	Weight matrix
w_0	A bias term weight of hidden neuron
c_j	The center of the jth Gaussian function
σ_j	The width of the Gaussian function
φ_n	White Gaussian noise
$d(p)$	The pth desired value
$y(p)$	The pth network output
$e(p)$	The pth difference between the desired value and the network output, i.e., $e(p)=d(p)-y(p)$
E	The total values of $e(p)$ in network
$y(t)$	The n-tuple of outputs of the n-processing neurons at time t
$x(t)$	The m-tuple of external inputs to the network at time t
$d_k(t)$	The desired value of the k-th neuron at time t
$z_k(t)$	The network output
$e_k(t)$	The difference between the desired value and the network output at time t, i.e., $e_k(t)= d_k(t)- z_k(t)$
$E(t)$	The total values of $e_k(t)$ at time t
η_1 , η_2	The learning rate
t_{occi}	The individual occupancy time (seconds)
t_{if}	The instant time that i^{th} vehicle is detected (seconds)
t_{ir}	The instant time that i^{th} vehicle is off detected (seconds)
$\dot{x}_i, \dot{x}_{i+1}$	Speed of i^{th} and $(i+1)^{th}$ vehicle
D_A, D_B	Detector A and detector B length
D	Distance between detector A and detector B
q_i	Flow rate at i^{th} time interval
u_i	Time-mean-speed at i^{th} time interval
q^T	Accumulated flow rate
u^T	Weighted time-mean-speed

APPENDIX C VITA

Name: Yi-San Huang
Gender: Male
Birth: 1963.01.15

Education:

1. Ph. D. Course in Institute of Traffic and Transportation, National Chiao Tung University (September 2002 ~ December 2007).
2. Master Course in Department of Traffic Science, Central Police University (September 1999 ~ July 2002).
3. Bachelor Course in Department of Traffic Science, Central Police College (September 1983 ~ July 1986).

Work Experience:

1. Traffic Sub-Lieutenant, Traffic Division, Taipei City Police Department.
2. Sub-Chief, Zhongzheng Second and Wanhua Police District.
3. Captain, Traffic Division, Taipei City Police Department.
4. Inspector, Taipei City Police Department.
5. Section Chief, Traffic Division and Criminal Investigation Division.

Publications:

A. Refereed Papers

1. Lan, L. W., Sheu, J. B. and Huang, Y. S. (2007), "Features of Traffic Time-series on Multi-dimensional Space," *Journal of the Chinese Institute of Transportation*, in press. (**TSSCI**, Accepted)

2. Lan, L. W., Sheu, J. B. and Huang, Y. S. (2007), "Investigation of temporal freeway traffic patterns in reconstructed state spaces," *Transportation Research Part C*, in press. (**SCI**, Accepted)
3. Lan, L. W., Sheu, J. B. and Huang, Y. S. (2007), "The characteristics of temporal traffic flow dynamics," *Journal of the Eastern Asia Society for Transportation Studies*, Vol. 7, in CD-ROM.
4. Lan, L. W., Sheu, J. B. and Huang, Y. S. (2007), "Prediction of short-interval traffic dynamics in multidimensional spaces," *Journal of the Eastern Asia Society for Transportation Studies*, Vol. 7, in CD-ROM.

B. Conference Papers

1. Sheu, J. B., Lan, L. W. and Huang, Y. S. (2007), "Prediction of short-interval nonlinear traffic dynamics using real-time recurrent learning," *Proceedings of the* 2007 *International Conference and Annual Meeting of Chinese Institute of Transportation*, in CD-ROM.
2. Lan, L. W., Sheu, J. B. and Huang, Y. S. (2006), "Features of Traffic Time-series on Multi-dimensional Space," *Proceedings of the 21th Conference of Chinese Institute of Transportation*, in CD-ROM.
3. Lan, L. W. and Huang, Y. S. (2005), "A refined parsimony procedure to exploring the nonlinear patterns of traffic dynamics," *Proceedings of the 10th Conference of Hong Kong Society for Transportation Studies*, pp. 23-32.
4. Lan, L. W., Lin, F. Y. and Huang, Y. S. (2004), "Some evidences of chaotic phenomena in short-term traffic flow dynamics: surrogate data approach," *Proceedings of the 9th Conference of Hong Kong Society for Transportation Studies*, pp. 566-574.
5. Lan, L. W., Lin, F. Y. and Huang, Y. S. (2004), "Confined space fuzzy proportion model for short-term traffic flow prediction," *Proceedings of the 9th Conference of Hong Kong Society for Transportation Studies*, pp. 370-379.

C. Other Refereed Papers

1. 曾平毅、黃益三（2003），改善我國駕照管理作業之研究，*運輸學刊*，第十五卷第四期，頁 411-436。
2. 曾平毅、蔡中志、黃益三、姜心怡、王旭昌（2002），駕照換發作業之民眾與醫師意見調查分析，*都市交通*，第十七卷第二期，頁 1-16。